National Library
of Canada

Acquisitions and
Bibliographic Services Branch

395 Wellington Street
Ottawa, Ontario
K1A 0N4

Bibliothèque nationale
du Canada

Direction des acquisitions et
des services bibliographiques

395, rue Wellington
Ottawa (Ontario)
K1A 0N4

Your file Votre référence

Our file Notre référence

NOTICE

The quality of this microform is heavily dependent upon the quality of the original thesis submitted for microfilming. Every effort has been made to ensure the highest quality of reproduction possible.

If pages are missing, contact the university which granted the degree.

Some pages may have indistinct print especially if the original pages were typed with a poor typewriter ribbon or if the university sent us an inferior photocopy.

Reproduction in full or in part of this microform is governed by the Canadian Copyright Act, R.S.C. 1970, c. C-30, and subsequent amendments.

AVIS

La qualité de cette microforme dépend grandement de la qualité de la thèse soumise au microfilmage. Nous avons tout fait pour assurer une qualité supérieure de reproduction.

S'il manque des pages, veuillez communiquer avec l'université qui a conféré le grade.

La qualité d'impression de certaines pages peut laisser à désirer, surtout si les pages originales ont été dactylographiées à l'aide d'un ruban usé ou si l'université nous a fait parvenir une photocopie de qualité inférieure.

La reproduction, même partielle, de cette microforme est soumise à la Loi canadienne sur le droit d'auteur, SRC 1970, c. C-30, et ses amendements subséquents.

Canada

UNIVERSITY OF ALBERTA

FACIES, STRATIGRAPHY, AND DIAGENESIS OF THE UPPER DEVONIAN CARBONATES IN THE OBED AREA, WEST-CENTRAL ALBERTA, CANADA

by

Karen S. Patey ©

A thesis submitted to the
Faculty of Graduate Studies and Research
in partial fulfilment of the requirements for the degree of
Master of Science

Department of Earth and Atmospheric Sciences

EDMONTON, ALBERTA
© Fall, 1995

National Library of Canada
Acquisitions and Bibliographic Services Branch
395 Wellington Street
Ottawa, Ontario
K1A 0N4

Bibliothèque nationale du Canada
Direction des acquisitions et des services bibliographiques
395, rue Wellington
Ottawa (Ontario)
K1A 0N4

Your file Votre référence

Our file Notre référence

THE AUTHOR HAS GRANTED AN IRREVOCABLE NON-EXCLUSIVE LICENCE ALLOWING THE NATIONAL LIBRARY OF CANADA TO REPRODUCE, LOAN, DISTRIBUTE OR SELL COPIES OF HIS/HER THESIS BY ANY MEANS AND IN ANY FORM OR FORMAT, MAKING THIS THESIS AVAILABLE TO INTERESTED PERSONS.

L'AUTEUR A ACCORDE UNE LICENCE IRREVOCABLE ET NON EXCLUSIVE PERMETTANT A LA BIBLIOTHEQUE NATIONALE DU CANADA DE REPRODUIRE, PRETER, DISTRIBUER OU VENDRE DES COPIES DE SA THESE DE QUELQUE MANIERE ET SOUS QUELQUE FORME QUE CE SOIT POUR METTRE DES EXEMPLAIRES DE CETTE THESE A LA DISPOSITION DES PERSONNE INTERESSEES.

THE AUTHOR RETAINS OWNERSHIP OF THE COPYRIGHT IN HIS/HER THESIS. NEITHER THE THESIS NOR SUBSTANTIAL EXTRACTS FROM IT MAY BE PRINTED OR OTHERWISE REPRODUCED WITHOUT HIS/HER PERMISSION.

L'AUTEUR CONSERVE LA PROPRIETE DU DROIT D'AUTEUR QUI PROTEGE SA THESE. NI LA THESE NI DES EXTRAITS SUBSTANTIELS DE CELLE-CI NE DOIVENT ETRE IMPRIMES OU AUTREMENT REPRODUITS SANS SON AUTORISATION.

ISBN 0-612-06519-7

Canada

UNIVERSITY OF ALBERTA

Library Release Form

Name of Author:	**Karen S. Patey**
Title of Thesis:	**Facies, stratigraphy, and diagenesis of the Upper Devonian carbonates in the Obed area, west-central Alberta, Canada**
Degree:	**Master of Science**
Year this Degree Granted:	**1995**

Permission is hereby granted to the University of Alberta Library to reproduce single copies of this thesis and to lend or sell such copies for private, scholarly, or scientific research purposes only. The author reserves all other publication and other rights in association with the copyright in the thesis, and except as herein before provided neither the thesis nor any substantial portion thereof may be printed or otherwise reproduced in any material form whatever without the author's prior written permission.

Karen S. Patey

1158 Memorial Drive N.W.
Calgary, Alberta
T2N 3E5

October 5, 1995

UNIVERSITY OF ALBERTA

FACULTY OF GRADUATED STUDIES AND RESEARCH

The undersigned certify that they have read, and recommended to the Faculty of Graduate Studies and Research for acceptance, a thesis entitled FACIES, STRATIGRAPHY, AND DIAGENESIS OF THE UPPER DEVONIAN CARBONATES IN THE OBED AREA, WEST-CENTRAL ALBERTA, CANADA submitted by KAREN S. PATEY in partial fulfillment of the requirements for the degree of MASTER OF SCIENCE.

Hans G. Machel

Dr. H.G. Machel (Supervisor)

J F Lerbekmo

Dr. J. Lerbekmo

Carl Mendoza

Dr. C. Mendoza

Donald J. Pluth

Dr. D. Pluth

July 10, 1995

ABSTRACT

An understanding of the stratigraphic framework and the associated depositional facies of the Frasnian carbonates of the Obed area, west-central Alberta, is necessary for the understanding of their reservoir characteristics. Reservoir facies include dolomitized grainstone to fossil floatstone/rudstone of the back-reef, reef crest, and reef slope paleoenvironments in the Leduc Formation (Woodbend Group) and Lower Blueridge Member (Winterburn Group). Mapping and reconstruction of the stratigraphy with the use of core descriptions has resulted in the recognition of seven westward prograding, shallowing upwards cycles in the Lower Blueridge Member (Graminia Formation), representative of reef to basin transitions.

The carbonates in the Obed area of west-central Alberta have undergone a complex diagenetic history. The platform facies have been affected by early widespread, pervasive dolomitization, which replaced the original limestones. Pyrite formed as a result of bacterial sulfate reduction (BSR) before and during pervasive dolomitization. Later diagenetic phases, post-dating pervasive dolomitization and hydrocarbon migration, include secondary (post-depositional) anhydrite, planar dolomite, saddle dolomite, calcite, pyrite, and native sulfur. The geochemistry of these late phases provides evidence for thermochemical sulfate reduction (TSR). Carbon, oxygen, and strontium isotope data for carbonates (calcites and dolomites) in the Obed area demonstrate that they underwent deep burial cementation and recrystallization.

ACKNOWLEDGEMENTS

Financial support of this thesis study was provided by Amoco Canada Petroleum Company Limited and strategic grants from the Natural Science and Engineering Research Council (NSERC). I would like to thank Amoco and Dr. H.G. Machel for providing the opportunity to work on this project.

There are several people I would like to acknowledge for their advice and editing in the final stages of writing: Hans Machel, Pat Cavell, Lee Riciputi, Bill Martindale, and Marc Villéger. Their comments are greatly appreciated.

I would like to thank Amoco Canada Petroleum Company Limited, Norcen Energy Resources Limited, Gulf Canada Resources Limited, and Home Oil Company Limited for providing contract employment during the course of my thesis. The knowledge I gained was invaluable to the production of my thesis and, undoubtedly, to my future career as a geologist in the petroleum industry.

Technical assistance was provided by several institutions. I would like to thank the following people: the staff at the ERCB core depository in Calgary; Don Resultay at the University of Alberta for preparing the majority of thin sections used in this study; Core Laboratories for supplying some thin sections; Nanita, Maria, and Jesusa who provided assistance and guidance in Roy Krouse's stable isotope lab at the University of Calgary; Martin Fowler at the ISPG for providing office space and use of a microscope; Karlis Muehlenbachs for use of the stable isotope lab and analyses at U of A; Kim Manzano for providing some stable isotope data from the Obed area which she used as part of a graduate course report; Gulf Canada for allowing me use of their lab for thin section studies and drafting services; Bud Baadsgaard for use of the radiogenic isotope lab at the University of Alberta and Pat Cavell for her guidance, support, and work in this lab; and, Scott Hadley of Amoco who initially provided invaluable assistance and guidance.

Kim Manzano, Harold Huebscher, Paul Blanchon, Heather Blyth, as well as other fellow graduate students, provided welcomed companionship and discussions. Special thanks are extended to my parents back on "the rock" who have always supported my decisions and choices in life and were always there when I needed a reality check, or anything...

TABLE OF CONTENTS

Page

CHAPTER 1: 1

GENERAL INTRODUCTION

REFERENCES 8

CHAPTER 2: 10

Depositional facies and stratigraphy of the Upper Devonian carbonates in the Obed area, west-cental Alberta

ABSTRACT 10
2.1. INTRODUCTION 10
2.2. PREVIOUS WORK AND METHODOLOGY 15
2.3. REGIONAL GEOLOGIC SETTING 15
2.4. DEPOSITIONAL FACIES AND ENVIRONMENTS 20
    2.4.1. Tidal Flat (Facies A) 21
    2.4.2. Lagoon (Facies B) 28
    2.4.3. Back-reef (Facies C) 28
    2.4.4. Reef Crest (Facies D) 31
    2.4.5. Reef Slope (Facies E) 31
    2.4.6. Reef Front (Facies F) 34
    2.4.7. Basinal (Facies G) 37
    2.4.8. Supratidal to Intertidal Facies Assemblage 37
2.5. STRATIGRAPHIC FRAMEWORK 37
    2.5.1. Woodbend Group 43
    2.5.2. Winterburn Group 44
2.6. RESERVOIR CHARACTER 46
2.7. CORRELATION TO OUTCROP 50
2.8. CONCLUSIONS 55
2.9. REFERENCES 56

CHAPTER 3: 59

Diagenesis of the Upper Devonian carbonates in the Obed area, west-central Alberta

ABSTRACT 59
3.1. INTRODUCTION 59
3.2. METHODOLOGY 66
3.3. PETROGRAPHY AND PARAGENETIC SEQUENCE 72
    3.3.1. Dolomitization and Dolomite Cementation 72
    3.3.2. Calcite Cementation 80
    3.3.3. Sulfur Phases 80
    3.3.4. Other Diagenetic Phases 88
    3.3.5. Porosity Generation and Destruction 91
3.4. INORGANIC GEOCHEMISTRY - EFFECTS OF BSR AND TSR 92
    3.4.1. Carbonates 96
    3.4.2. Anhydrite 98
    3.4.3. Pyrite 108
    3.4.4. Elemental Sulfur 111
3.5. DISCUSSION AND CONCLUSIONS 114
3.6. REFERENCES 119

CHAPTER 4:

CONCLUSIONS AND RECOMMENDATIONS **124**
REFERENCES 126

APPENDIX A:

CORE INFORMATION **127**

APPENDIX B:

GEOCHEMICAL ANALYSES **129**
B.1. Carbon and Oxygen Isotope Analysis 129
B.2. Strontium Isotope Analysis 129
B.3. Sulfur and Oxygen Isotope Analysis 130
REFERENCES CITED IN APPENDICES **147**

LIST OF FIGURES

Page

Figure 1-1 Obed study area, west-central Alberta 3
Figure 1-2 Major Woodbend reef complexes, Wild River sub-basin 5
Figure 1-3 Obed platform geometry and well control 7
Figure 2-1 Table of Woodbend and Winterburn formations and members 12
Figure 2-2 Obed study area, west-central Alberta 14
Figure 2-3 Major Woodbend reef complexes, Wild River sub-basin 17
Figure 2-4 Obed platform geometry, wells with core, and cross-section lines 19
Figure 2-5 Reef model with depositional environment and facies zonations 23
Figure 2-6 Facies classification 25
Figure 2-7 Tidal flat (facies A) and lagoon (facies B) photos 27
Figure 2-8 Back-reef (facies C) and reef crest (facies D) photos 30
Figure 2-9 Reef slope (facies E) photos 33
Figure 2-10 Reef front (facies F) and basinal (facies G) photos 36
Figure 2-11a Stratigraphic cross-section A (Woodbend and Winterburn Groups) 39
Figure 2-11b Stratigraphic cross-section B (Woodbend and Winterburn Groups) 41
Figure 2-12 Schematic structural cross-section across the Obed area 49
Figure 2-13 Shematic diagram of Jasper Basin stratigraphy and nomenclature 52
Figure 2-14 Schematic stratigraphic cross-section across the Obed area 54
Figure 3-1 Obed study area, west-central Alberta 61
Figure 3-2 Obed platform geometry and well and core control 63
Figure 3-3 Schematic structural cross-section across the Obed area 65
Figure 3-4 Swan Hills burial history curve 68
Figure 3-5 Schematic stratigraphic cross-section across the Obed area 70
Figure 3-6 Paragenetic sequence 74
Figure 3-7 Photos of replacive dolomite matrix and planar dolomite cements 77
Figure 3-8 Photos of saddle dolomite cements 79
Figure 3-9 Photos of early replacive calcite and late calcite cements 82
Figure 3-10 Photos of primary anhydrite and anhydrite replacements and cement 85
Figure 3-11 Pyrite photos 87

Figure 3-12 Native sulfur photos 90
Figure 3-13 Reaction scheme for bacterial and thermochemical sulfate reduction 94
Figure 3-14 Plot of $\delta^{13}C$ versus $\delta^{18}O$ for calcites and dolomites of Obed 100
Figure 3-15 Plot of $^{87}Sr/^{86}Sr$ versus $\delta^{18}O$ for calcites and dolomites of Obed 102
Figure 3-16 Plot of $\delta^{34}S$ versus $\delta^{18}O$ for Nisku anhydrites 105
Figure 3-17 Plot of $\delta^{34}S$ versus $\delta^{18}O$ for Obed anhydrites 107
Figure 3-18 Plot of depth below Graminia versus $\delta^{34}S$ of Obed pyrite 110
Figure 3-19 Plot of depth below Graminia versus $\delta^{34}S$ of Obed native sulfur 113

LIST OF TABLES

Table A-1 List of wells with core in the Obed area 128
Table B-1 Calcite geochemistry 131
Table B-2 Dolomite geochemistry 135
Table B-3 Anhydrite geochemistry 137
Table B-4 Pyrite geochemistry 141
Table B-5 Native sulfur geochemistry 144

What does the "D" stand for in "D-day"?

CHAPTER 1:
GENERAL INTRODUCTION

Late Frasnian (Upper Devonian) reef complexes in the subsurface of the Whitecourt area in west-central Alberta are host to several groups of hydrocarbon reservoirs. The Obed field, situated in the area of Townships 52-55 and Ranges 21-24 W5M (Figure 1-1), was discovered in 1964 by Imperial Oil. It is located on the margin of the Wild River sub-basin (Switzer *et al.*, 1994), surrounded by other Devonian carbonate reef complexes including Simonette, Bigstone, and Windfall, and is a promontory of the Southesk-Cairn carbonate complex (Figure 1-2). The Obed reef complex is host to the designated D2A and D3 hydrogen sulfide gas pools (approximately 20-30% H_2S; Energy Resources Conservation Board, 1992). The study area (Townships 52-55, Ranges 21-24W5M) encompasses these pools, which are situated in the updip portion of the complex (Figures 1-2 and 1-3).

The comprehension of the stratigraphic framework and associated depositional facies of the Late Devonian strata in the Obed area is required to contribute to the understanding of the spatial distribution and geochemical signatures of primary (syn-depositional) anhydrite and early calcite and dolomite, as well as secondary (post-depositional) anhydrite, early and late diagenetic pyrite, and late elemental sulphur, dolomite cement, and calcite cement and replacement. The geology of the Obed field and seismic and production data are briefly outlined in the Geophysical Atlas of Western Canadian Hydrocarbon Pools (Anderson *et al.*, 1989), and the Geological Atlas of the Western Canada Sedimentary Basin (Mossop and Shetsen, 1994) provides an overview of the Devonian Woodbend and Winterburn strata. No detailed depositional facies information, petrography, or stratigraphic framework is provided, nor are there any geochemical analyses and interpretations in these sources.

This study attempts to provide a comprehensive interpretation of the diagenetic history of the Obed area in the framework of its complex stratigraphy. Petrographic and geochemical studies, involving stable (carbon, oxygen, sulfur) and radiogenic (strontium) isotope analyses of the carbonates (calcite, dolomite), sulfides, and sulfates are

Figure 1-1 Obed study area, west-central Alberta, encompassing Townships 52 to and Ranges 21 to 24 W5M.

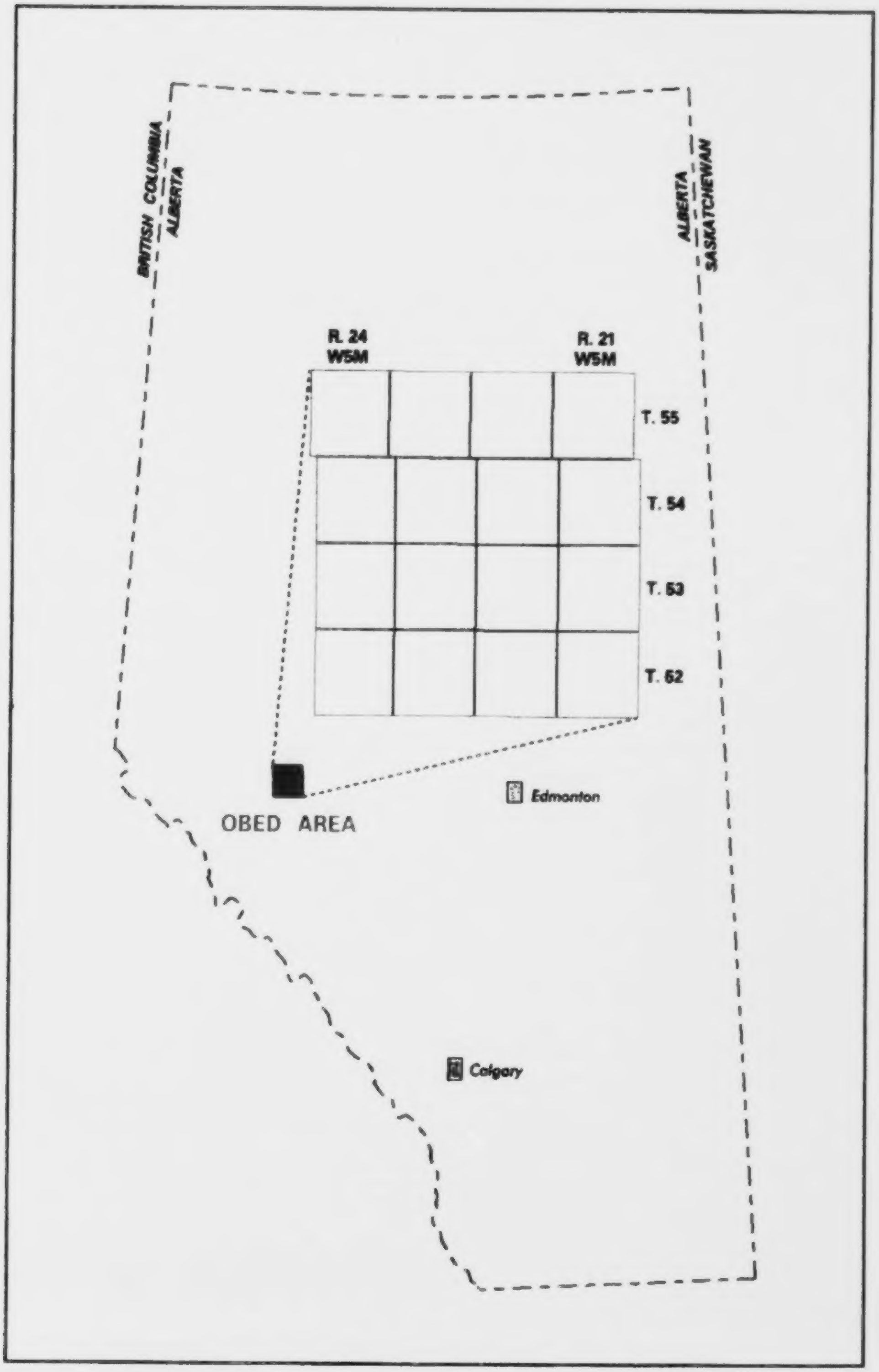
BRITISH COLUMBIA
ALBERTA
ALBERTA
SASKATCHEWAN
R. 24 W5M
R. 21 W5M
T. 55
T. 54
T. 53
T. 52
OBED AREA
Edmonton
Calgary

Figure 1-2 Major Woodbend reef complexes and basins in the Obed area, west-central Alberta (modified after Switzer *et al.*, 1994). Palinspastically restored areas are modified from Andrews (1987).

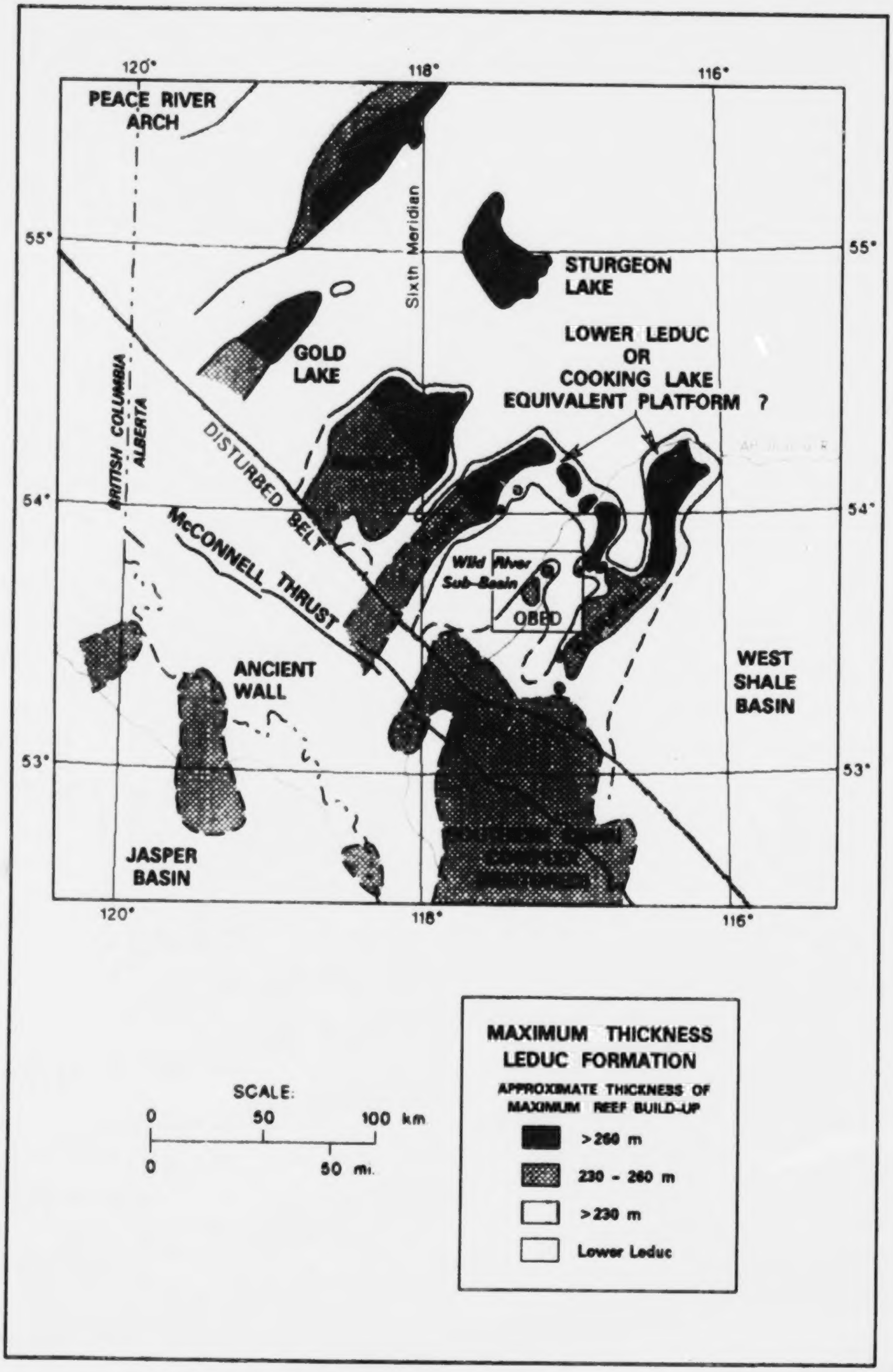
120°
118°
116°
55°
54°
53°
PEACE RIVER ARCH
Sixth Meridian
STURGEON LAKE
GOLD LAKE
LOWER LEDUC OR COOKING LAKE EQUIVALENT PLATFORM ?
BRITISH COLUMBIA
ALBERTA
DISTURBED BELT
McCONNELL THRUST
Wild River Sub-Basin
OBED
WEST SHALE BASIN
ANCIENT WALL
JASPER BASIN
MAXIMUM THICKNESS LEDUC FORMATION
APPROXIMATE THICKNESS OF MAXIMUM REEF BUILD-UP
>260 m
230 - 260 m
>230 m
Lower Leduc
SCALE:
0
50
100 km
0
50 mi.

Figure 1-3 Obed study area showing Leduc platform geometry and well control.

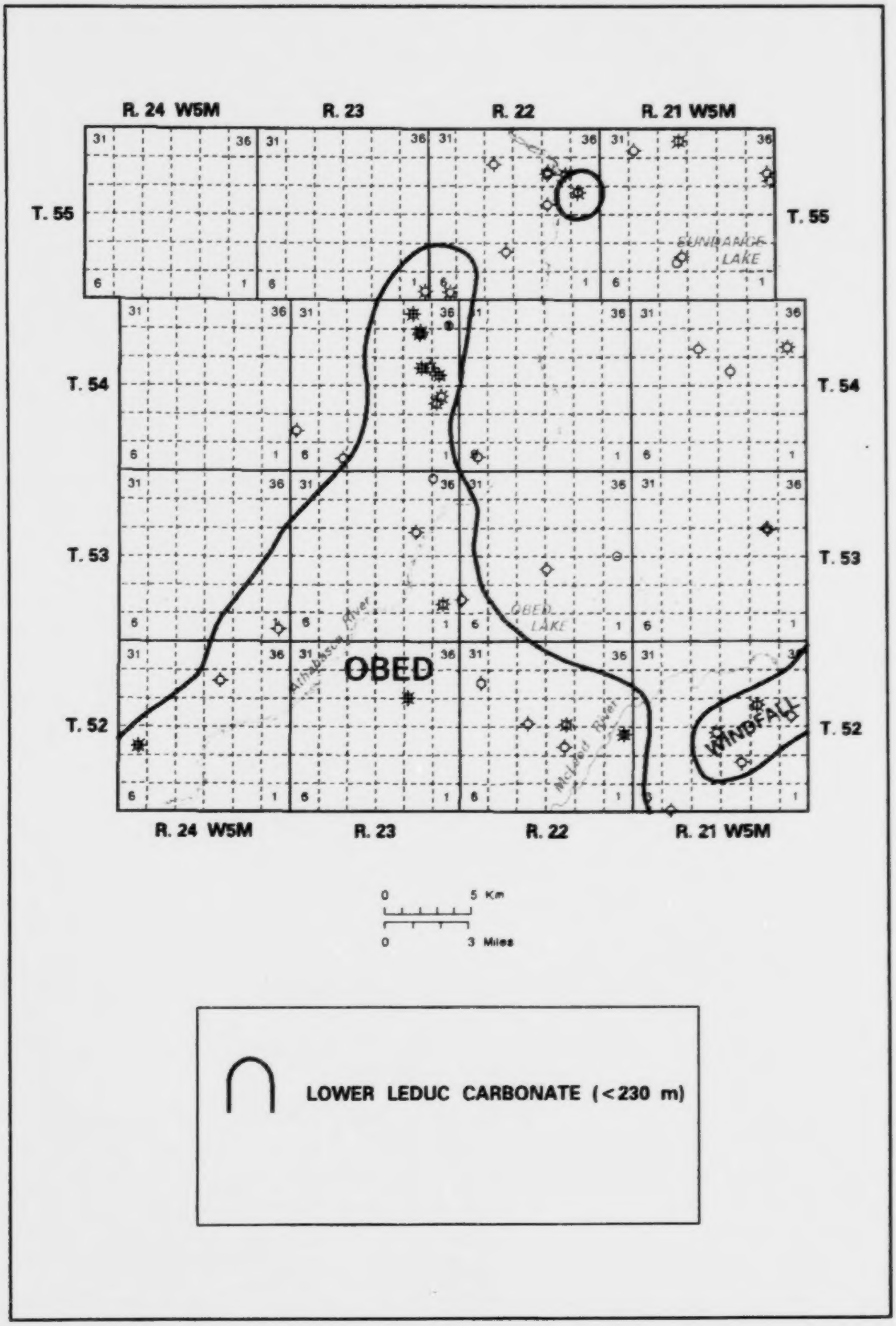
R. 24 W5M
R. 23
R. 22
R. 21 W5M
T. 55
T. 54
T. 53
T. 52
SUNDANCE LAKE
OBED LAKE
Athabasca River
McLeod River
OBED
WINDFALL
0 5 Km
0 3 Miles
LOWER LEDUC CARBONATE (<230 m)

documented. The main objective is to constrain their origin in relation to timing and geochemical processes involving bacterial sulfate reduction (BSR) and thermochemical sulphate reduction (TSR) in strata of the Winterburn Group (Blueridge Member) and Woodbend Group (Leduc Formation).

This thesis is comprised of four chapters, with Chapter 1 being a general introduction. Chapter 2 and Chapter 3 are written as self-contained manuscripts. Chapter 2 is entitled "Depositional facies and stratigraphy of the Upper Devonian carbonates in the Obed area, west-central Alberta". It is a compilation of mapping and descriptions of the different reefal and reef proximal facies, as well as a detailed description of the stratigraphic framework. Chapter 3 is entitled "Diagenesis of the Upper Devonian carbonates in the Obed area, west-central Alberta", with an emphasis on the geochemistry of diagenetic phases such as carbonates (calcite and dolomite), anhydrite, pyrite, and elemental sulfur. Chapter 4 consists of conclusions derived from Chapters 2 and 3. The two papers which comprise the main body of this thesis provide original information about the Devonian carbonates of the Obed area and are useful in the characterization of these reservoirs. This information may be applied to other carbonate complexes in this and other parts of the Western Canada Sedimentary Basin.

REFERENCES

Anderson, N.L., Hills, L.V., Cederwall, D.A. (editors), 1989, Geophysical Atlas of Western Canadian Hydrocarbon Pools, Alberta Research Council, 344p.

Andrews, G.D., 1987, Devonian Leduc outcrop reef-edge models and their potential seismic expression, *In* Devonian of the World, Proceedings of the Second International Symposium on the Devonian System, N.M., McMillan, A.F. Embry, and D.J. Glass (*eds.*), Can. Soc. Petrol. Geol., Memoir 14, v. II, p. 427-450.

Energy Resources Conservation Board, 1993, Alberta's reserves of crude oil, oil sands, gas, natural gas liquids and sulphur (December 31, 1992), Report Series ERCB93-18, 32nd Edition, Alberta Energy Conservation Board, Calgary, Alberta.

Mossop, G.D, and Shetsen, I. (compilers), 1994, Geologic Atlas of the Western Canada Sedimentary Basin. Calgary, Canadian Society of Petroleum Geologists and Alberta Research Council, 510p.

Switzer, S.B., Holland, W.G., Christie, D.S., Graf, G.C., Hedinger, A.S., McAuley, R.J., Wierzbicki, R.A., Packard, J.J., 1994, Devonian Woodbend-Winterburn strata of the Western Canada Sedimentary Basin. *In* Geologic Atlas of the Western Canada Sedimentary Basin. G.D. Mossop and I. Shetsen (compilers), Canadian Society of Petroleum Geologists and Alberta Research Council (Calgary), p. 165-195.

CHAPTER 2:

Depositional facies and stratigraphy of the Upper Devonian carbonates in the Obed area, west-central Alberta

ABSTRACT

An understanding of the stratigraphic framework and the associated depositional facies of the Frasnian carbonates of the Obed area, west-central Alberta, is necessary for the understanding of their reservoir characteristics. Reservoir facies include dolomitized grainstone to fossil floatstone/rudstone of the back-reef, reef crest, and reef slope environments in the Leduc Formation (Woodbend Group) and Lower Blueridge Member (Winterburn Group). The stratigraphy of the Obed area is complex. Mapping and reconstruction of the stratigraphy with the use of core descriptions has resulted in the recognition of seven westward prograding, shallowing upwards cycles in the Lower Blueridge Member, representative of reef to basin transitions. The stratigraphy in the subsurface of the Obed area is compared to that of Jasper Basin outcrops.

2.1. INTRODUCTION

The Woodbend and Winterburn Groups, both Frasnian in age (Figure 2-1) in the Obed area of west-central Alberta (Figure 2-2), contain reservoir units within the Leduc Formation and Blueridge Member (Graminia Formation), respectively, at depths greater than 3500m. The aim of this paper is to describe the depositional facies and stratigraphy of these reservoir units. The Nisku Formation also contains local intervals with reservoir potential. The Woodbend Group, comprising the Leduc Formation, Ireton Formation, source rock Duvernay Formation (Allan and Creaney, 1991), and the underlying Beaverhill Lake Group, consists principally of carbonate reef facies assemblages (Leduc and Beaverhill Lake) and shales (Ireton and Duvernay). The Winterburn Group overlies the Leduc and Ireton and is comprised of the Nisku Formation (carbonates, argillaceous carbonates and shale), Calmar Formation (green siltstone), Blueridge Member of the Graminia Formation (carbonates, argillaceous carbonates, and interbedded dolomite and anhydrite), and the uppermost Graminia Formation (siltstone). The Wabamun Group,

Figure 2-1 Table of formations and selected members of the Woodbend and Winterburn strata of Western Canada (Switzer *et al.*, 1994).

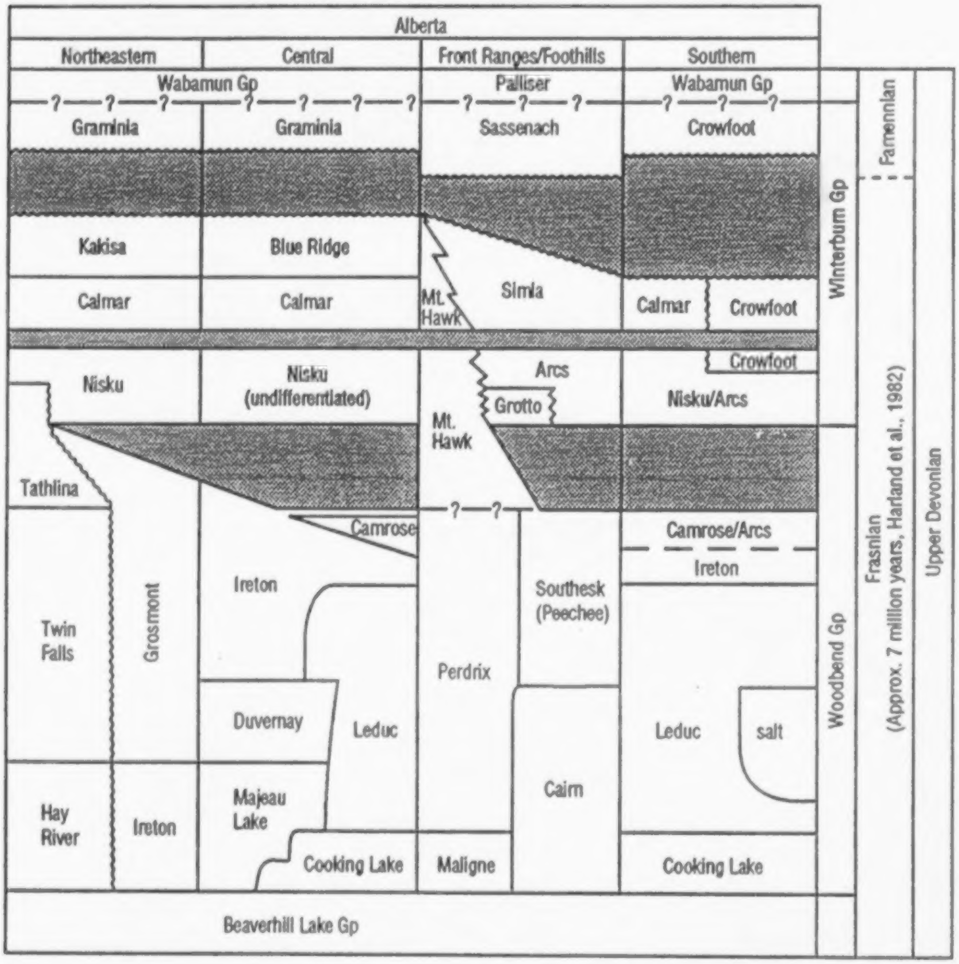
Alberta
Northeastern
Central
Front Ranges/Foothills
Southern
Wabamun Gp
Palliser
Wabamun Gp
Graminia
Graminia
Sassenach
Crowfoot
Kakisa
Blue Ridge
Simla
Mt. Hawk
Calmar
Calmar
Calmar
Crowfoot
Crowfoot
Nisku
Nisku (undifferentiated)
Arcs
Grotto
Nisku/Arcs
Mt. Hawk
Tathlina
Camrose
Camrose/Arcs
Ireton
Ireton
Twin Falls
Grosmont
Southesk (Peechee)
Perdrix
Duvernay
Leduc
Leduc
salt
Cairn
Hay River
Ireton
Majeau Lake
Cooking Lake
Maligne
Cooking Lake
Beaverhill Lake Gp
Winterburn Gp
Woodbend Gp
Famennian
Frasnian (Approx. 7 million years, Harland et al., 1982)
Upper Devonian

Figure 2-2 Obed study area, west-central Alberta, encompassing Townships 52 to 55 and Ranges 21 to 24 W5M.

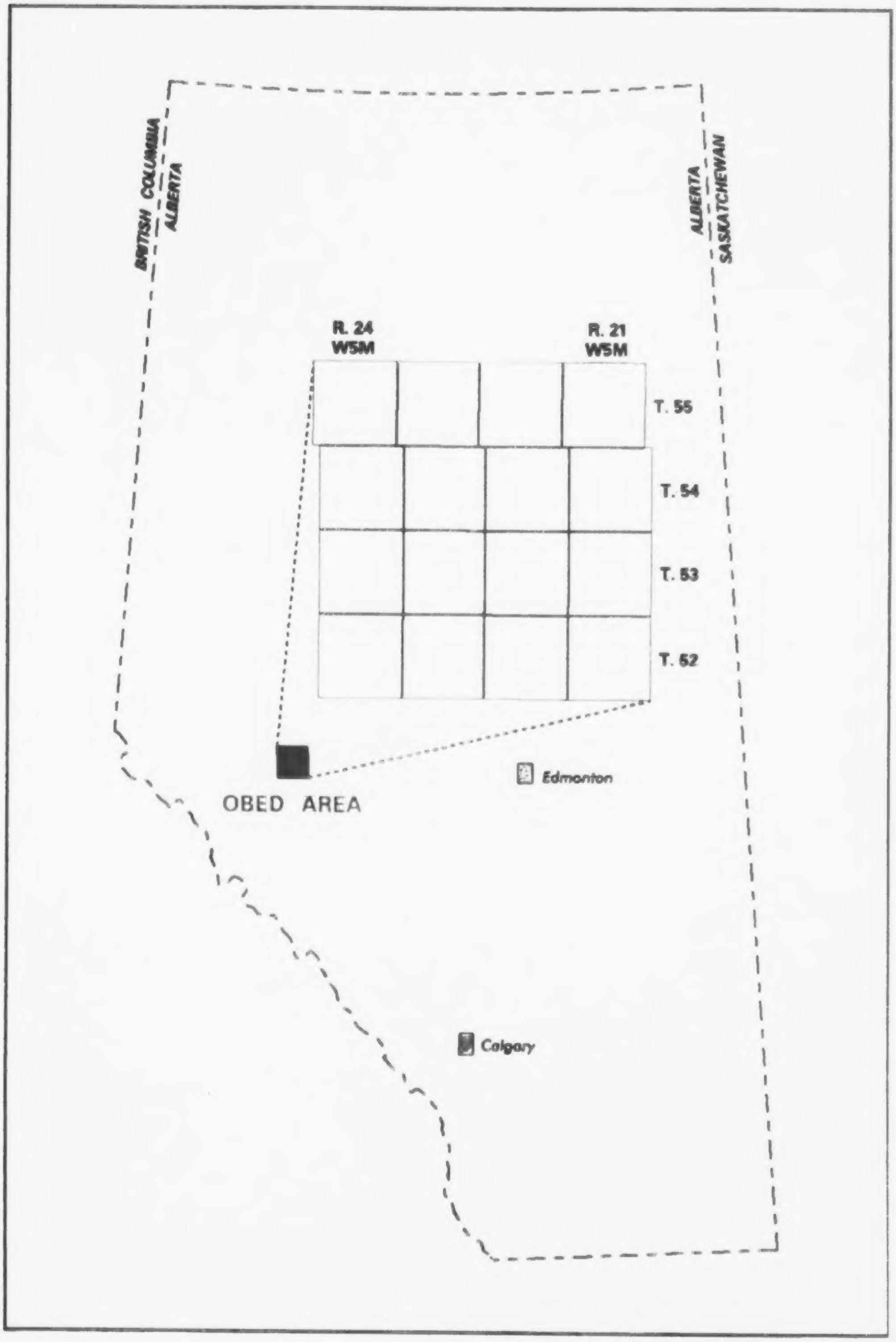
BRITISH COLUMBIA
ALBERTA
ALBERTA
SASKATCHEWAN
R. 24
W5M
R. 21
W5M
T. 55
T. 54
T. 53
T. 52
OBED AREA
Edmonton
Calgary

Famennian in age, overlies the Graminia Formation, and its erosional upper surface represents the top of the Devonian section.

2.2. PREVIOUS WORK AND METHODOLOGY

The geology of the Obed field and seismic and production data are briefly outlined in the Geophysical Atlas of Western Canadian Hydrocarbon Pools (Anderson *et al.*, 1989). The Geological Atlas of the Western Canada Sedimentary Basin provides an overview of the Devonian Woodbend and Winterburn strata (Switzer *et al.*, 1994). Otherwise, little has been published on this area. The Obed area is located on the margin of the Wild River sub-basin (Switzer *et al.*, 1994), surrounded by other Devonian carbonate reef complexes including Simonette, Bigstone, and Windfall, and is a promontory of the Southesk-Cairn carbonate complex (Figure 2-3).

For this study, mapping and stratigraphic interpretations were accomplished using cross-sections based on well log and core descriptions, where available (Figure 2-4). Although there are over 50 wells that penetrate the top of the Devonian section (Wabamun Group) in the Obed area, well control over the Obed platform is generally fair to poor. There are only 32 available cores (Appendix A) in the area, collectively representative of the Woodbend and Winterburn Groups. These cores were logged in detail and photographed at the Energy Resources Conservation Board (ERCB), Calgary. Over 700 core photos were taken of depositional facies characteristics, cements, and other sedimentary and diagenetic features, and over 300 core samples were obtained. The core sample depths recorded in this paper are the stratigraphic depths and have not been adjusted to true vertical depth, as the conversion factor is negligible. An allostratigraphic (North American Commission on Stratigraphic Nomenclature, 1984) approach to the stratigraphy is taken where possible to map and correlate discontinuity-bounded cycles of similar lithology.

2.3. REGIONAL GEOLOGIC SETTING

"Western Canada Sedimentary Basin" is the general name given to the wedge of sedimentary rocks that thickens to the west from the Canadian Shield in northeast Alberta

Figure 2-3 Major Woodbend reef complexes and basins in the Obed area, west-central Alberta (modified after Switzer *et al.*, 1994). Palinspastically restored areas are modified from Andrews (1987).

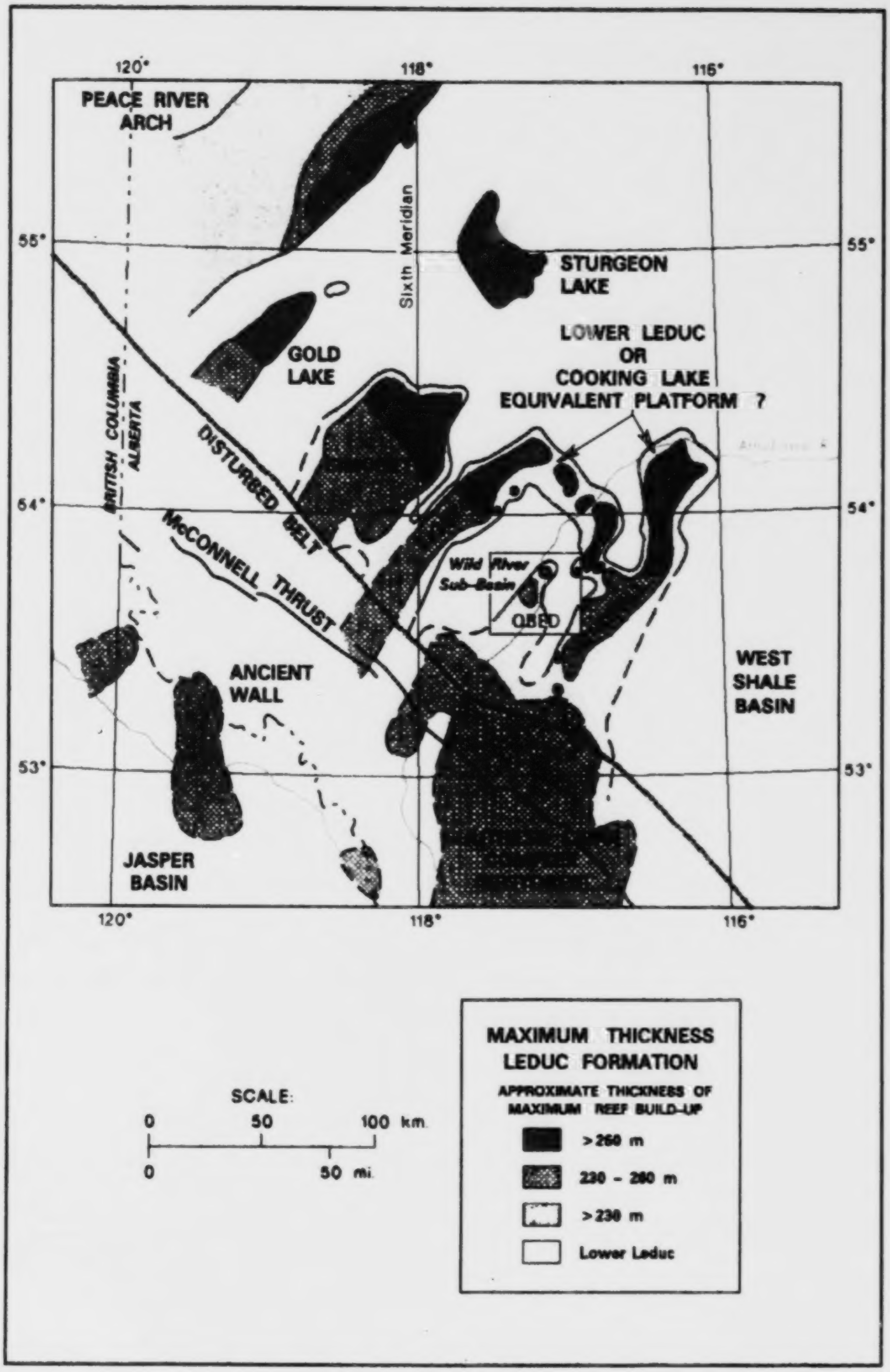
120°
118°
116°
55°
54°
53°
PEACE RIVER ARCH
Sixth Meridian
STURGEON LAKE
GOLD LAKE
LOWER LEDUC OR COOKING LAKE EQUIVALENT PLATFORM ?
BRITISH COLUMBIA
ALBERTA
DISTURBED BELT
McCONNELL THRUST
Wild River Sub-Basin
OBED
ANCIENT WALL
WEST SHALE BASIN
JASPER BASIN
SCALE:
0
50
100 km.
0
50 mi.
MAXIMUM THICKNESS LEDUC FORMATION
APPROXIMATE THICKNESS OF MAXIMUM REEF BUILD-UP
■ >260 m
▨ 230 - 260 m
☐ >230 m
☐ Lower Leduc

Figure 2-4 Obed study area showing Leduc platform geometry, well control, wells with core, and stratigraphic cross-section lines.

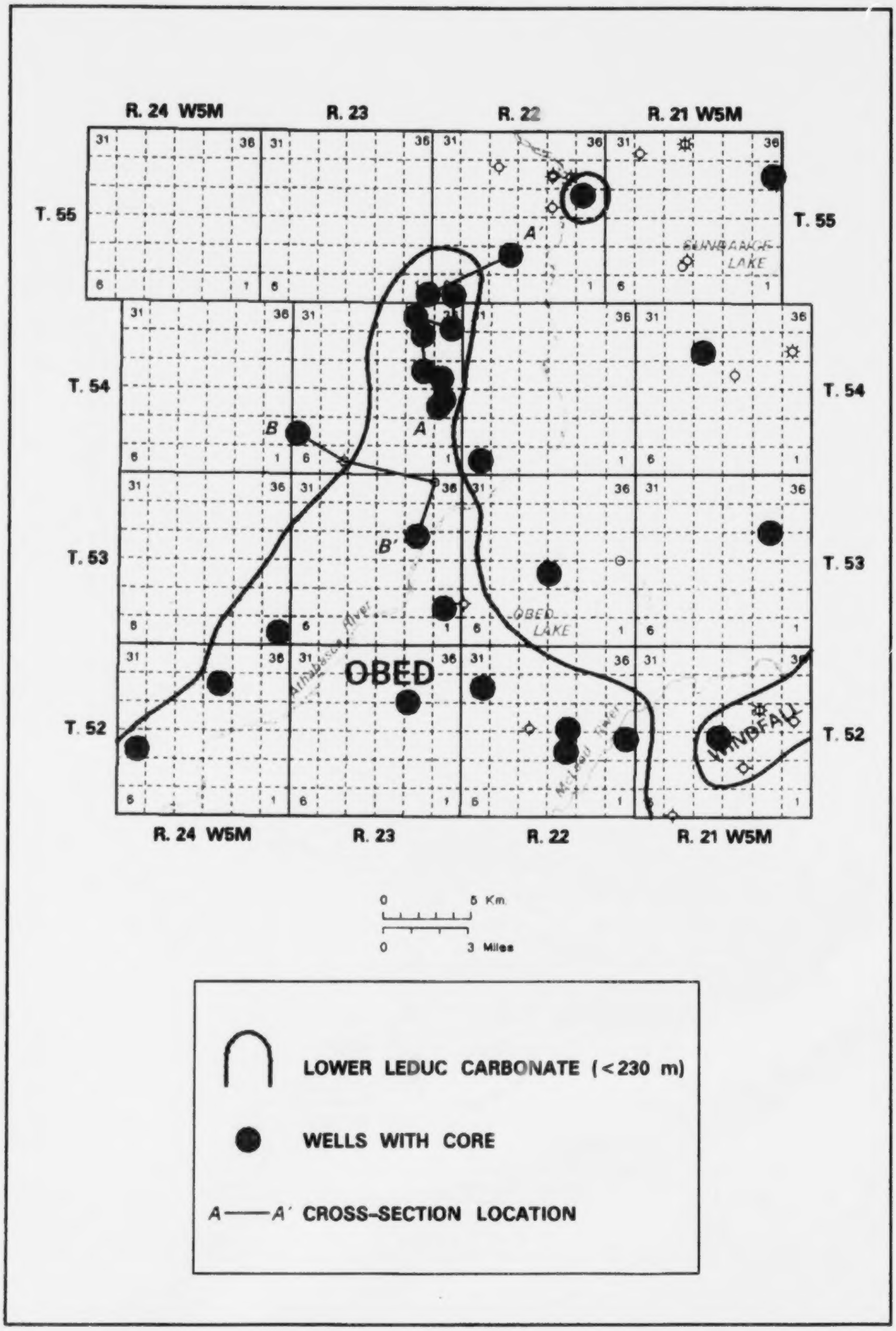
R. 24 W5M
R. 23
R. 22
R. 21 W5M
T. 55
T. 54
T. 53
T. 52
31
36
6
1
A
A'
B
B'
SUNDANCE LAKE
OBED LAKE
Athabasca River
McLeod River
OBED
WINDFALL
0
5 Km
0
3 Miles
LOWER LEDUC CARBONATE (<230 m)
WELLS WITH CORE
A——A' CROSS-SECTION LOCATION

to the Rocky Mountain tectonic belt (Ricketts, 1989). The Devonian Obed reef complex lies stratigraphically at approximately 4000m depth in the subsurface of west-central Alberta within the Western Canada Sedimentary Basin (Figure 2-2). For this study, the strata of interest are within the Woodbend (Leduc Formation) and Winterburn (Blueridge Member) Groups. These groups lie between the Beaverhill Lake and Wabamun Groups, and contain several distinct chronostratigraphic intervals composed largely of cyclic carbonate deposits, separated by reefal and argillaceous carbonates of the Nisku Formation and shale and argillaceous carbonates of the Ireton Formation (Switzer *et al.*, 1994).

During deposition of the Beaverhill Lake Group, western Canada was covered by a broad epicontinental sea which underwent several transgressive and regressive phases. To the northwest of the study area, the Peace River Arch and part of the Western Alberta Ridge stood out as prominent landmasses (Fischbuch, 1968). Open marine conditions in Woodbend and Winterburn time led to reef growth in Leduc, Nisku, and Blueridge time.

2.4. DEPOSITIONAL FACIES AND ENVIRONMENTS

Numerous models have been proposed to account for reef growth and zonations (eg. Wilson, 1975; James, 1983; James and Bourque, 1992; Burchette, 1981; Machel, 1990; Machel and Hunter, 1994). A reef can be defined as a distinctive biofacies with genetically associated detrital material (Fishbuch, 1968). Reef size and shape is dependent on prevailing winds and water current direction, character of the substrate, post-depositional erosion, and relationship to adjacent carbonate bodies. The geometry of the basal platform and its paleotopography determine where buildups occur. Due to variations in sea level and the energy of the environment, different environments persist with characteristic facies constituents.

The principal factors in the recognition of the facies present in each environment are the dominant fossil (or other biochem) type and depositional texture. Despite alteration and modification by dolomitization, biochems and depositional textures can often be recognized, and there is preservation of primary fossil structures and texture locally. The core availability in the Obed area is sufficient to allow an understanding of the facies of the reef complex. Correlation of the reef facies with their laterally equivalent off-reef facies is possible within the Winterburn Group (Lower Blueridge Member). However, because of the variety of facies types produced by fluctuations in relative sealevel, and because of sparse well control over the platform, it is difficult to make meaningful associations.

For this study, the basic paleoenvironment zonations of back-reef, reef core, and fore-reef (Fischbuch, 1968; James, 1983; Machel and Hunter, 1994) have been used as a foundation for describing the Obed reef complex. Facies include tidal flat, lagoon, back-reef, reef crest, reef slope, reef front, and basin (labelled A to G, respectively; Figure 2-5). These facies are common to all reefal environments of the Woodbend and Winterburn Groups. Since the Upper Blueridge (dominantly supratidal-intertidal) facies is not directly influenced by reefal environments, it is not included as a facies zonation in Figure 2-5 and is described separately. The classification of Embry and Klovan (1972), modified after Dunham (1962; Figure 2-6), is used to describe the facies present in each facies zone.

2.4.1. Tidal Flat (Facies A)

The shallow tidal flat is a low energy environment with dark grey to light grey/brown packstone/wackestone to mudstone/grainstone facies. This sediment is commonly dolomitized and is massive to laminated (parallel and anastomosing; A, Figure 2-7); grey-green mudstone is also present locally. Locally, there are occurrences of an *Amphipora* floatstone facies where storms have washed *Amphipora* fragments and other reefal debris, such as crinoids, brachiopods, corals, and stromatoporoid fragments, into this environment from the lagoon and reef. Up to 15% biochems may occur in this facies, which constitute the fossil (type of fossil depends on which is dominant) rudstones in some locations.

The porosity in this facies is generally low, varying from up to 5%, where a mud matrix is present, to 10% where the sediment is grain supported or biochems are present. Intercrystalline porosity is the main porosity type, with the occurrence of moldic and rare vuggy porosity where biochems have been dissolved. Moldic porosity is present where there has been leaching of *Amphipora*. These facies may contain fenestral textures (B,

Figure 2-5 Reef model showing zonations of depositional environments and associated facies A to G (see text for descriptions).

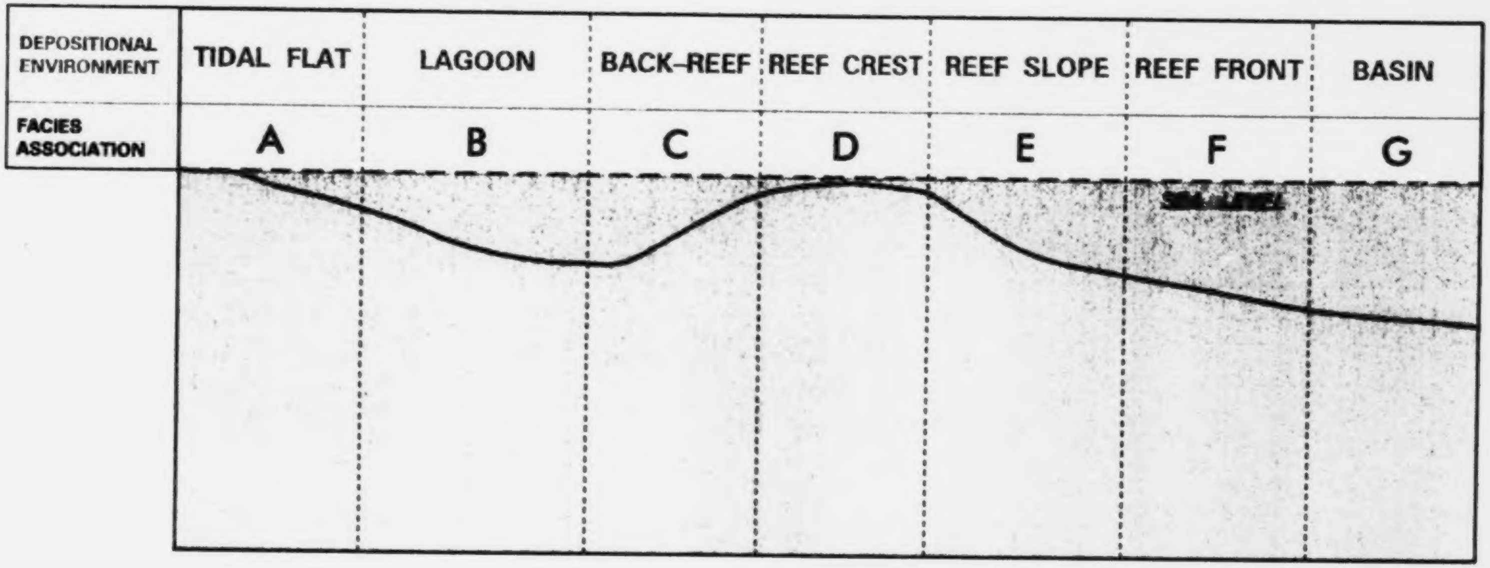
DEPOSITIONAL ENVIRONMENT
TIDAL FLAT
LAGOON
BACK-REEF
REEF CREST
REEF SLOPE
REEF FRONT
BASIN
FACIES ASSOCIATION
A
B
C
D
E
F
G
SEA LEVEL

Figure 2-6 Facies classification of Embry and Klovan (1972) modified after Dunham (1962).

DUNHAM (1962)				EMBRY & KLOVAN (1971)				
Original components not bound during deposition						Original components organically bound during deposition		
Contains mud, (clay- & silt-size carbonate)				More than 10% grains greater than 2 mm				
Mud-supported		Grain-support						
Less than 10% grains	More than 10% grains		Lacks mud and is grain supported	Matrix supported	Clast supported	by organisms which act as baffles	by organisms which encrust and bind	by organisms which build a rigid framework
MUDSTONE	**WACKESTONE**	**PACKSTONE**	**GRAINSTONE**	**FLOATSTONE**	**RUDSTONE**	**BAFFLESTONE**	**BINDSTONE**	**FRAMESTONE**
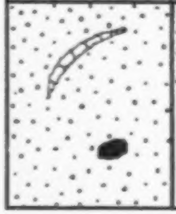	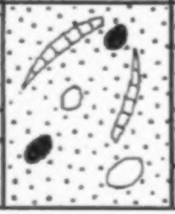	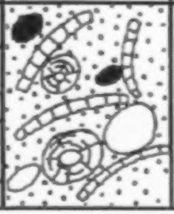	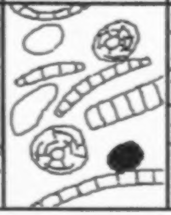	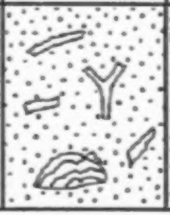	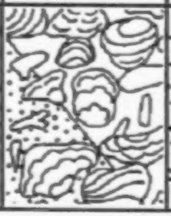	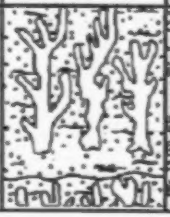	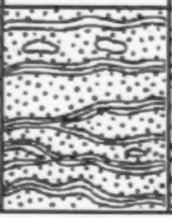	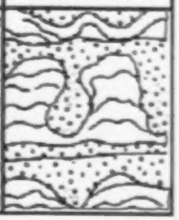

Figure 2-7 A. Light brown to light grey mudstone with parallel to anastomosing laminations; tidal flat (facies A; hand sample 5-23-55-22W5; 12862.8′).
B. Light grey grainstone with moldic porosity and fenestral textures; tidal flat (facies A; hand sample 11-35-54-23W5; 13826′).
C. Light brown to light grey *Amphipora* packstone to grainstone; lagoon (facies B; hand sample 11-35-54-23W5; 13854.5′).
D. Light brown *Amphipora* packstone with anastomosing laminations; lagoon (facies B; hand sample 5-23-55-22W5; 12751′).

Figure 2-7) due to the former presence of algal mats; algal laminations occur locally.

Also present locally is evidence of bioturbation and soft sediment deformation. The rock of this facies is relatively competent with minor fractures (horizontal, inclined, and vertical; up to 0.5cm thick, >7cm long) and tension gashes (2mm thick). Fracturing sometimes occurs along the wispy (1mm thick) stylolites, which are commonly associated with the anastomosing laminations. The tidal flat environment commonly alternates with the lagoon and back-reef environments.

2.4.2. Lagoon (Facies B)

The lagoon environment occurs in shallow, slightly agitated waters and is characterized by the dominance of *Amphipora*. The facies is generally a light brown to light grey *Amphipora* floatstone/rudstone to a mudstone/packstone or grainstone (C and D, Figure 2-7). There may be several fossil accessories due to the presence of debris from the reef crest and proximal areas. Biochems, comprising 5% to locally up to 50% of the sediment, include abundant *Amphipora* (locally large, 0.5cm diameter), *Euryamphipora*, stromatoporoids (*Stachyodes* up to 1cm), crinoids (locally large, 0.5-1.0cm), gastropods, brachiopods, and corals. The sediment may show wavy or parallel laminations, as well as bioturbation and burrowing. This facies has been dolomitized and the observed porosity is variable, ranging from very low to 20%. Intercrystalline porosity is common, as is moldic porosity due to the leaching of *Amphipora*; vuggy porosities are also present, but rare. Generally, permeability is low since porous *Amphipora* skeletons are not interconnected and the matrix mud percentage is high. Fenestral texture is present locally.

2.4.3. Back-reef (Facies C)

The back-reef is an area of moderately agitated waters, and generally contains abundant reef crest and lagoonal debris. The main facies present is a dolomitized, light to medium grey fossil floatstone/rudstone to grainstone (A and B, Figure 2-8). Fossil occurrences of *Stachyodes* and other fossil debris, including tabular stromatoporoid and bulbous stromatoporoid fragments, crinoids, *Amphipora* and *Euryamphipora*, characterize the back-reef environment. Corals, including *Syringopora* and *Thamnopora*, as well as

Figure 2-8 A. Light grey fossil (*Stachyodes*, coral, stromatoporoids, *Amphipora*) floatstone/rudstone; back-reef (facies C; hand sample 15-26-54-23W5; 13363.5′).

B. Light grey fossil (*Stachyodes*, coral (?), *Amphipora*) floatstone; back-reef (facies C; hand sample 10-13-52-22W5; 4373.7m).

C. Medium grey fossil (tabular stromatoporoid) floatstone/rudstone; reef crest (facies D; hand sample 11-13-54-23W5; 4016.4m).

D. Light grey fossil (bulbous stromatoporoid) floatstone; reef crest (facies D; hand sample 2-36-54-23W5; 13392′).

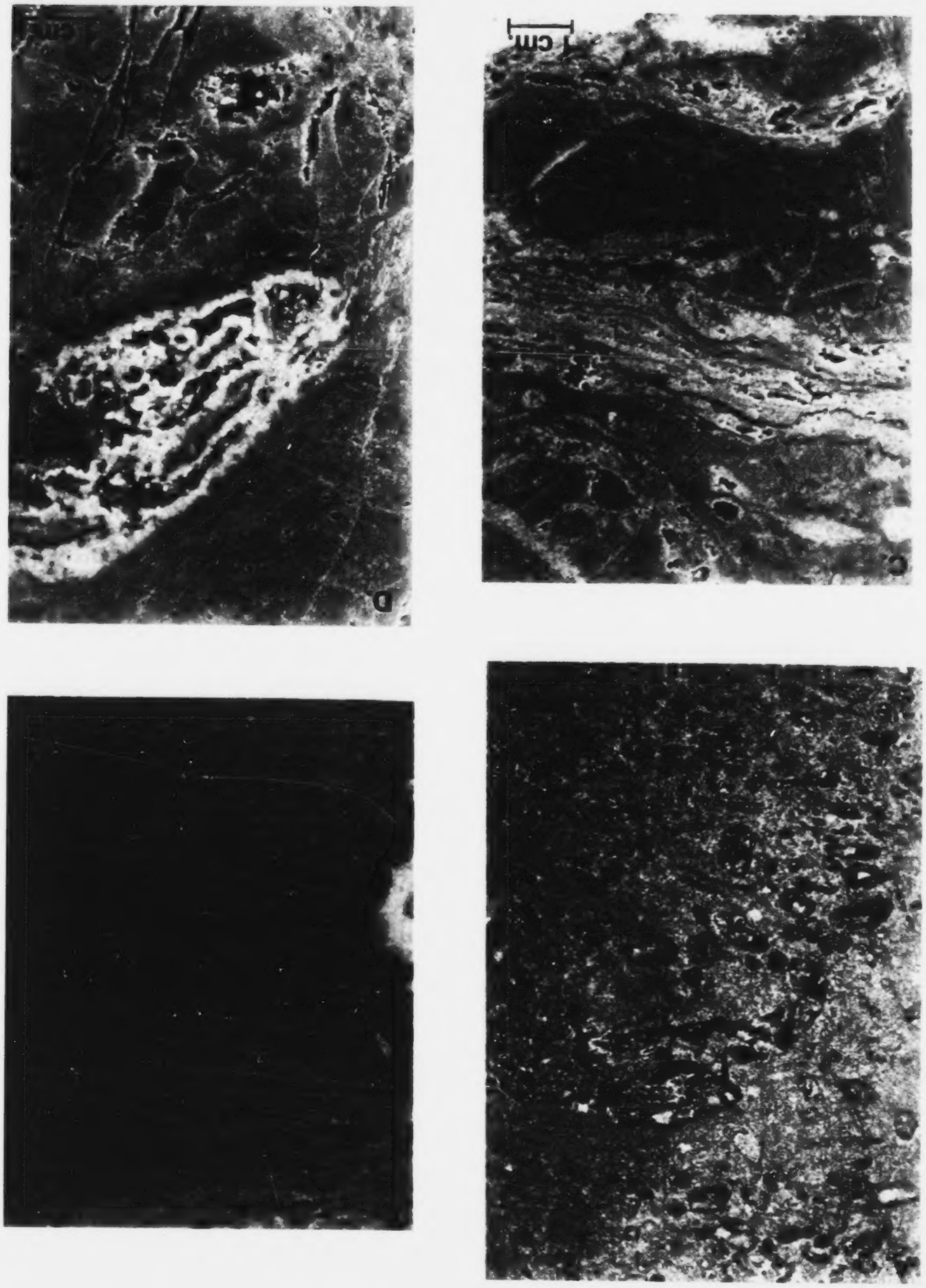
1 cm
D
1 cm
C

shell debris may also be present. These biochems comprise 40-80% of the sediment. Observed porosity in the Obed area is variable, ranging from 2% to 20%. Intercrystalline porosity is most common, with moldic and vuggy porosity present where fossil fragments have been leached. Anastomosing laminations are common with evidence locally of bioturbation, boring, and inclined bedding. This back-reef facies is very similar to the reef slope in front of the reef crest, but is less chaotic.

2.4.4. Reef Crest (Facies D)

The Woodbend and Winterburn high-energy reef crest environment present at Obed consists of medium grey to light brown, dolomitized, fossil floatstones and rudstones. Fossil framestones and a packstone/grainstone matrix are also common locally. The dominance of *in situ* tabular, bulbous, and hemispherical stromatoporoids (C and D, Figure 2-8) is the main criterion for recognizing the reef crest environment. Stromatoporoids are the most important frame-building organisms and appear to be in growth position locally, but are often fragmented. The range in size and shape of the fragments indicate only limited transport. Most tabular stromatoporoids, on the other hand, appear to be in place but are also found fragmented locally. Also common are *Stachyodes*, crinoids, *Amphipora*, *Euryamphipora*, as well as rugose, colonial (*Syringopora*), and/or *Thamnopora* corals. Brachiopods may also be present. These biochems can comprise up to 50% of the sediment in the Winterburn Group, and up to 90% of the sediment in the Woodbend Group. In the Obed area, there is very little mud in the facies characteristic of the reef crest environment, and reservoir rock has good intercrystalline, as well as leached moldic (1mm-1cm) and vuggy (2cm-0.5m), porosity ranging up to 25%.

2.4.5. Reef Slope (Facies E)

The slope environment is generally a moderate to high energy environment resulting in the deposition of reef rubble due to the water agitation proximal to the reef and local transport of reefal organisms. This zone displays a mixed lithology with skeletal debris and consists of a medium grey to light brown fossil floatstone/rudstone to grainstone facies (A and B, Figure 2-9); a packstone to wackestone matrix is present

Figure 2-9 A. Light brown fossil (bulbous stromatoporoid, coral) floatstone; reef slope (facies E; hand sample 8-6-55-22W5; 4021.5m).
B. Light brown to light grey fossil (coral, *Amphipora*) floatstone to rudstone; reef slope (facies E; hand sample 2-36-54-23W5; 13424').
C. Medium grey coral (*Syringopora*) floatstone to rudstone; reef slope (facies E; hand sample 8-6-55-22W5; 4015.8m).
D. Light grey crinoid packstone; storm deposit, reef slope (facies E; hand sample 8-6-55-22W5; 4015.3m).

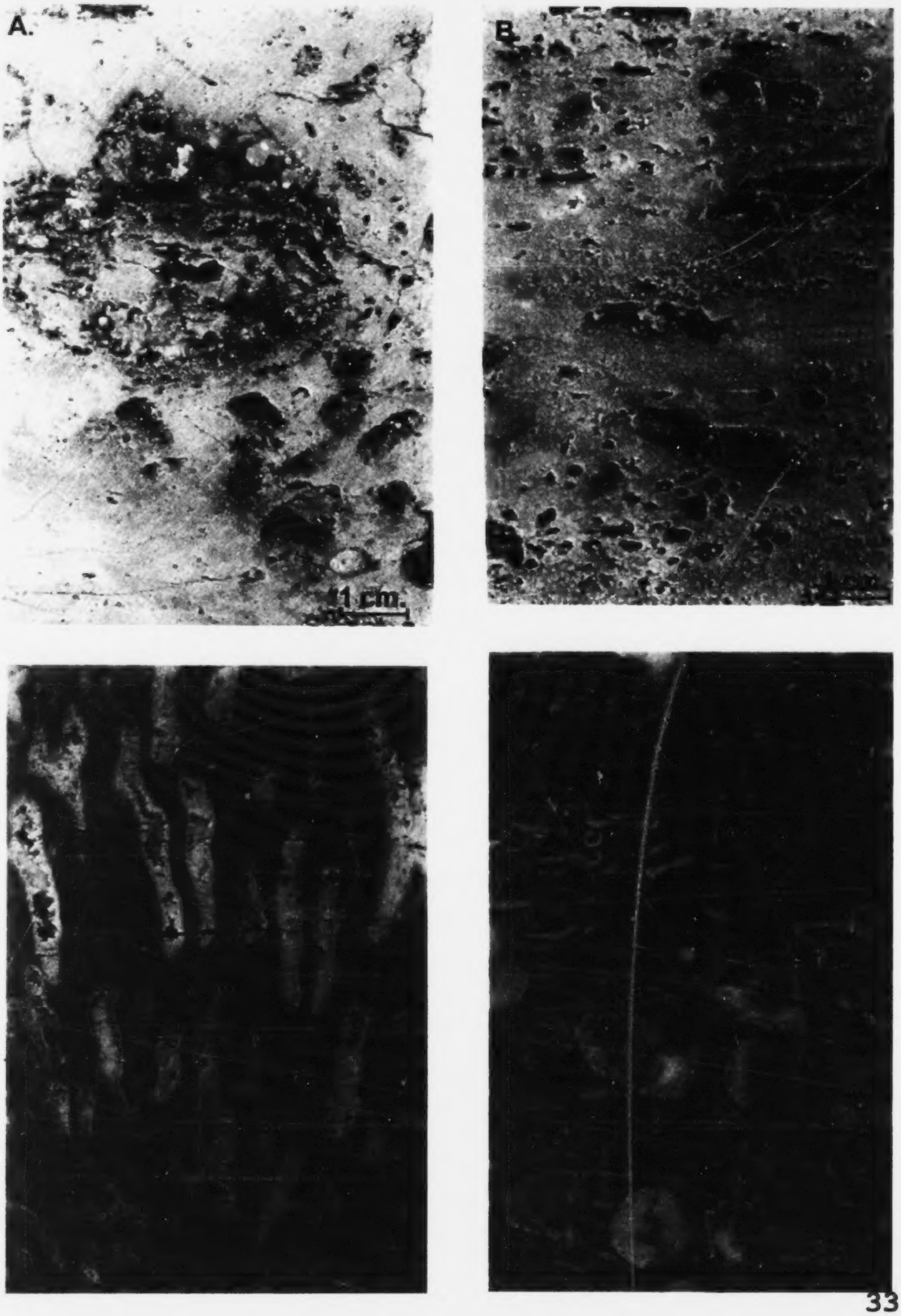
A.
1 cm.
B.

locally. Fossils, and fossil fragments, common to this zone are bulbous, hemispherical, and tabular stromatoporoids with local *Stachyodes*, large *Amphipora* (up to 0.5cm), and *Euryamphipora* (1mm) in a mudstone to grainstone matrix. Also common are large crinoid (up to 8cm long, 1cm wide), shell (brachiopod, gastropod), and coral (*Thamnopora*, *Syringopora*) intraclasts (C and D, Figure 2-9). The biochems comprise up to 40% of the sediment in the Lower Blueridge Member, and 60-90% of the sediment in the Leduc Formation. There is local evidence of bioturbation. This facies is dolomitized and is very complex with variable grain sizes. The sediment may be brecciated, and anastomosing laminations are present locally. Intercrystalline and moldic (mm-cm size) porosity development is common, with local vuggy (up to >7cm) pores. Moldic porosity is present where *Amphipora* has been leached. The porosity varies cosiderably from 5% to 20% and permeability appears to be very high.

2.4.6. Reef Front (Facies F)

The reef front, or lower reef slope, environment was slightly to intermittently (due to storm activity) agitated, yet with relatively high mud content. The mud matrix is massive (structureless) to finely laminated (anastomosing), with the local occurrence of mudclasts and bioturbation. Where dolomitized, the reef front facies is commonly a medium to dark grey mudstone to a fossil floatstone, with rare occurrences of a fossil rudstone or grainstone (A. and B., Figure 2-10). Crinoids (up to 0.5cm) and brachiopods are common. In areas relatively proximal to the reef, there may be up to 30% biochems which include corals (*Thamnopora*, *Syringopora*), brachiopods, *Amphipora* and *Euryamphipora*, as well as reef talus with larger skeletal debris such as stromatoporoid fragments. With increasing distance from the reef, the color of the matrix becomes darker and the number of biochems decreases. The percentage of fossil constituents varies from 2% to locally greater than 15%. The observed porosity is generally very low (nil to 3%), with local moderate porosity of 5 to 10% where moldic (1mm to 1cm), vuggy (up to 10cm), and rare intercrystalline porosity is present; permeability is also very poor.

Figure 2-10 A. Medium to dark grey mudstone to coral floatstone; reef front (facies F; hand sample 02/15-26-54-23W5; 4122.7m).

B. Medium grey coral (*Thamnopora*) floatstone; reef front (facies F; hand sample 9-23-54-23W5; 3961m).

C. Dark grey nodular lime mudstone with anastomosing laminations; basinal (facies G; hand sample 12-15-53-22W5; 13187.2').

D. Laminated (anastomosing) lime mudstone; basinal (facies G; hand sample 15-23-53-21W5; 4035.8m).

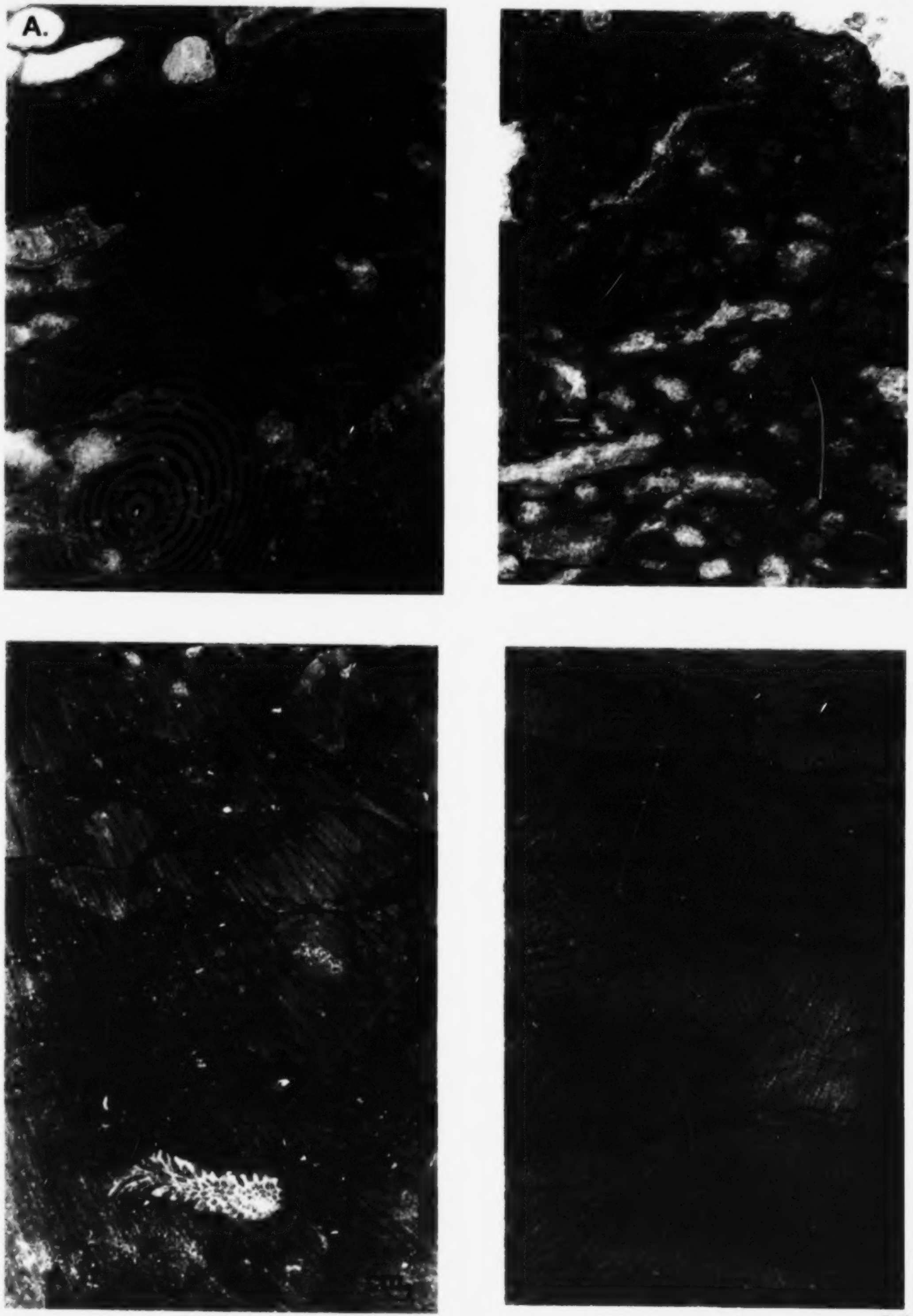
A.

2.4.7. Basinal (Facies G)

The basinal environment is one of quiet water with sediment deposition below wave base. In the basin of the Obed area, green to brown lime mudstone facies is dominant in this zone, with local rare occurrences of the wackestone/floatstone facies. These facies generally have a nodular to mottled texture (sedimentary boudinage structures) with anastomosing laminations (C and D, Figure 2-10). Evidence of bioturbation and burrowing is also present locally. There is very little to no observed porosity development (nil to 2%), and cores may be shaly and fissile. Rare moldic and intercrystalline void spaces may be present proximal to the reef front where skeletal fragments have been derived from the reef crest. Chert nodules of silica derived from radiolaria or siliceous sponges (Fishbuch, 1968) may be present locally .

2.4.8. Supratidal to Intertidal Facies Assemblage

The Upper Blueridge shallow water facies assemblage is interpreted as being formed in restricted, evaporitic supratidal, intertidal, and locally lagoonal environments. The dominant supratidal and intertidal facies consists of interlaminated, interbedded, and/or nodular primary, or syndepositional, anhydrite with cryptocrystalline dolomite. Synsedimentary deformation is also present. Fenestral mudstones with algal laminations are common, and occasional shallow water grainstones are present. The less dominant lagoonal sediments are predominantly mudstones with minor interbedded floatstones with possible burrow forms. Moldic porosity after *Amphipora* occurs locally within this facies, but overall, this evaporitic environment results in very little to no porosity. This facies assemblage is not present in the Woodbend and Winterburn Groups.

2.5. STRATIGRAPHIC FRAMEWORK

A simplified illustration of the Devonian (Frasnian) lithostratigraphic nomenclature utilized in this study of the Obed area is presented in Figure 2-1. The lithostratigraphic nomenclature has been modified for the purposes of presenting the Obed stratigraphic framework, illustrated through the designation of stratigraphic intervals in two cross-sections (Cross-sections A and B; Figure 2-11a and 2-11b). The location of the

Figure 2-11a Stratigraphic cross-section A of Woodbend and Winterburn Groups in the Obed area (see text for explanation).

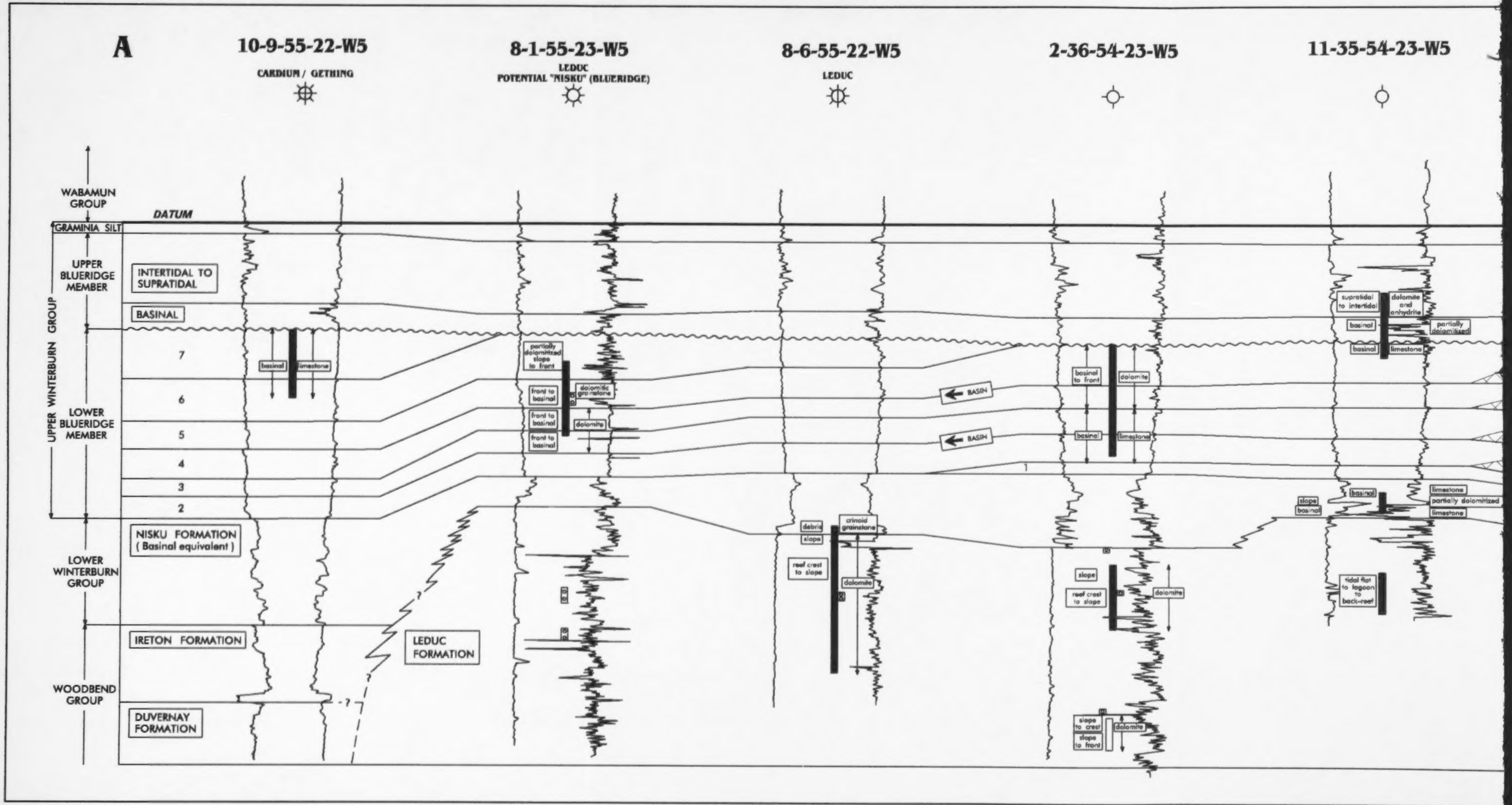

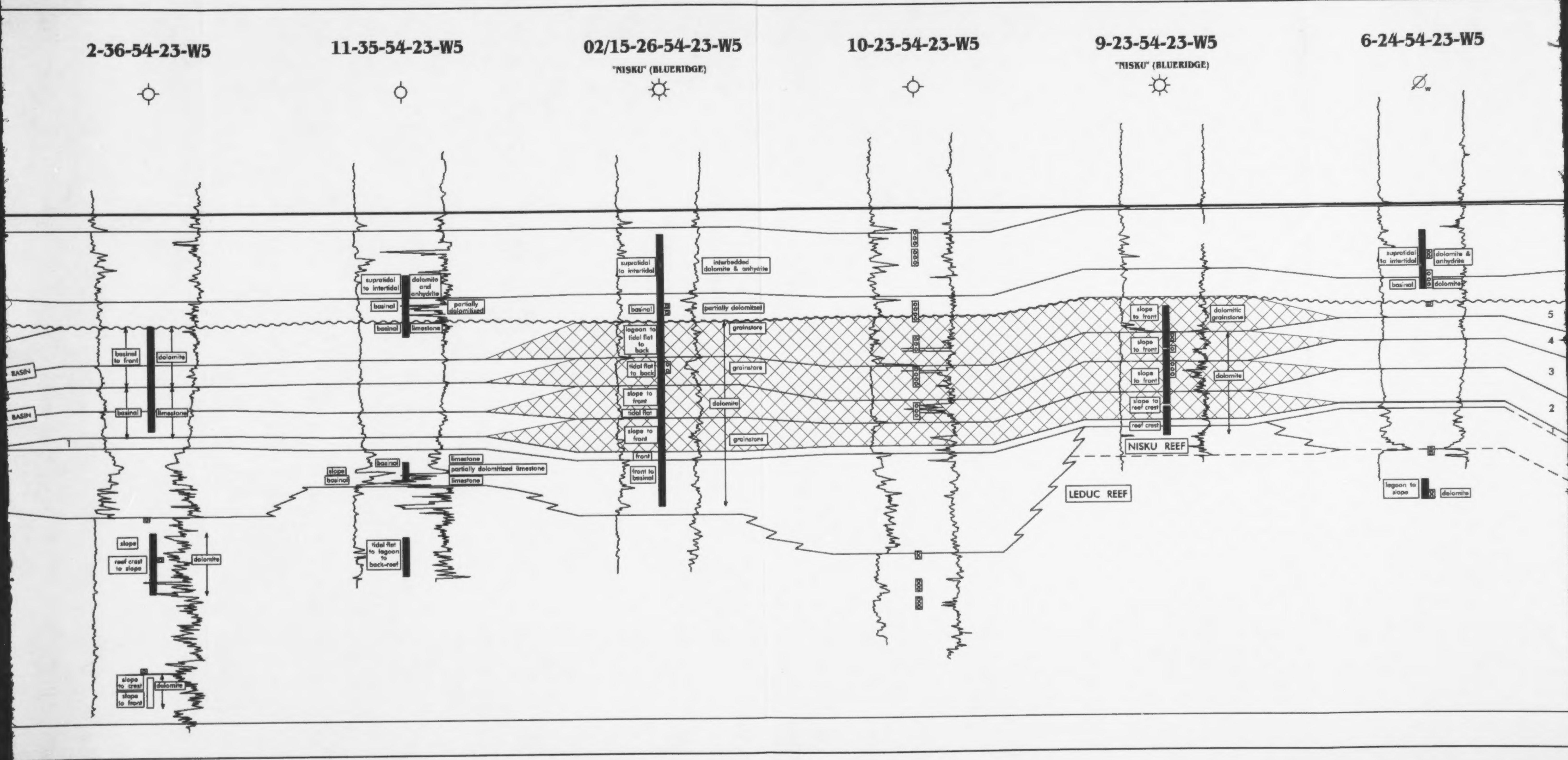
2-36-54-23-W5
11-35-54-23-W5
02/15-26-54-23-W5
"NISKU" (BLUERIDGE)
10-23-54-23-W5
9-23-54-23-W5
"NISKU" (BLUERIDGE)
6-24-54-23-W5
BASIN
BASIN
1
basinal to front
dolomite
basinal
limestone
slope
reef crest to slope
dolomite
slope to crest
slope to front
dolomite
supratidal to intertidal
dolomite and anhydrite
basinal
partially dolomitized
basinal
limestone
slope
basinal
basinal
limestone
partially dolomitized limestone
limestone
tidal flat to lagoon to back-reef
supratidal to intertidal
interbedded dolomite & anhydrite
basinal
partially dolomitized
lagoon to tidal flat to back
grainstone
tidal flat to back
grainstone
slope to front
dolomite
tidal flat
slope to front
grainstone
front
front to basinal
slope to front
dolomitic grainstone
slope to front
slope to front
dolomite
slope to reef crest
reef crest
NISKU REEF
LEDUC REEF
supratidal to intertidal
dolomite & anhydrite
basinal
dolomite
lagoon to slope
dolomite
5
4
3
2
1

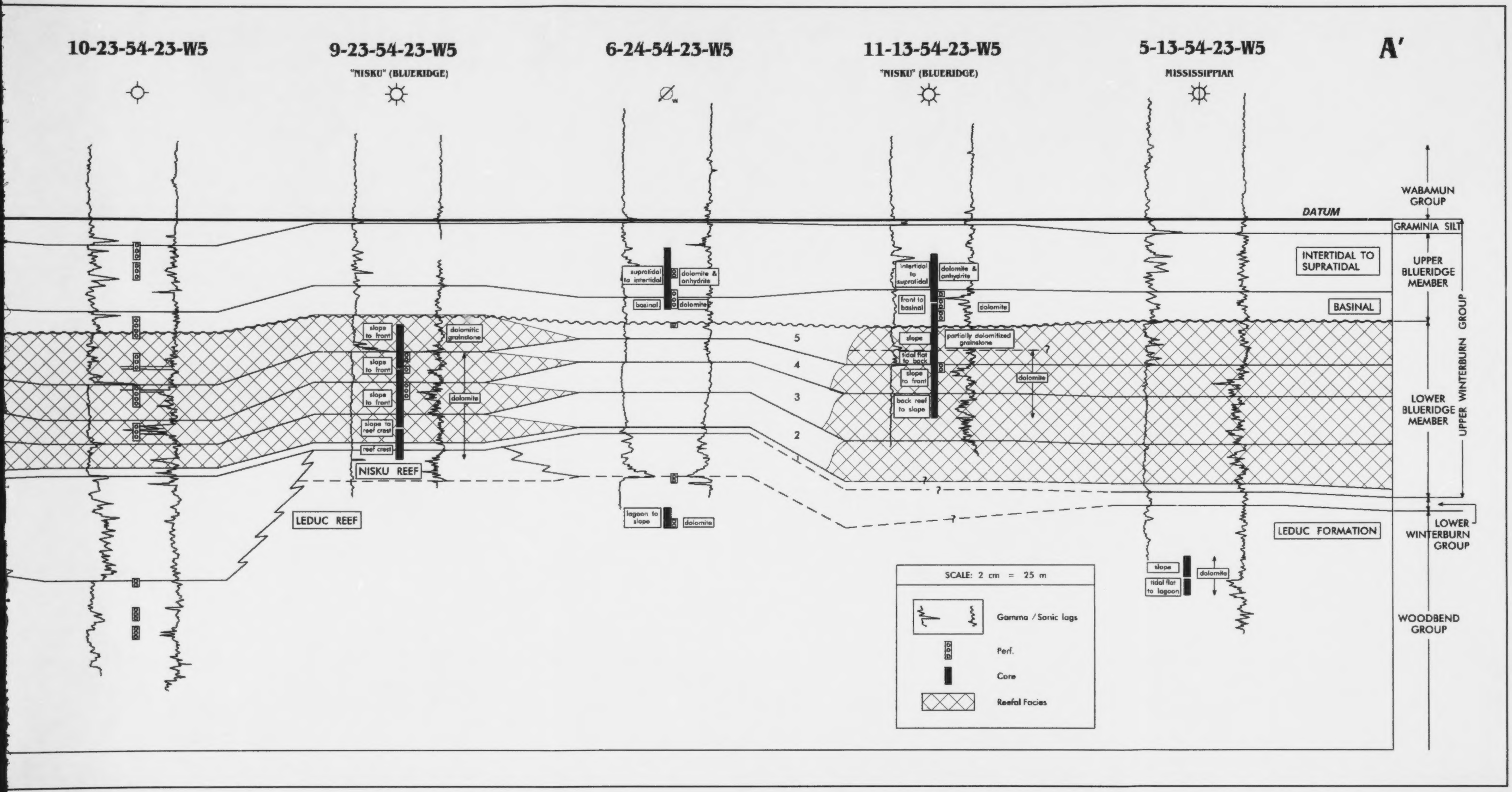
10-23-54-23-W5
9-23-54-23-W5
"NISKU" (BLUERIDGE)
6-24-54-23-W5
11-13-54-23-W5
"NISKU" (BLUERIDGE)
5-13-54-23-W5
MISSISSIPPIAN
A'
DATUM
WABAMUN GROUP
GRAMINIA SILT
UPPER BLUERIDGE MEMBER
LOWER BLUERIDGE MEMBER
UPPER WINTERBURN GROUP
LOWER WINTERBURN GROUP
WOODBEND GROUP
INTERTIDAL TO SUPRATIDAL
BASINAL
LEDUC FORMATION
LEDUC REEF
NISKU REEF
slope to front
slope to front
slope to front
slope to reef crest
reef crest
dolomitic grainstone
dolomite
supratidal to intertidal
dolomite & anhydrite
basinal
dolomite
lagoon to slope
dolomite
intertidal to supratidal
dolomite & anhydrite
front to basinal
dolomite
slope
partially dolomitized grainstone
tidal flat to back
slope to front
back reef to slope
dolomite
slope
tidal flat to lagoon
dolomite
5
4
3
2
1
?
?
?
?
SCALE: 2 cm = 25 m
Gamma / Sonic logs
Perf.
Core
Reefal Facies

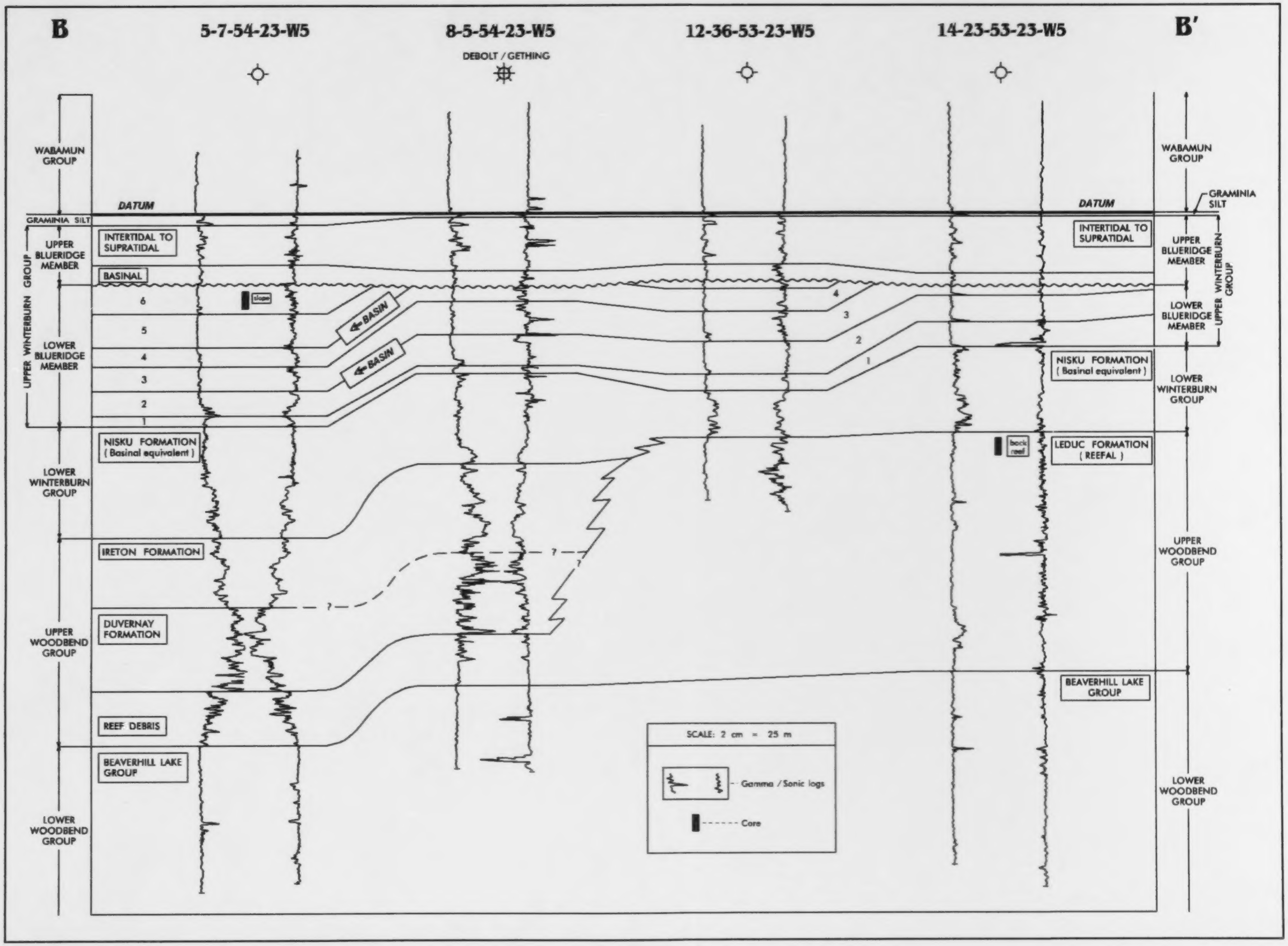
B
5-7-54-23-W5
8-5-54-23-W5
DEBOLT / GETHING
12-36-53-23-W5
14-23-53-23-W5
B'
WABAMUN GROUP
DATUM
GRAMINIA SILT
UPPER BLUERIDGE MEMBER
INTERTIDAL TO SUPRATIDAL
BASINAL
UPPER WINTERBURN GROUP
6
5
4
3
2
1
slope
BASIN
BASIN
LOWER BLUERIDGE MEMBER
NISKU FORMATION (Basinal equivalent)
LOWER WINTERBURN GROUP
IRETON FORMATION
?
?
?
?
DUVERNAY FORMATION
UPPER WOODBEND GROUP
REEF DEBRIS
BEAVERHILL LAKE GROUP
LOWER WOODBEND GROUP
4
3
2
1
back reef
LEDUC FORMATION (REEFAL)
SCALE: 2 cm = 25 m
Gamma / Sonic logs
Core

Figure 2-11b Stratigraphic cross-section B of Woodbend and Winterburn Groups in the Obed area (see text for explanation).

stratigraphic cross-sections, relative to their position on the platform or in the basin of the Obed area are shown in Figure 2-4, as are well locations representative of those wells penetrating the Wabamun Group. The Obed complex lies at the western edge of the West Shale Basin and the eastern edge of the Jasper Basin (Figure 2-3). The subsurface geology in the Obed area is compared with outcrop nomenclature (Figure 2-1) and descriptions (Workum and Hedinger, 1992) of the Rocky Mountain Front Ranges.

The emphasis of this investigation is placed upon the Upper Woodbend Group (Leduc Formation), at a depth in excess of 4000m, and the overlying Upper Winterburn Group (Blueridge Member) with its coeval lateral units. Facies and depositional environments, as previously discussed, have been identified in the Leduc Formation and have been mapped in terms of stacked prograding cycles and lateral facies changes across the Obed platform in the Lower Blueridge Member. Similar Leduc reef complexes have been studied by McCrossen (1957), Klovan (1964), McGillivray and Mountjoy (1975), Stoakes (1980), Andrews (1987), Workum and Hedinger (1987, 1992), Dix (1990), McNamara and Wardlaw (1991), and others. The Upper Woodbend, as well as the Lower Winterburn, contain cycles of reef to basin transitions which form westerly trending wedges of sediments. Where the sedimentary cycles attain a maximum thickness, reefs are present. In the Obed area, however, the Leduc Formation could not be correlated in terms of internal cyclicity, and distinctions between post-reef and reef equivalent basin fill deposits were not made because geophysical well logs seldom penetrate the entire Woodbend succession. The complex architecture of the reef and surrounding environments may have been the result of processes such as sea level fluctuations and erosion.

The top of the Graminia Formation has been used as a datum for presentation of the cross-sections (Figure 2-11a and 2-11b), as it is considered to be a chronostratigraphic marker and is assumed to have been relatively flat and continuous over the entire study area and beyond (Switzer *et al.*, 1994). The working datum was at or near the base of the Lower Blueridge cycles and well to well correlations were made primarily from log response. Core descriptions verified the confidence in these correlations. The stratigraphic relationships of the units of the Woodbend Group and Winterburn Group in the Obed area are best understood through the investigation of these stratigraphic cross-sections (Figure 2-11a and 2-11b).

2.5.1. Woodbend Group

During early phases of Woodbend Group deposition, the Western Canada Sedimentary Basin underwent gradual deepening, resulting in the development of a thick aggradational succession of carbonates with substantial topographic relief between shelf and basinal areas (Switzer *et al.*, 1994). Stratigraphic cross-sections A and B (Figures 2-11a and 2-11b), across the Obed area, provide a representative illustration of the Woodbend Group, and its relation between platform and reefal stages (Leduc Formation) of development and basin fill (Duvernay and Ireton) on the Obed carbonate platform (Beaverhill Lake Group).

The Beaverhill Lake Group is an extensive carbonate platform underlying the entire area with very little apparent relief and a relatively uniform thickness (Anderson *et al.*, 1989). It forms the base upon which the basal Leduc platform, overlying carbonate buildups, and other units of the Woodbend Group were deposited (Figure 2-1). The thickness of this platform (cross-section B, Figure 2-11b) in the Obed area is approximately 140m, according to wells which penetrate the Beaverhill Lake Group.

The basal Leduc platform extends over most of the Obed reef complex area with some basinal wells showing poor platform development over the Beaverhill Lake Group. Where the platform is present and not overlain by Leduc buildups, the average thickness varies from 60m to 80m. The stratigraphic cross-sections do not fully distinguish the basal Leduc platform from the Leduc buildups (Figures 2-11a and 2-11b).

The reefal carbonates of the Leduc Formation buildups have an average thickness of approximately 160m. There is also evidence of the presence of Leduc reefal debris at the outer margins of the reefal complex (Figure 2-11a). The Leduc buildups appear to be concentrated in the north and the south regions of the platform. This, however, may be a function of the lack of well control in the central region. The Leduc carbonate buildups consist primarily of reef crest (stromatoporoid-coral rudstone/floatstone) and reef slope (coral or crinoid dominated rudstone) facies with intervals of back-reef and lagoon facies associations. Lateral and vertical relationships are difficult to interpret due to relatively poor core control. The equivalents to the Leduc Formation in the Rocky Mountain Front Ranges are represented by the Cairn Formation (basal Leduc platform) and Peechee Member (reefal buildups) of the Southesk Formation (Workum and Hedinger, 1992).

The dark brown, bituminous shales and limestones of the Duvernay Formation (Allan and Creaney, 1991) are developed basinward of the Leduc Formation buildups. Overlying the shales of the Duvernay Formation (Perdrix Formation) are transgressive shales of the Ireton Formation, or Mount Hawk equivalent in the Jasper Basin (Switzer *et al.*, 1994). The Duvernay and Ireton Formations were deposited penecontemporaneously with the Leduc reefs (Switzer *et al.*, 1994). The Ireton Formation consists of illitic shales grading to marl and argillaceous limestones towards the top (Anderson *et a*l., 1989). This formation directly overlies the Leduc reef buildups locally, but may be confused with the basinal Winterburn Nisku Formation, also equivalent to the Mount Hawk Formation. Basement movement of block faults during late stage Ireton deposition resulted in variable Ireton thicknesses (Switzer *et al.*, 1994).

2.5.2. Winterburn Group

By the end of Woodbend deposition, during a period of reduced rate of subsidence and/or relative sealevel fall, most of the basin was filled by shales of the Winterburn Group (Switzer *et al.*, 1994). The Nisku Formation overlies the shales of the Ireton Formation and reefal buildups of the Leduc Formation (Figure 2-11a and 2-11b). Recent regional correlations and mapping suggest that the Nisku Formation is diachronous in central Alberta (Villéger and Webb, 1992; Villéger, 1994). By extrapolation, this interpretation can be extended into the West Shale Basin and Wild River sub-basin (Figure 2-3) where the Nisku Formation consists of shelf carbonates that grade into thin basinal cycles. In the Obed area, the Nisku Formation is comprised of basinal facies, consisting of dark grey, fossiliferous, argillaceous dolomites and limestones, equivalent to the Mount Hawk Formation of the Rocky Mountain Front Ranges (Workum and Hedinger, 1992). The Nisku may appear as a thin transitional argillaceous unit between the Leduc Formation and the Blueridge Member or may have a substantial thickness

(>10m). Reef buildups, possibly of Nisku age (Arcs and Grotto Members), occur locally and can be seen directly overlying Leduc carbonate buildups in cross-section A (Figure 2-11a) with a thickness of approximately 30m. Since the basinal Nisku Formation can be considered equivalent to the Mount Hawk Formation (McLean and Mountjoy, 1993), as can the Ireton Formation (Switzer *et al.*, 1994), it is difficult to distinguish the boundary between the two on geophysical well logs. The regionally defined "Z" marker, a depositional hiatus dividing Upper Woodbend and overlying Winterburn shales (Stoakes, 1980), of the Nisku Formation is occasionally recognizable on petrophysical well logs, but is difficult to correlate across the Obed area. Because of the difficulty in correlations, the Nisku reef-to-basin facies changes are not mapped. Transgression, and possible cessation of fine clastic input into the basin, marked the end of Nisku time.

Green shales and silts of the Calmar Formation regionally cap the Nisku facies but are only seen locally and cannot be mapped across the Obed area. Deposition of these shales and silts was followed by deposition of Upper Winterburn regressive cycles. Within the Lower Blueridge Member, seven prograding, generally shallowing-up cycles have been recognized, with four being continuous across the entire Obed platform. These cycles are illustrated in stratigraphic cross-sections A and B (Figure 2-11a and 2-11b, respectively). The lowermost cycle is clinoformic and pinches out basinward, and the two uppermost cycles have been cut by erosion. The correlatable Lower Blueridge cycles show reef to basin transitions. Reef and basinal facies are indicated on the cross-sections (Figure 2-11a and 2-11b) where core is available. The location of reefal facies is related to the underlying topography and structure, with a back-stepping relationship with respect to the Nisku and Leduc reefal buildups. The three-dimensional geometry and complex stratigraphic relationships within the reef cannot be illustrated on cross-section A (Figure 2-11a). Correlations of cycles may be made, but the well and core control does not provide the means to provide an accurate reef model. The vertical stacking of lateral facies changes within the cycles show both prograding and retrograding relationships, dependent on the geometry of the reef complex. Locally, the Lower Blueridge buildups are rooted directly on Nisku carbonate buildups. Each cycle has a thickness of about 20m in reefal areas and about 15m in basinal portions of these prograding units. The cumulative thickness of the overall regressive, prograding Lower Blueridge cycles ranges from an average of 80m in the reefal areas, where topography is the highest and is cut by the unconformity, to 105m where basin fill is the thickest due to underlying topography, and where the cycles are most numerous before erosion. The Lower Blueridge Member is equivalent to the Simla or Ronde Member in reefal strata and the Mount Hawk Formation basinward (Workum and Hedinger, 1992 and references therein). These vertically aggrading, upward shallowing cycles formed in response to changes in relative sea level and show a diversity of reef to basin transitions. The top surface of each cycle represents a relative sealevel rise (flooding surface) or stillstand.

The top of the Lower Blueridge cycles (Figure 2-11a and 2-11b) is marked by an abrupt facies change and local erosion of the uppermost cycles. Overlying the planar unconformity surface is a widespread basinal unit (15m) and an evaporitic unit (45m) that comprise the Upper Blueridge. The interbedded dolomite and anhydrite of the intertidal-supratidal facies assemblage of the Upper Blueridge Member were deposited during a relative sealevel lowstand.

The Graminia Silt was deposited during a subsequent transgressive phase, and is indicative of the cessation of Blueridge carbonate accumulation. Its deposition coincided with one of the most significant global mass extinctions of the Phanerozoic (Switzer *et al.*, 1994). It is equivalent to the Sassenach Formation in the Jasper Basin (Workum and Hedinger, 1992) and marks the end of Frasnian deposition.

2.6. RESERVOIR CHARACTER

Reservoir facies are generally found in the back-reef, reef crest, and reef slope environments of the Woodbend and Winterburn Groups where the grain size is coarse and fossils are abundant, allowing for secondary porosity development and preservation. The percentage of mud in a facies influences porosity. Mud is most common in lagoonal and basinal platform rocks. Diagenetic attributes, independent of facies characteristics, are also important to the development of porosity and permeability in these rocks. The Obed D2A (Lower Blueridge, previously regarded as Nisku) and D3 (Leduc) hydrogen sulfide gas pools are located at the northern, updip edge of the Leduc, Nisku, and Blueridge reef complex at Obed. Nisku reefs, where present, also have characteristics of a paleoaquifer, and thus have reservoir potential. Hydrocarbon migration occurred locally through the Leduc carbonates, and when not trapped in a Leduc reef the hydrocarbons migrated into the Nisku reef, and finally into the Lower Blueridge reefal units. Where argillaceous sediments of the Nisku Formation form a barrier between the Leduc and Lower Blueridge reefs, there are two possibilities for oil migration. Firstly, the reefs may be connected three dimensionally, which cannot be illustrated due to poor well control. Secondly, the argillaceous carbonates may have sufficient permeability to allow for fluid migration through this unit into the overlying reef.

A structural cross-section across the Obed area (Figure 2-12), along with the stratigraphic cross-sections (Figures 2-11a and 2-11b), help to explain the interrelationships of the stratigraphy, depositional facies, and structural control on the two gas pools. Strata on the platform dip to the southwest at a gradient of 20m/km. The average structural depth of the top of the Graminia Silt is -2400m in the northeast (Township 55, Range 20W5M) and -3400m in the southwest (Township 52, Range 24W5M). The structural cross-section (Figure 2-12) illustrates the relative fault movements which elevated the producing Leduc reef (D3 pool) to a higher structural level than expected, at about the same structural level as the Lower Winterburn reefs. Faulting probably occurred either syndepositionally due to extensional fault movements during Ireton to Nisku time, or by later reactivation of fault blocks. The structural history of the Obed area is very complex. Because of the lack of seismic data and available time, structural aspects are not further addressed in this paper.

The Leduc buildup hosting the D3 pool is seen in updip wells at 8-1-55-23W5M and 8-6-54-23W5M (Figure 2-11a), with the gas-water contact at -2955 sub-sealevel (Figure 2-12). The D2A pool, with gas-water contact at -2963m sub-sealevel (Figure 2-12), is located within the Lower Blueridge reefal buildups in wells 5-13-54-23W5M and 11-13-54-23W5M, as well as in a possible separate Lower Blueridge reef in up-dip well 9-23-54-23W5M (Figure 2-11a). The gas-water contacts were delineated through detailed log analyses. Since the gas-water contacts for the D2A and D3 pools are at similar structural elevations, with the D3 pool located up-dip from the D2A pool, the two

Figure 2-12 Schematic structural cross-section across the Obed area showing the gas/water contacts of the Leduc (D3) and Lower Blueridge (D2) sour gas pools.

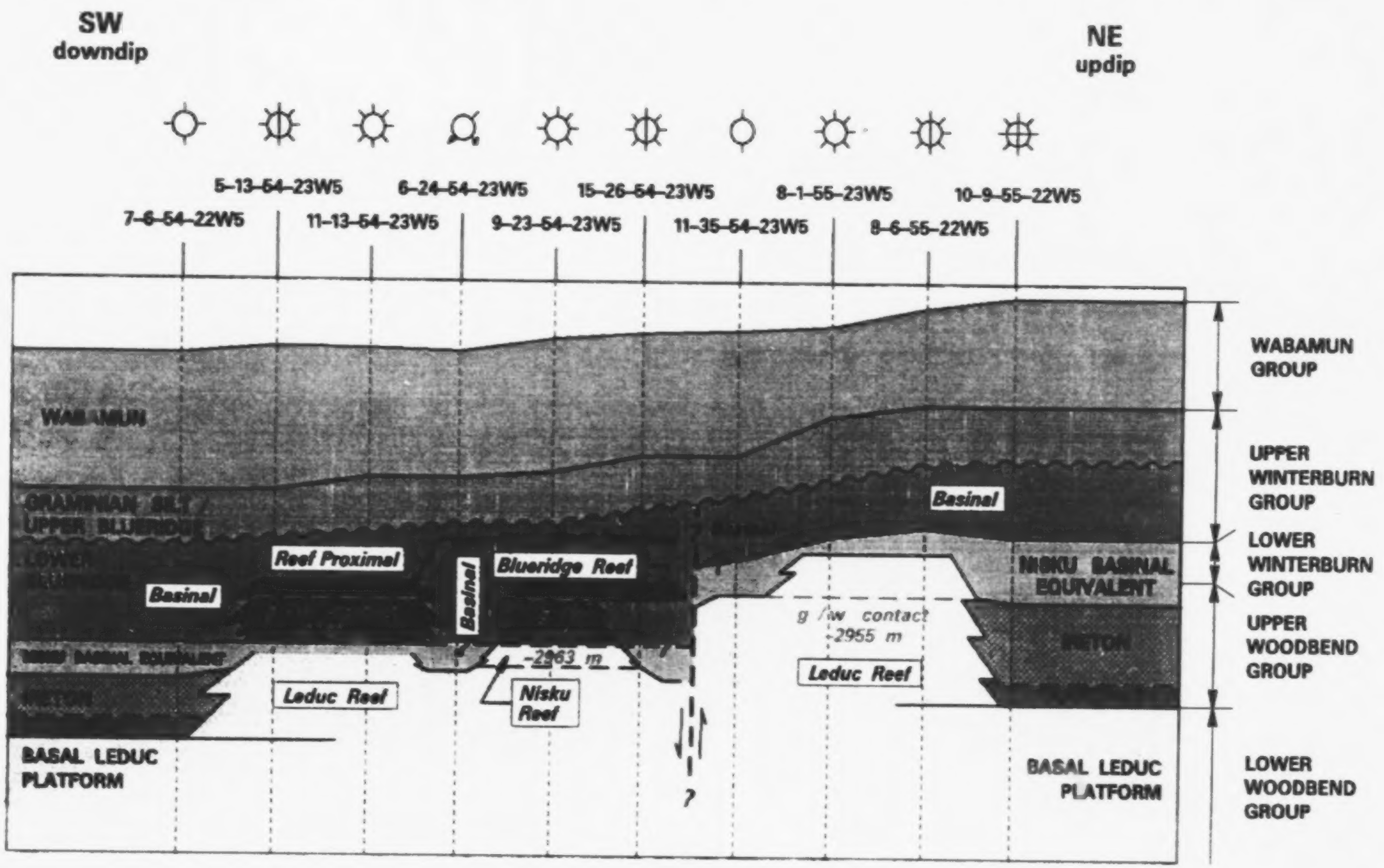
SW
downdip
NE
updip
7-6-54-22W5
5-13-54-23W5
11-13-54-23W5
6-24-54-23W5
9-23-54-23W5
15-26-54-23W5
11-35-54-23W5
8-1-55-23W5
8-6-55-22W5
10-9-55-22W5
WABAMUN
GRAMINIAN SILT / UPPER BLUERIDGE
LOWER BLUERIDGE
Basinal
Reef Proximal
Basinal
Blueridge Reef
Basinal
NISKU BASINAL EQUIVALENT
IRETON
Leduc Reef
-2963 m
Nisku Reef
g /w contact -2955 m
Leduc Reef
NISKU BASINAL EQUIVALENT
IRETON
?
BASAL LEDUC PLATFORM
BASAL LEDUC PLATFORM
WABAMUN GROUP
UPPER WINTERBURN GROUP
LOWER WINTERBURN GROUP
UPPER WOODBEND GROUP
LOWER WOODBEND GROUP

reservoirs may be in hydrologic communication.

The distribution of hydrocarbons is also influenced by post-depositional structure, due to a combination of differential compaction and basin subsidence. Anderson *et al.* (1989) prefer to classify reefs, such as the Obed reefal complex, as combination structural and stratigraphic traps. Some isolated buidups in the surrounding area have impermeable shale seals and could form traps regardless of the sense of regional dip. The traps for the Lower Blueridge (D2A) and Leduc (D3) reservoirs are sealed laterally and vertically by shales and off-reef argillaceous carbonates. The unconformity and tight sediments of the basinal and restricted evaporitic Upper Blueridge seem to form a widespread seal over the entire platform. The producing units, with a lower porosity limit on the sonic logs of 3% and gamma ray cut-off of <15 API, appear to be the clean reefal or reef-proximal carbonate facies of both the Leduc and the Lower Blueridge Formation.

The Woodbend and Winterburn Groups were subjected to post-depositional dolomitization and structural movements which influenced reservoir quality and trap configuration. The thick accumulations of dolomite, limestone, evaporites, and basin-filling shales during Frasnian time reflect the interplay between eustatic and tectonic sealevel changes, rapid sedimentation, and high rate of basin subsidence. Infilling of the basin was from the northeast to southwest (Stoakes, 1980). The distribution of pore types in the reservoir is dependent on the depositional environment and facies assemblages, but effective porosity and permeability is controlled by post-depositional processes.

2.7. CORRELATION TO OUTCROP

The use of Jasper Basin, Rocky Mountain Front Ranges, stratigraphy and nomenclature (Figure 2-13) helps to explain the stratigraphic framework in the subsurface of the Obed area. A schematic of the stratigraphy in the Obed area is shown in Figure 2-14. It provides a comparison of the stratigraphic nomenclature of the subsurface and outcrop Devonian units common to this area. Within Alberta, similar Frasnian reefal facies are observed within the Golden Spike, Redwater, Strachan, and Ricinus buildups in the Woodbend Group (Walls and Burrowes, 1985), within the Mount Hawk Formation (Hedinger and Workum, 1988), as well as east of the Windfall complex (Switzer *et al.*,

Figure 2-13 Schematic diagram of Jasper Basin, Rock Mountain Front Ranges, stratigraphy and nomenclature (Workum and Hedinger, 1992).

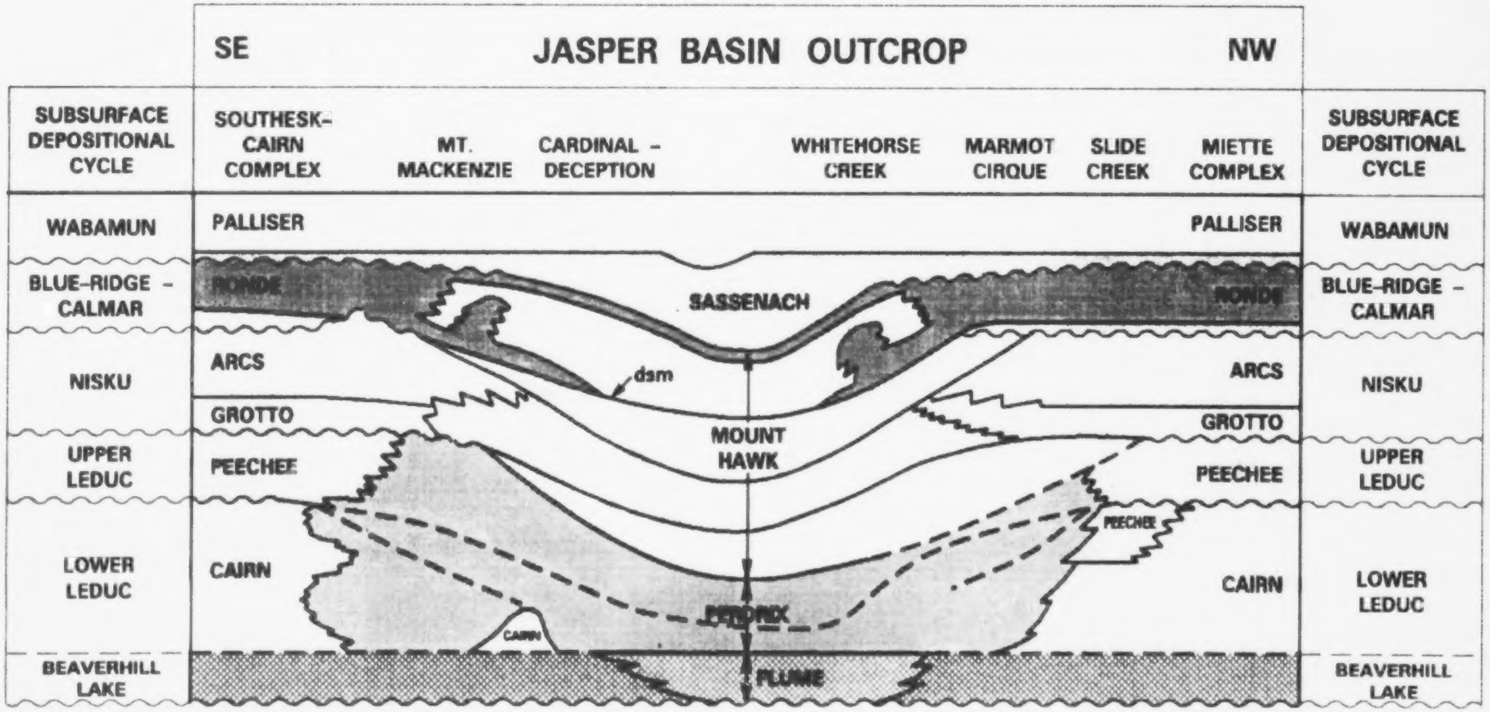
SE
JASPER BASIN OUTCROP
NW
SUBSURFACE DEPOSITIONAL CYCLE
SOUTHESK-CAIRN COMPLEX
MT. MACKENZIE
CARDINAL - DECEPTION
WHITEHORSE CREEK
MARMOT CIRQUE
SLIDE CREEK
MIETTE COMPLEX
SUBSURFACE DEPOSITIONAL CYCLE
WABAMUN
PALLISER
PALLISER
WABAMUN
BLUE-RIDGE - CALMAR
RONDE
SASSENACH
RONDE
BLUE-RIDGE - CALMAR
NISKU
ARCS
dsm
ARCS
NISKU
GROTTO
MOUNT HAWK
GROTTO
UPPER LEDUC
PEECHEE
PEECHEE
UPPER LEDUC
LOWER LEDUC
CAIRN
PEECHEE
PERDRIX
CAIRN
CAIRN
LOWER LEDUC
BEAVERHILL LAKE
FLUME
BEAVERHILL LAKE

Figure 2-14 Schematic stratigraphic cross-section across the Obed area showing both subsurface and outcrop nomenclature of the Devonian carbonates.

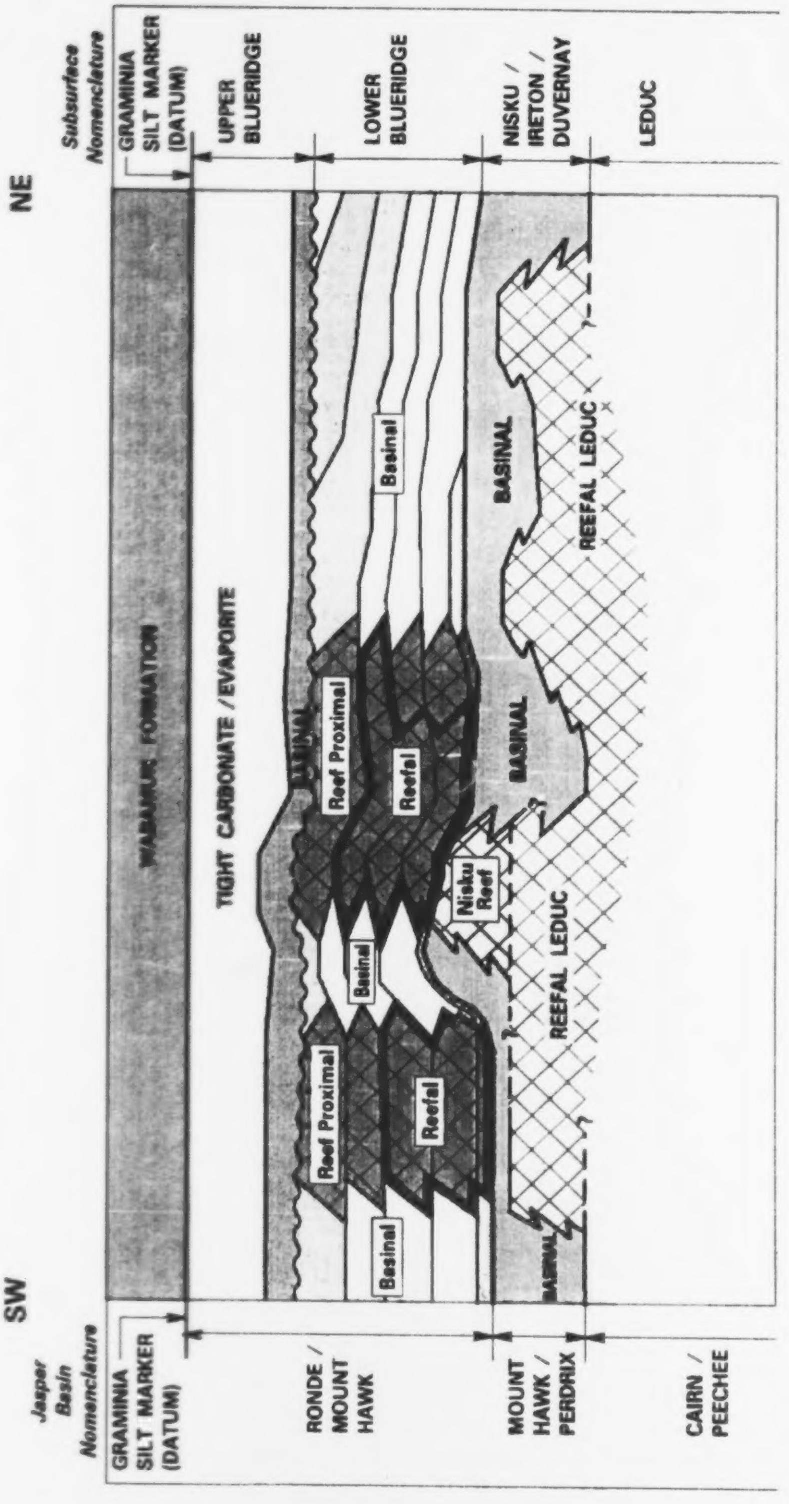
SW
NE
Jasper Basin Nomenclature
GRAMINIA SILT MARKER (DATUM)
RONDE / MOUNT HAWK
MOUNT HAWK / PERDRIX
CAIRN / PEECHEE
Subsurface Nomenclature
GRAMINIA SILT MARKER (DATUM)
UPPER BLUERIDGE
LOWER BLUERIDGE
NISKU / IRETON / DUVERNAY
LEDUC
WABAMUN FORMATION
TIGHT CARBONATE / EVAPORITE
BASINAL
Basinal
Reef Proximal
Reefal
Basinal
Reef Proximal
Reefal
Basinal
Nisku Reef
BASINAL
REEFAL LEDUC
BASINAL
BASINAL
REEFAL LEDUC
?
?
?
?
?

1994), and thus east of Obed, in the Winterburn Group. The Jasper Basin appears to be a better comparison than the West Pembina area for the stratigraphy of the Obed reef complex based on its proximity and the observations and interpretations of this study.

2.8. CONCLUSIONS

The major influences on Woodbend sedimentation were localized movement of basement fault blocks, differential subsidence, and the nature and volume of terrigenous clastics introduced to the basin (Switzer at al., 1994). Conditions allowed for the development of an extensive Leduc carbonate platform (Cairn Formation) over the Beaverhill Lake platform, and subsequent localized Leduc reefal buildups (Peechee Formation). The end of Woodbend deposition marks the cessation of basin infill and marine incursion, resulting in shallow water shelf carbonate deposition of the Winterburn Group. The Ireton (Mount Hawk) Formation is the last Woodbend interval and needs additional detailed mapping and biostratigraphic control to distinguish it from the Winterburn Nisku (Mount Hawk) Formation. The thickness of the Ireton and overlying Nisku Formations varies. They thin where they drape reefs and thicken where they fill the basin and Leduc topography is relatively low. Where probable Nisku reefs overly Leduc reefs, the Ireton Formation is very thin and generally indistinguishable from the Nisku Fromation.

The Nisku Formation is primarily basinal in the West Shale Basin, and hence the Obed area, due to lateral shifts of the basin depocenter and relative sea level changes in Nisku time (Villéger, 1994). Isolated Nisku carbonate buildups may occur locally. The stratigraphic cross-sections integrating geophysical log and core data illustrate prograding cycles with associated reefal facies within the Lower Blueridge Member (Ronde Formation) which are both aggradational and progradational, and which thin into the basin (Mount Hawk Formation). The superposition of these cycles and their related facies illustrate the complexity and diversity of the Lower Blueridge Member. Shifts in reef location due to sea level fluctuations is evident in the lateral changes of reefal facies through time. The distribution of Lower Blueridge reefs are apparently related to the underlying Nisku and Leduc topography in a back-stepping relationship. Erosional topography carves into the Lower Blueridge cycles before the deposition of a basinal and an intertidal-supratidal unit. The basin had a relatively flat topography by the end of Woodbend and Winterburn time.

2.9. REFERENCES

Allan, J. and Creaney, S., 1991, Oil families of the Western Canada Basin, Bull. Can. Petrol. Geol., v. 39, p. 107-122.

Anderson, N.L., Hills, L.V., Cederwall, D.A. (editors), 1989, Geophysical Atlas of Western Canadian Hydrocarbon Pools, Alberta Research Council, 344p.

Andrews, G.D., 1987, Devonian Leduc outcrop reef-edge models and their potential seismic expression, *In* Devonian of the World, Proceedings of the Second International Symposium on the Devonian System, N.M., McMillan, A.F. Embry, and D.J. Glass (eds.), Can. Soc. Petrol. Geol., Memoir 14, v. II, p. 427-450.

Burchette, T.P., 1981, European Devonian reefs: A review of current concepts and models, In Toomey, D.F. (ed.), European Fossil Reef Models, Soc. Econ. Paleont. Mineral. Spec. Publ., v. 30, p. 85-142.

Dix, G.R., 1990, Stages of platform development in the Upper Devonian (Frasnian) Leduc Formation, Peace River Arch, S.C. O'Connell and J.S. Bell (eds.), Bull. Can. Petrol. Geol., v. 38A, p. 66-92.

Dunham, R.J., 1962, Classification of carbonate rocks according to depositional texture, *In* Ham, W.E. (ed.): Classification of Carbonate Rocks, Amer. Assoc. Petrol. Geol. Mem., v. 1, p. 108-121.

Embry, A.F., III and Klovan, J.E., 1972, Absolute water depths of Late Devonian paleoecological zones, Geol. Rund., v. 61, p. 672-686.

Fischbuch, N.R., 1968, Statigraphy, Devonian Swan Hills reef complexes of central Alberta, Bull. Can. Petrol. Geol., v. 16, p. 446-587.

James, N.P., 1983, Reef environment, In Scholle, P.A., Bebout, D.G., and Moore, D.H. (eds.), Carbonate Depositional Environments, Amer. Assoc. Petrol. Geol. Mem., v. 33, p. 345-440.

James, N.P. and Bourque, P.A., 1992, Reefs and mounds, In Walker, R.G. and James, N.P. (eds.), Facies Models: Response to Sea Level Change, Geol. Assoc. Canada, p. 323-347.

Klovan, J.E., 1964, Facies analysis of the Redwater complex, Alberta, Canada, Bull. Can. Petrol. Geol., v. 12, p. 1-100.

Machel, H.G., 1990, Nisku oil and sour gas play, subsurface of central Alberta, In The development of porosity in carbonate reservoirs, Canadian Society Petroleum Geologists Short Course Notes, 8-1 to 8-6.

Machel, H.G. and Hunter, I., 1994, Facies models for Middle to Late Devonian shallow-marine carbonates, with comparisons to modern reefs: a guide for facies analysis, Facies, v. 30, p. 155-176.

McCrossan, R.G., 1957, Colour variations in the Ireton shale, Journal of the Alberta Society of Petroleum Geologists, v. 5, p. 48-51.

McGillivray, J.G. and Mountjoy, E.W., 1975, Facies and related reservoir characteristics, Golden Spike reef complex, Alberta, Bull. Can. Petrol. Geol., v. 23, p. 753-809.

McLean, D.J. and Mountjoy, E.W., 1993, Upper Devonian buildup-margin and slope development in the southern Canadian Rocky Mountains, Geological Society of America Bulletin, v. 105, p. 1263-1283.

McNamara, L.B. and Wardlaw, N.C., 1991, Geological and statistical description of the Westerose reservoir, Alberta, Bull. Can. Petrol. Geol., v. 39, p. 332-351.

Mountjoy, E.W., 1980, Some questions about the development of Upper Devonian carbonate buildups (reefs), western Canada, Bulletin of Canadian Petroleum Geology, v. 28, p. 315-344.

North American Commission on Stratigraphic Nomenclature (NACSN), 1883, North American Stratigraphic Code, American Association of Petroleum Geologists Bulletin, v. 67, p. 841-875.

Ricketts, B.D. (ed.), 1989, Western Canada Sedimentary Basin - a case history, Canadian Society of Petroleum Geologists, 320p.

Stoakes, F.A., 1980, Nature and control of shale basin fill and its effect on reef growth and termination: Upper Devonian Duvernay and Ireton Formations of Alberta, Canada, Bull. Can. Petrol. Geol., v. 28, p. 345-410.

Switzer, S.B., Holland, W.G., Christie, D.S., Graf, G.C., Hedinger, A.S., McAuley, R.J., Wierzbicki, R.A., Packard, J.J., 1994, Devonian Woodbend-Winterburn strata of the Western Canada Sedimentary Basin. In Geologic Atlas of the Western Canada Sedimentary Basin. G.D. Mossop and I. Shetsen (compilers). Calgary, Canadian Society of Petroleum Geologists and Alberta Research Council, p. 165-195.

Villéger, M., 1994, Diachronism of Upper Devonian Nisku Formation (Alberta, Canada): geometry and sequence stratigraphy, C.R. Acad. Sci. Paris, t. 318, series II, p. 1527-1533.

Villéger, M. and Webb, T.K., 1992, Upper Devonian diachronous pinnacle reef generation (Alberta, Canada), C.R. Acad. Sci. Paris, t. 315, series II, p. 1381-1387.

Walls, R.A. and Burrowes, O.G., 1985, The role of cementation in the diagenetic history of Devonian reefs, *In* Carbonate Cements, N. Schneidermann and P.M. Harris (eds.), Society of Economic Paleontologists and Mineralogists Special Publication No. 36, p. 185-220.

Wilson, J.L., 1975, Carboante Facies in Geologic History, Springer-Verlag, New York, 471p.

Workum, R.H. and Hedinger, A.S., 1987, Geology of the Fairholme Group, Cline Channel, Alberta, Second International Symposium on the Devonian System, Field Excursion A6 Guidebook, 45p.

Workum, R.H. and Hedinger, A.S., 1988, Kananaskis area Frasnian Reefs, In Geldsetzer, H.H.J., James, N.P., and Tebbutt, G.E. (eds.), Reefs, Canada and adjacent areas, Canadian Society of Petroleum Geologists, Memoir 13, p. 522-556.

Workum, R.H. and Hedinger, A.S., 1992, Devonian Frasnian stratigraphy, Rocky Mountain Front Ranges, Crowsnest Pass to Jasper, Alberta, Geological Survey of Canada, Open File 2509, 106p.

CHAPTER 3:

Diagenesis of the Upper Devonian carbonates in the Obed area, west-central Alberta

ABSTRACT

The carbonates in the Obed area of west-central Alberta have undergone a complex diagenetic history. The platform facies have been affected by early widespread, pervasive dolomitization, which replaced the original limestones. Pyrite formed as a result of bacterial sulfate reduction before and during pervasive dolomitization. Later diagenetic phases, post-dating dolomitization and hydrocarbon migration, include secondary (post-depositional) anhydrite, planar dolomite, saddle dolomite, calcite, pyrite, and native sulfur. The geochemistry of these late phases provides evidence and thermochemical sulfate reduction (TSR). Reduction of sulfate from the primary (syn-depositional) anhydrite of the Upper Blueridge Member is the likely source of the sulfide involved in the BSR and TSR redox reactions. Carbon, oxygen, and strontium isotope data for carbonates (calcites and dolomites) in the Obed area demonstrate that they underwent deep burial cementation and recrystallization. Late calcites were effected by geochemical alteration more severely than the early calcites, early replacement dolomite, and late dolomite cements.

3.1. INTRODUCTION

Upper Devonian carbonates of the Obed sour gas field in west-central Alberta have a complex diagenetic history. Carbonate samples were obtained from the reef and off-reef facies in cores of the Woodbend and Winterburn Groups from the study area (Figure 3-1), which is defined by the Leduc platform and basinal wells (Figure 3-2). These samples were studied petrographically and geochemically. Dolomitized reefal facies are present in the Leduc Formation (Woodbend Group) and Lower Blueridge Member (Winterburn Group) and are host to at least two sour gas (up to 30% H_2S; Energy Resources Conservation Board, 1993) pools in the updip portion of the platform (Figure 3-2 and 3-3). The present subsurface depth at Obed is greater than 3500m. It has been estimated that about 1700m of sediment had been removed from the deeper part of the

Figure 3-1 Obed study area, west-central Alberta, encompassing Townships 52 to 55 and Ranges 21 to 24 W5M.

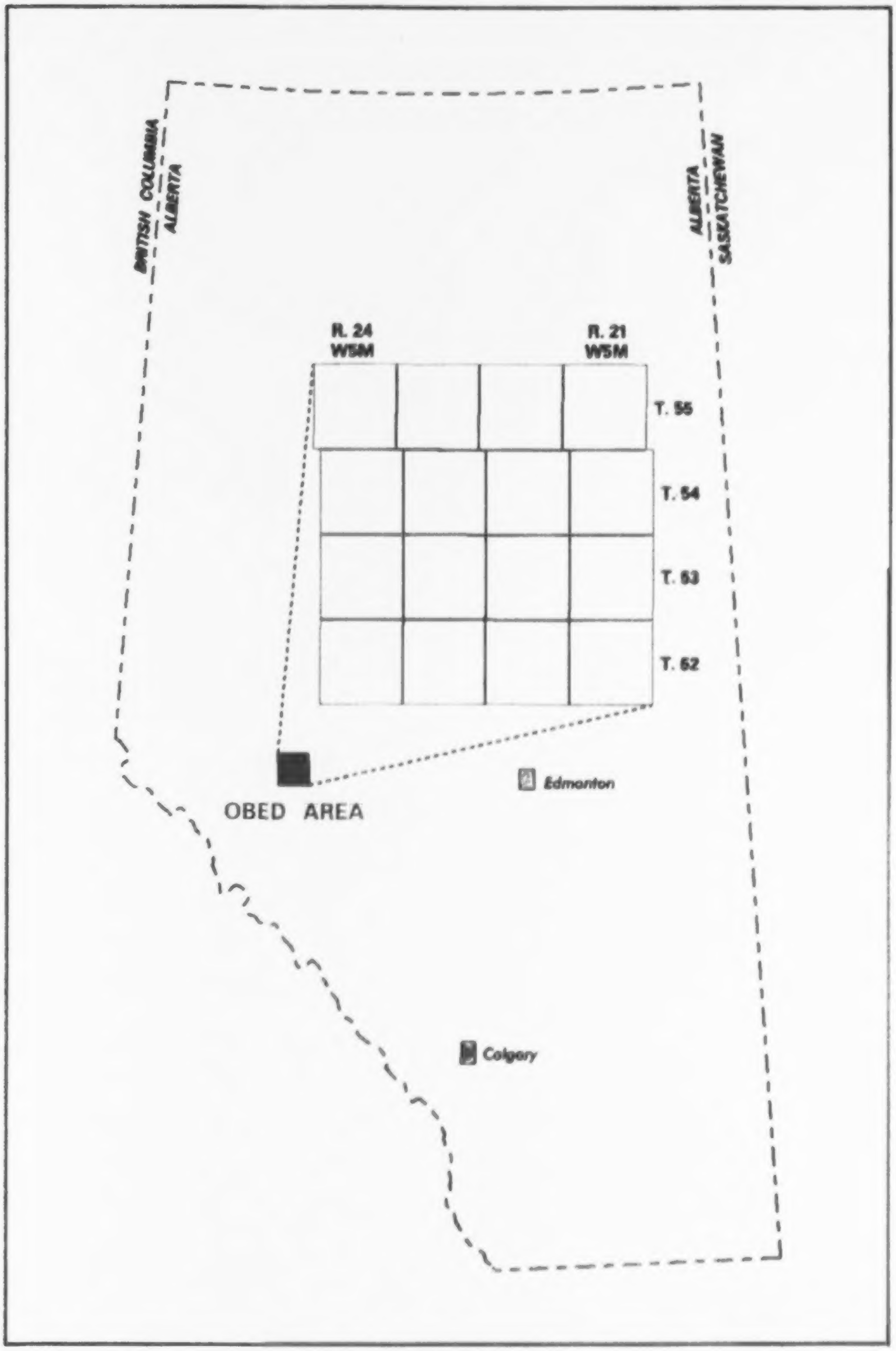
BRITISH COLUMBIA
ALBERTA
ALBERTA
SASKATCHEWAN
R. 24
W5M
R. 21
W5M
T. 55
T. 54
T. 53
T. 52
OBED AREA
Edmonton
Calgary

Figure 3-2 Obed study area showing Leduc platform geometry and well and core control.

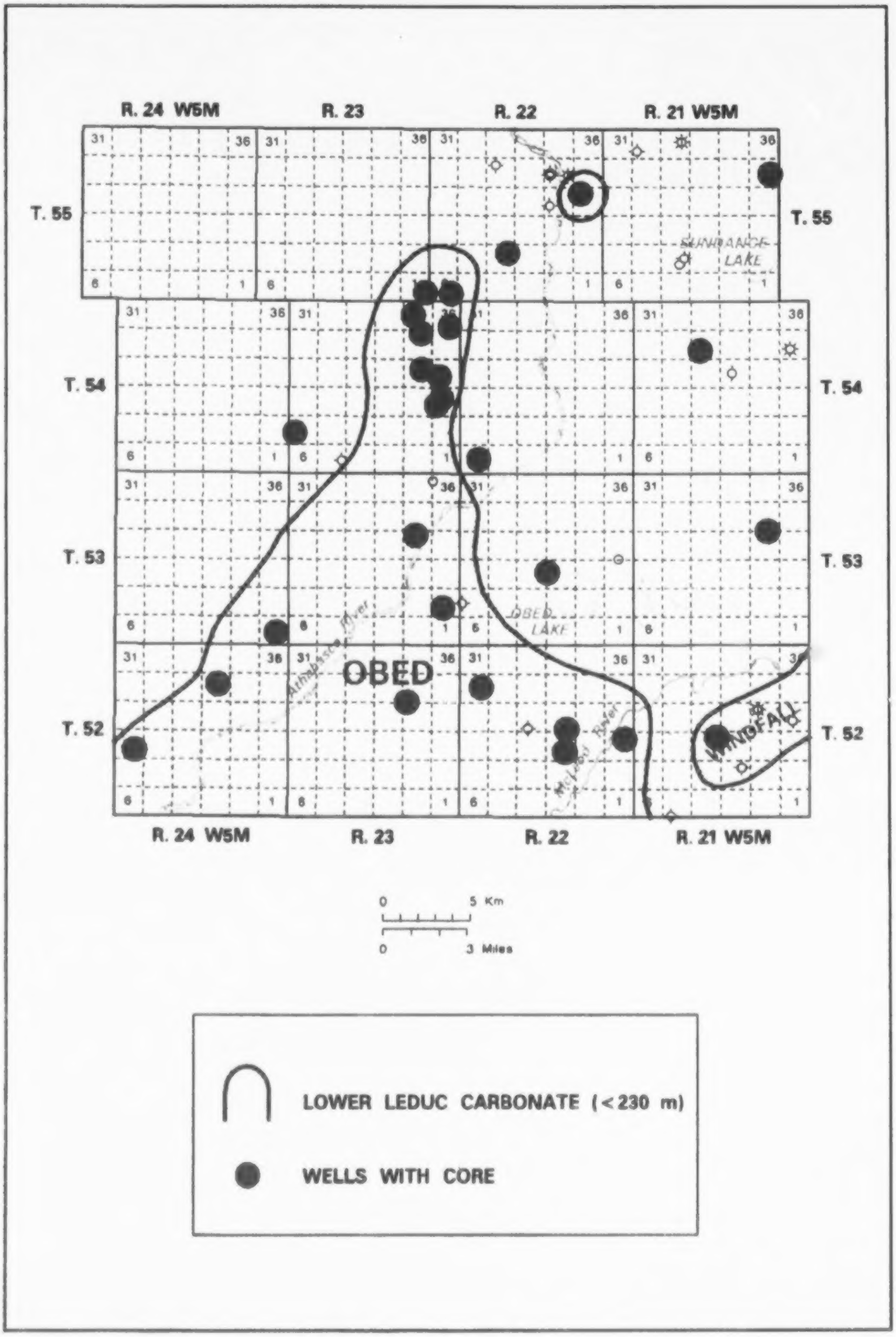
R. 24 W5M
R. 23
R. 22
R. 21 W5M
T. 55
T. 54
T. 53
T. 52
SUNDANCE LAKE
OBED LAKE
OBED
WINDFALL
Athabasca River
McLeod River
0 5 Km
0 3 Miles
LOWER LEDUC CARBONATE (<230 m)
WELLS WITH CORE

Figure 3-3 Schematic structural cross-section across the Obed area showing the gas/water contacts of the Leduc (D3) and Lower Blueridge (D2) sour gas pools.

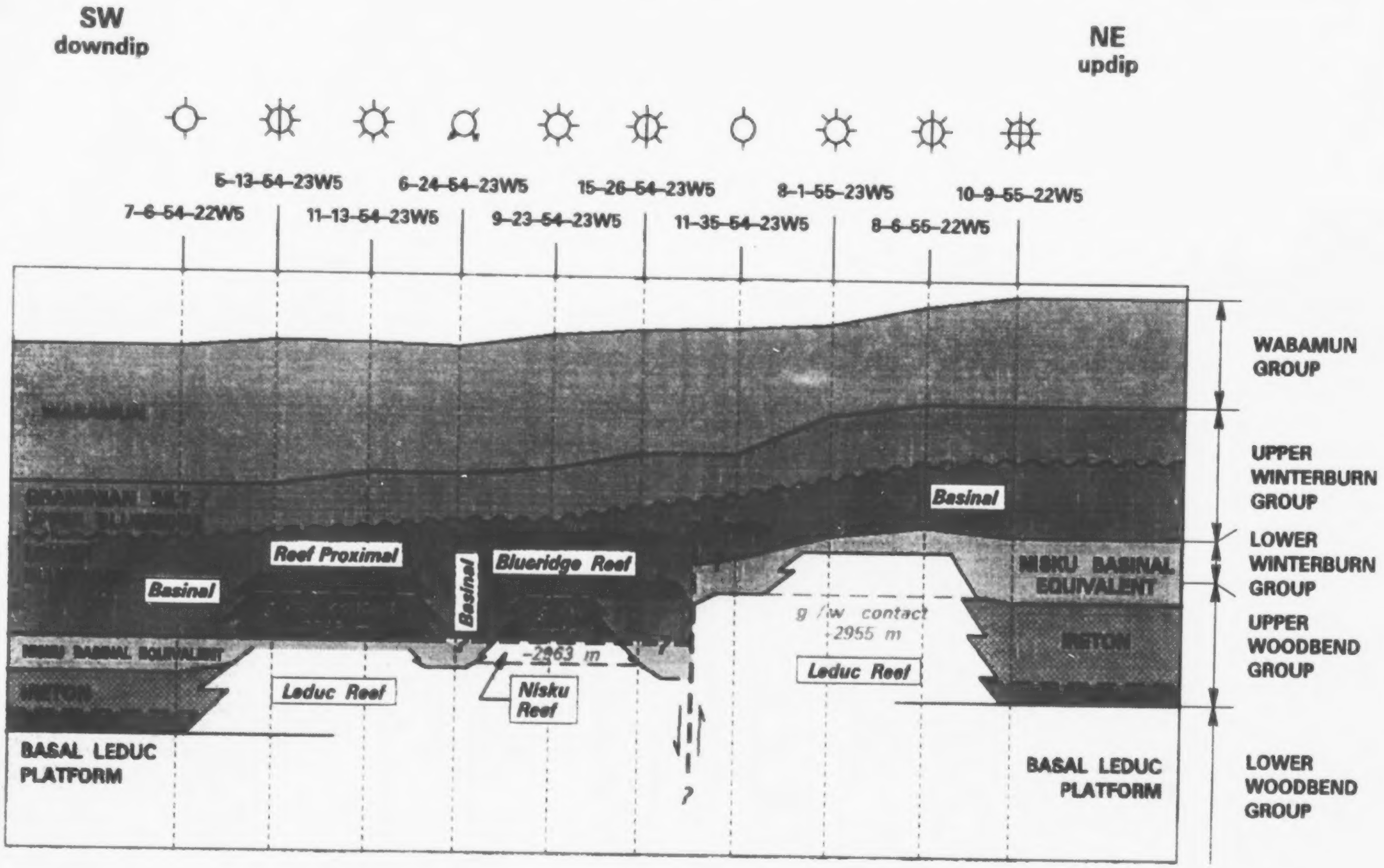
SW
downdip
NE
updip
7-6-54-22W5
5-13-54-23W5
11-13-54-23W5
6-24-54-23W5
9-23-54-23W5
15-26-54-23W5
11-35-54-23W5
8-1-55-23W5
8-6-55-22W5
10-9-55-22W5
WABAMUN GROUP
UPPER WINTERBURN GROUP
LOWER WINTERBURN GROUP
UPPER WOODBEND GROUP
LOWER WOODBEND GROUP
Basinal
Reef Proximal
Basinal
Blueridge Reef
Basinal
NISKU BASINAL EQUIVALENT
g /w contact
2955 m
-2963 m
Nisku Reef
Leduc Reef
Leduc Reef
IRETON
IRETON
NISKU BASINAL EQUIVALENT
?
BASAL LEDUC PLATFORM
BASAL LEDUC PLATFORM

Western Canada Sedimentary Basin by post-Laramide time, which renders the maximum burial depth about 5200m at Obed. Using two geothermal gradients of 30°C/km and 20°C/km for the Paleocene and Early Tertiary, respectively (Kaufman *et al.*, 1990; Figure 3-4), the maximum burial temperature at Obed is estimated to have been 104 to 156°C.

The main emphasis of this study is placed on dolomitic reservoir rocks and inorganic cement phases. The porosity and permeability of the reservoir facies was preconditioned by the depositional facies (Figure 3-5), whereby reefal and reef proximal facies constitute the most porous and permeable lithologies. The geology of the Obed field and seismic and production data are briefly outlined in the Geophysical Atlas of Western Canadian Hydrocarbon Pools (Anderson *et al.*, 1989). The Geological Atlas of the Western Canada Sedimentary Basin provides an overview of the Devonian Woodbend and Winterburn strata (Switzer *et al.*, 1994). Otherwise, there is little published data on the Obed area.

The major objectives of this paper are to document new petrographical and geochemical data on the Upper Devonian carbonates of the Obed area, with an emphasis on the dolomite reservoir rocks and diagenetically late, inorganic cement phases, and to investigate evidence for bacterial sulfate reduction and thermochemical sulfate reduction reactions. Detailed core logging and thin section studies, as well as sulfur, oxygen, carbon, and strontium isotope analyses, are used to interpret the diagenetic evolution of the reefal buildups and constrain the relative timing of dolomitization and cementation. The textures and geochemistry of the late-diagenetic phases are the most important, as they will be shown to be genetically related to the sour gas in the area.

3.2. METHODOLOGY

Mapping and reconstruction of the Upper Devonian carbonate formations in the Obed area was accomplished using well log data and incorporating core descriptions where available. Although there are many wells in the Obed area, the well control over the platform is fair to poor. In the Obed study area, there are more than 50 wells that penetrate the top of the Devonian section (Wabamun Group), but only 32 available cores (Appendix A) of the Leduc Formation and Blueridge Member, which are the units of

Figure 3-4 The Cretaceous through Recent portion of the Swan Hills burial history curve. Temperatures outside of parentheses correspond to a paleogeothermal gradient of 30°C/km calculated for the Paleocene; temperatures within parentheses correspond to a paleogeothermal gradient of 20°C/km operative in the Early Tertiary. Approximately 1700m of post-Laramide erosion is estimated for this burial curve (Kaufman *et al.*, 1990).

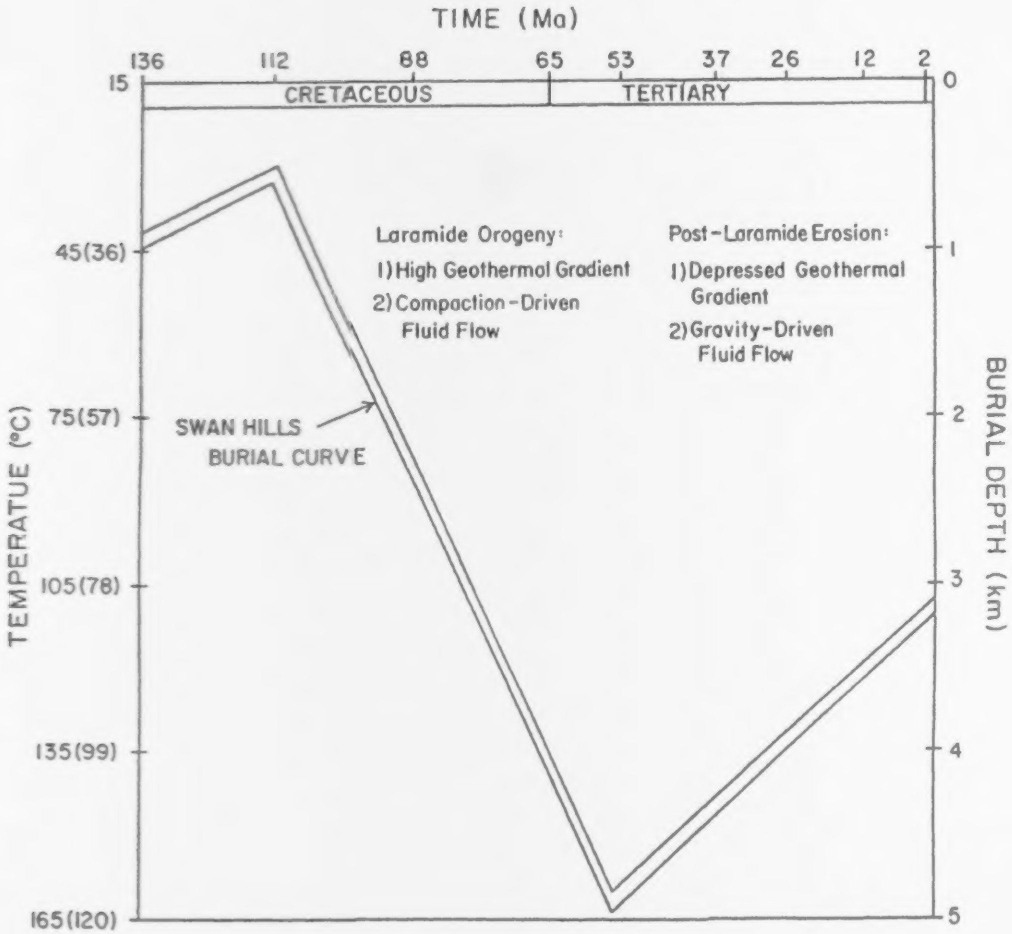
TIME (Ma)
136
112
88
65
53
37
26
12
2
CRETACEOUS
TERTIARY
15
45(36)
75(57)
105(78)
135(99)
165(120)
TEMPERATUE (°C)
0
1
2
3
4
5
BURIAL DEPTH (km)
Laramide Orogeny:
1) High Geothermal Gradient
2) Compaction-Driven Fluid Flow
Post-Laramide Erosion:
1) Depressed Geothermal Gradient
2) Gravity-Driven Fluid Flow
SWAN HILLS BURIAL CURVE

Figure 3-5 Schematic stratigraphic cross-section across the Obed area showing both subsurface and outcrop nomenclature of the Devonian carbonates.

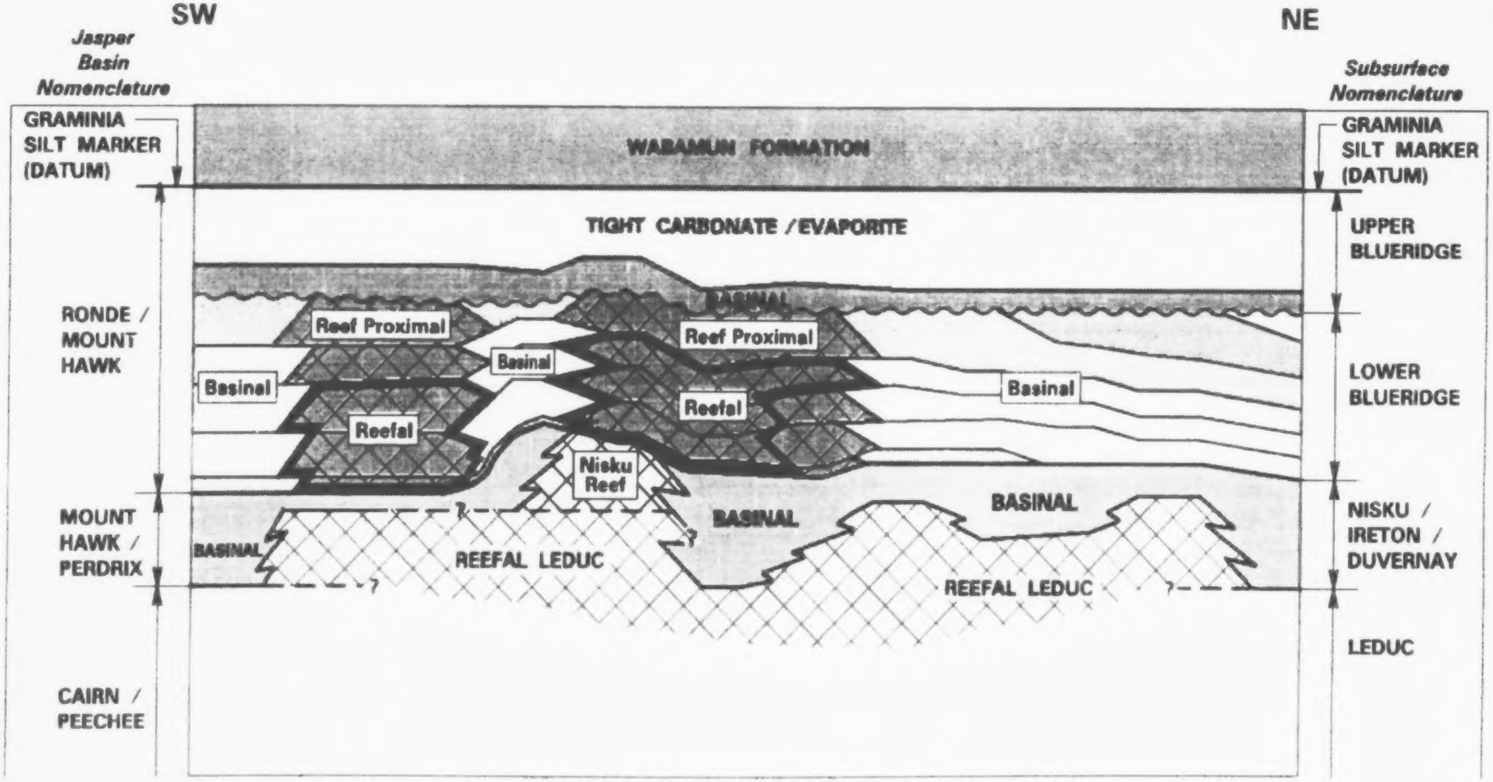
SW
NE
Jasper Basin Nomenclature
Subsurface Nomenclature
GRAMINIA SILT MARKER (DATUM)
GRAMINIA SILT MARKER (DATUM)
WABAMUN FORMATION
TIGHT CARBONATE / EVAPORITE
RONDE / MOUNT HAWK
MOUNT HAWK / PERDRIX
CAIRN / PEECHEE
UPPER BLUERIDGE
LOWER BLUERIDGE
NISKU / IRETON / DUVERNAY
LEDUC
BASINAL
Reef Proximal
Reef Proximal
Basinal
Basinal
Basinal
Reefal
Reefal
Nisku Reef
BASINAL
BASINAL
BASINAL
REEFAL LEDUC
REEFAL LEDUC
?

interest in this study. These cores were logged in detail and photographed at the Energy Resources Conservation Board (ERCB), Calgary. More than 700 core photos were taken of depositional facies characteristics, cements, and other sedimentary and diagenetic features. Samples from which thin sections were made and powders prepared for geochemical analyses were selected from about 300 core samples. Powdered samples from various wells and stratigraphic levels in the study area were removed with a dental drill. Thin sections (more than 200) were made from core samples, half-stained with Alizarin-red (Dickson, 1965).

Departmental facilities at the University of Alberta were used to conduct the strontium isotope analyses and some of the carbon and oxygen isotope analyses. A supplementary set of carbon and oxygen isotope data, as well as the sulfur and oxygen isotope analyses, were run at the University of Calgary, Department of Physics. Lead isotope compositions were determined as part of a larger reconaissance study of the Western Canada Sedimentary Basin. These data (Appendix B) proved to be of little value in interpretation of diagenesis in the Obed area and are not addressed further. Sample preparations and purifications were conducted by the author and the isotopic determinations were carried out by the staff at the aforementioned facilities (Appendix B). Carbon and oxygen isotope analyses of carbonates were conducted using procedures outlined in McCrea (1950) and Epstein *et al.* (1964). The precision of these measurements is ± 0.2‰ for $\delta^{13}C$ and ± 0.2‰ for $\delta^{18}O$. Sulfur and oxygen isotope ratios of anhydrite, pyrite, and elemental sulfur were analyzed by the methods described in Shakur (1982), Krouse (1983), and Ueda and Krouse (1986). The precision of isotope measurements of the sulfates are ± 0.2‰ for $\delta^{34}S$ and ± 0.8‰ for $\delta^{18}O$. Strontium isotope analyses of carbonates were carried out according to Baadsgaard *et al.* (1986), with a precision of better than 0.00005 (2σ). The data in all plots in this study have analytical precision better than the size of the symbols used on these graphs. Data tables are found in Appendix B.

3.3. PETROGRAPHY AND PARAGENETIC SEQUENCE

The paragenetic sequence of 15 events (Figure 3-6) was determined through visual examination of core and the petrographic study of thin sections from core samples of the Obed area. Individual events are described later in this section. Textural and geochemical changes during late-diagenetic events are the main focus of this research, with a secondary focus on the early dolomitization and primary anhydrites of the Upper Blueridge Member (Winterburn Group). Late diagenetic cements include dolomite and calcite, with secondary anhydrite, sulfur and pyrite also contributing to the destruction of porosity. The depths and timing of the paragenetic events are indicated in Figure 3-6. Shallow (<500m), intermediate (500-2000m), and deep (>2000m) burial regimes are defined by Drivet (1993, and references therein). Burial curves, for timing of events relative to burial depth in this part of the Western Canada Sedimentary Basin may be found in Drivet (1993) and Kaufman *et al.* (1990). The temperature-depth-time relations were derived by the aforementioned authors through the use of fluid inclusions in rocks of various ages to determine paleotemperatures, and by assuming a geothermal gradient of 30°C/km (Hudson and Anderson, 1989) and a surface temperature of 30°C (Walls *et al.*, 1979) to determine burial depth.

The percentages of diagenetic cement phases were visually estimated from cores. Within the platform area, secondary anhydrite is the only phase that, in the Leduc Formation (Woodbend Group), does not seem to be present in abundance in the updip portion of the platform, but is present throughout in the Winterburn carbonates. All other diagenetic phases appear in both the Woodbend and Winterburn Groups in similar abundances throughout the platform area (Figure 3-2). The presence and percentage of dolomitization and cementation are very low in the basinal regions. This distribution is probably controlled by the ease of migration of fluids, including hydrocarbons, through the porous reefal facies of the platform, relative to the less porous and permeable basinal facies.

3.3.1. Dolomitization and Dolomite Cementation

Dolomite types in the Obed study area occur as replacive dolomite (Event 5,

Figure 3-6 Paragenetic sequence in the Obed area. Designations of depths of burial are explained in Drivet (1993) and Kaufman et al. (1990); they were derived through the use of fluid inclusions to determine paleotemperatures. By assuming a geothermal gradient of 30°C/km (Hudson and Anderson, 1989) and a surface temperature of 30°C (Walls et al., 1979), burial depths were derived.

PARAGENETIC SEQUENCE

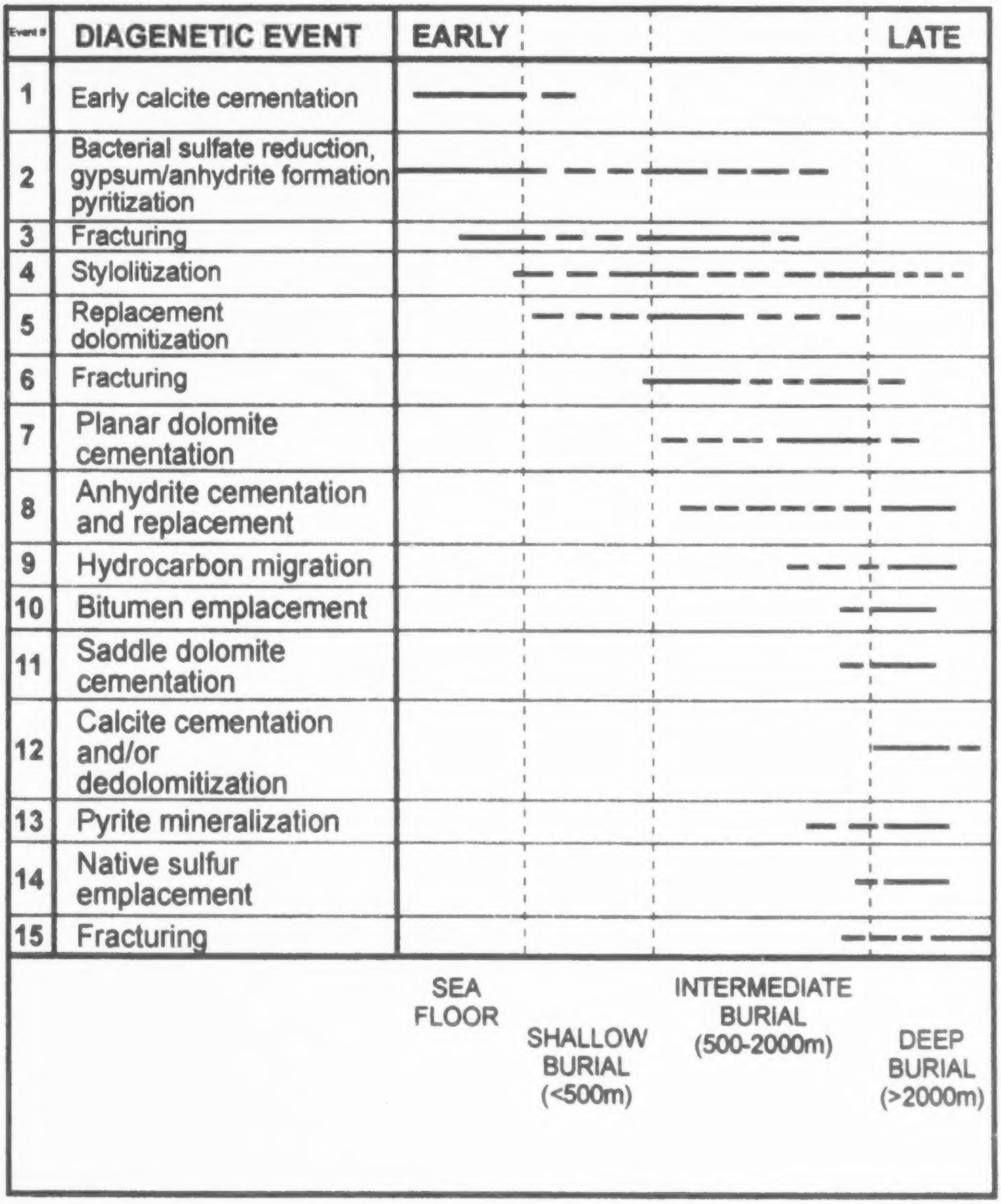
EARLY
LATE
SEA FLOOR
SHALLOW BURIAL (<500m)
INTERMEDIATE BURIAL (500-2000m)
DEEP BURIAL (>2000m)

Event #	DIAGENETIC EVENT
1	Early calcite cementation
2	Bacterial sulfate reduction, gypsum/anhydrite formation pyritization
3	Fracturing
4	Stylolitization
5	Replacement dolomitization
6	Fracturing
7	Planar dolomite cementation
8	Anhydrite cementation and replacement
9	Hydrocarbon migration
10	Bitumen emplacement
11	Saddle dolomite cementation
12	Calcite cementation and/or dedolomitization
13	Pyrite mineralization
14	Native sulfur emplacement
15	Fracturing

Figure 3-6) and dolomite cements (Events 7 and 11, Figure 3-6). Widespread, pervasive, matrix-selective dolomitization of Event 5 has resulted in the replacement of the original limestones. Pervasive replacement dolomitization is inferred to have occurred mainly during intermediate burial in Late Devonian to Mississippian time throughout the Western Canada Sedimentary Basin (Amthor *et al.*, 1993). Later, minor dolomite cements filled, or partially filled, pore spaces during deeper burial. Similar dolomite types have been observed by Drivet (1993) and Amthor *et al.* (1993).

Replacive matrix dolomite (Event 5, Figure 3-6) crosscuts all formations and facies. This dolomite is light to dark grey and light to medium brown, with xenotopic to hypidiotopic replacive texture, and ranges in crystal size from fine-crystalline to medium-crystalline and exhibits straight to undulose extinction (A and B, Figure 3-7). Commonly, this dolomite also occurs as a hypidiotopic to idiotopic medium to coarse grained texture. The abundance and nature of each texture type depends on the facies zone in which the dolomite occurs and the amount of mud comprising the matrix. Medium to coarse grained dolomites retain fossil outlines but are fabric destructive, whereas primary structures and textures may be well preserved where marine limestone (mudstone to grainstone) has been replaced by fine grained dolomite. In basinal limestones, fossils such as brachiopods exhibit neomorphism of their primary calcite shells.

Two common types of dolomite cement are coarse, planar dolomite (Event 7, Figure 3-6) and very coarse saddle dolomite (nonplanar; Event 11, Figure 3-6). These late dolomite cements fill intercrystalline, moldic, and vuggy porosity, as well as fractures, especially where brecciated. Corrosion rims are present locally and zoning is very common.

Medium to coarse crystalline, idiotopic to hypidiotopic planar dolomite cement (C and D, Figure 3-7) is generally light brown in color. Planar dolomite cements exhibit a straight extinction. It is generally found directly adjacent to the matrix replacement dolomite. Both dolomite cements comprise a volumetrically small component of the rock, on average less than 2%. The idiotopic to hypidiotopic saddle dolomite is typically white in color (A and C, Figure 3-8) and has curved crystal faces (B and D, Figure 3-8). Saddle dolomite can range in size from coarse to very coarse crystalline and overgrew,

Figure 3-7 A. Fine grained, medium grey replacive dolomite matrix with moldic porosity (hand sample 5-13-54-23W5; 13400').
B. Photomicrograph (30X magnification; cross polarization) of medium brown xenotopic to hypidiotopic replacive dolomite (thin section, sample 2-36-54-23W5; 13664').
C. and D. Photomicrographs (60X magnification; plane polarization) of idiotopic to hypidiotopic zoned planar dolomite (thin sections, samples 2-36-54-23W5; 13350' and 2-36-54-23W5; 13411', respectively). Alizarin-red staining shows the presence of calcite.

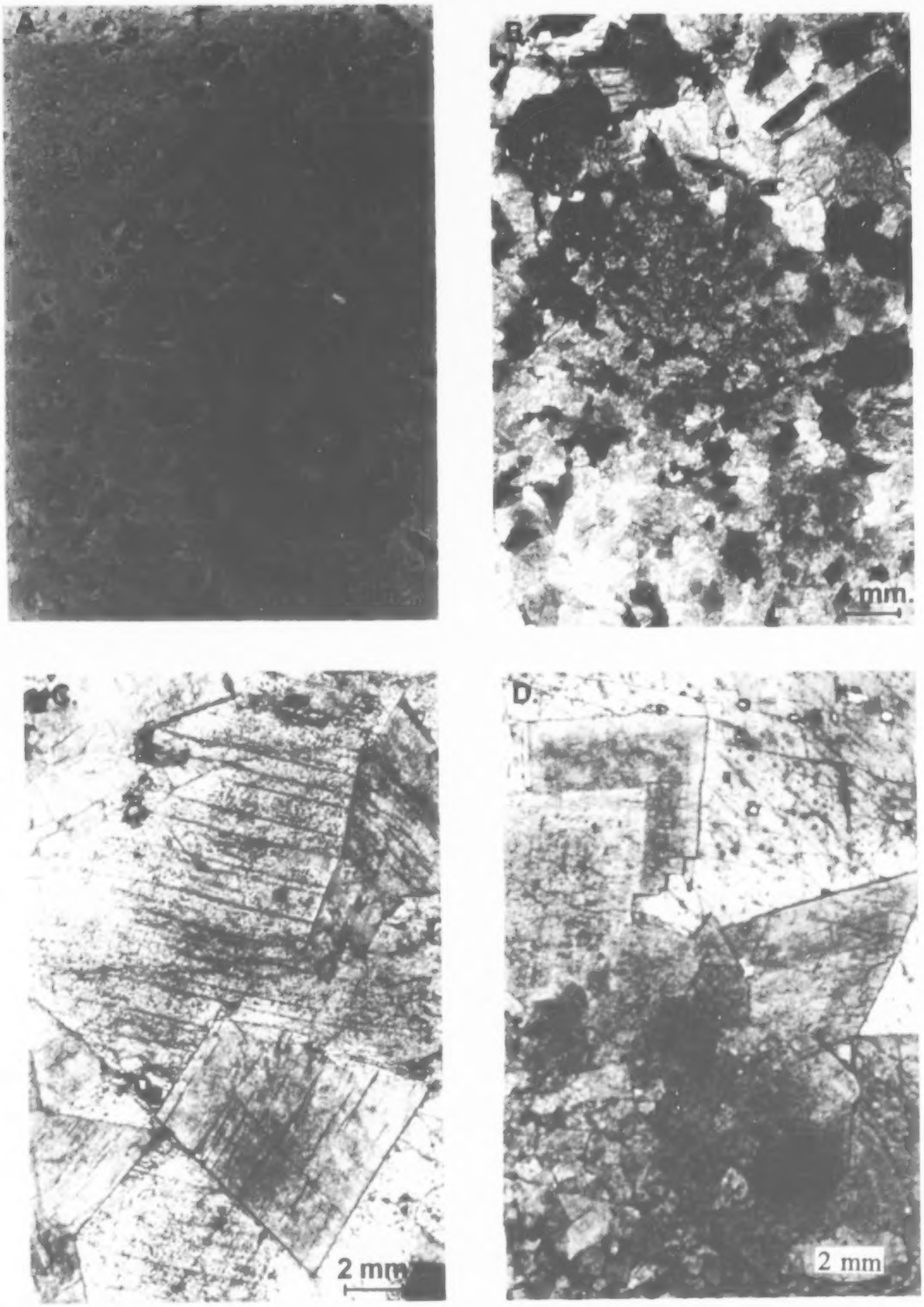
A
B
mm.
C
2 mm
D
2 mm

Figure 3-8 A. and C. White saddle dolomite cement filling moldic porosity in medium grey replacive dolomite matrix (hand samples 9-30-52-22W5; 4527.6m and 10-27-52-24W5; 4690.2m, respectively).

B. and D. Photomicrographs (30X and 60X magnification, respectively; plane polarization and cross-polarzation, respectively) of saddle dolomite crystals in replacive dolomite matrix (thin sections, samples 6-24-54-23W5; 4103.25m and 5-13-54-23W5; 13376′, respectively). Alizarin-red staining shows the presence of calcite.

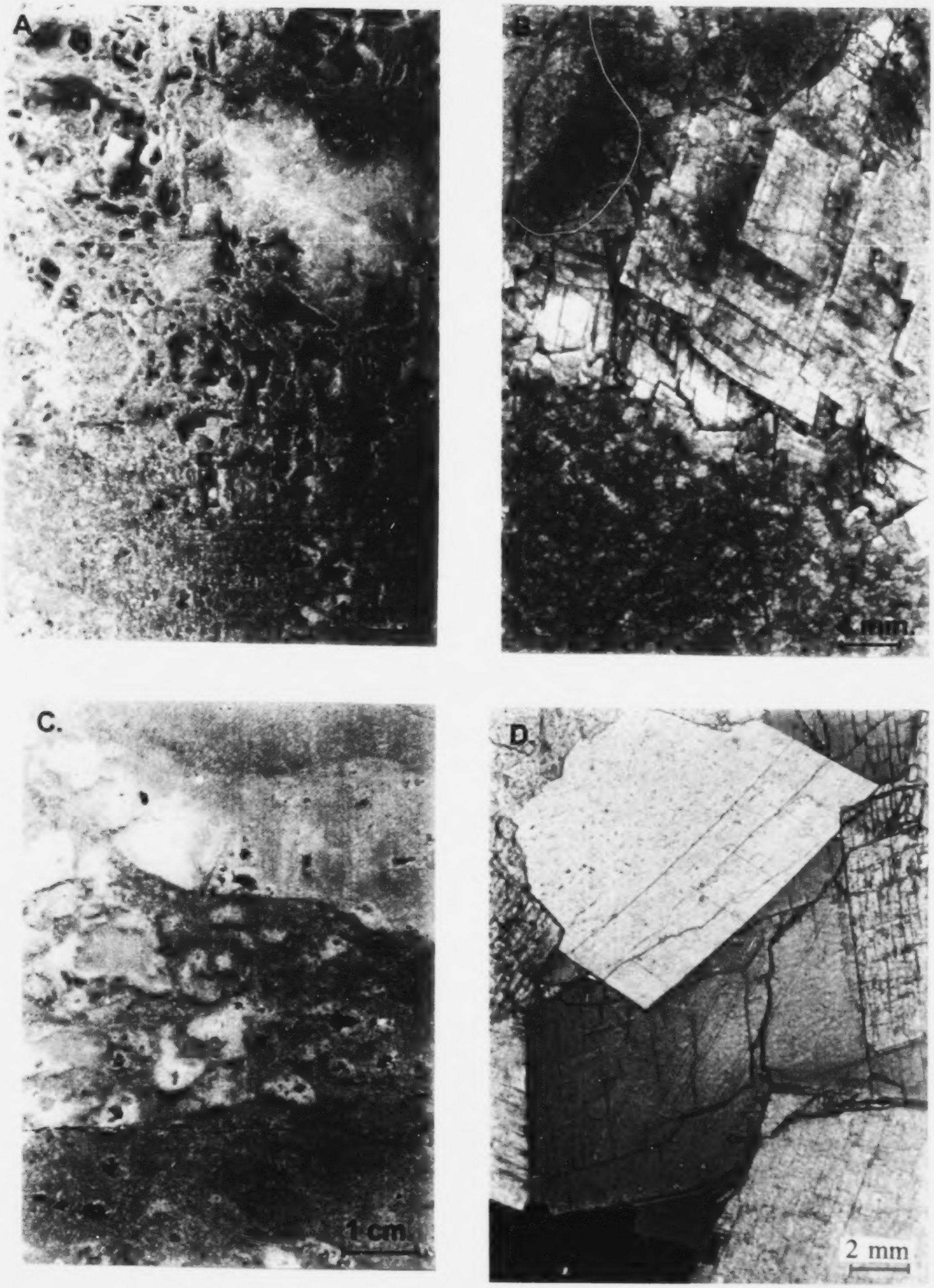
A
B
1 mm.
C.
1 cm.
D.
2 mm

and therefore post-dates, the medium to coarse planar dolomite cement lining the void space. Saddle dolomite also occurs directly adjacent to the replacement dolomite matrix. Saddle dolomite exhibits a sweeping extinction.

3.3.2. Calcite Cementation

Early diagenetic calcite (Event 1, Figure 3-6) is found only in the basinal facies as fossil replacements (A, Figure 3-9). Late-diagenetic calcite cement (Event 12, Figure 3-6) is much more common and formed during late diagenesis under deep burial conditions. It fills intercrystalline, moldic and vuggy porosity, as well as fracture and tension gash porosity (B, C, and D, Figure 3-9). This calcite cement post-dates and corrodes replacive dolomites and dolomite cements. Late-diagenetic calcite ranges in crystal size from very fine grained, anhedral to very coarse grained, euhedral, with common twinning. Crystals are limpid to translucent. Large calcite crystals are blocky, ranging in size from less than 0.5cm to 1cm (C, Figure 3-9) with abundant fluid inclusions. This calcite is replacive as well as void filling, commonly replacing anhydrite void fill (D, Figure 3-9), in which case it is very fine grained and appears sucrosic. It also replaces dolomite rimming pore spaces. Late calcite that corroded and replaced dolomite is generally cleaved with microfractures and contains inclusions of the dolomite which it replaced. Dedolomitization is also common. In general, late calcite cement is much finer grained where replacive than where it is void filling, and it commonly comprises 2-5% of the rock.

3.3.3 Sulfur Phases

Primary (syn-depositional) anhydrite (Event 2, Figure 3-6) is abundant in the Upper Blueridge and has been altered by early diagenetic processes. Secondary (post-depositional) anhydrite (Event 8, Figure 3-6), early and late pyrite (Events 2 and 13, respectively, Figure 3-6), and late native sulfur (Event 14, Figure 3-6) volumetrically constitute a minor percentage of the total rock. The late diagenetic phases post-date pervasive replacement dolomitization and the initiation of hydrocarbon migration (Event 9, Figure 3-6). They occur as intercrystalline, moldic, vuggy, and fracture void fill, either

Figure 3-9 A. Calcite replaces fossils in basinal lime mudstone (hand sample 12-15-53-22W5; 13176′).

B. Calcite fills moldic porosity in fossil packstone/floatstone (hand sample 7-18-52-24W5; 4824.5m).

C. Coarse calcite crystals fill fractures (hand sample 14-23-53-23W5; 4126.85m).

D. Fine to coarse (0.5cm) calcite crystals ($^{87}Sr/^{86}Sr$ = 0.72010) fill moldic and fracture porosity (hand sample 5-7-54-23W5; 4381.3m).

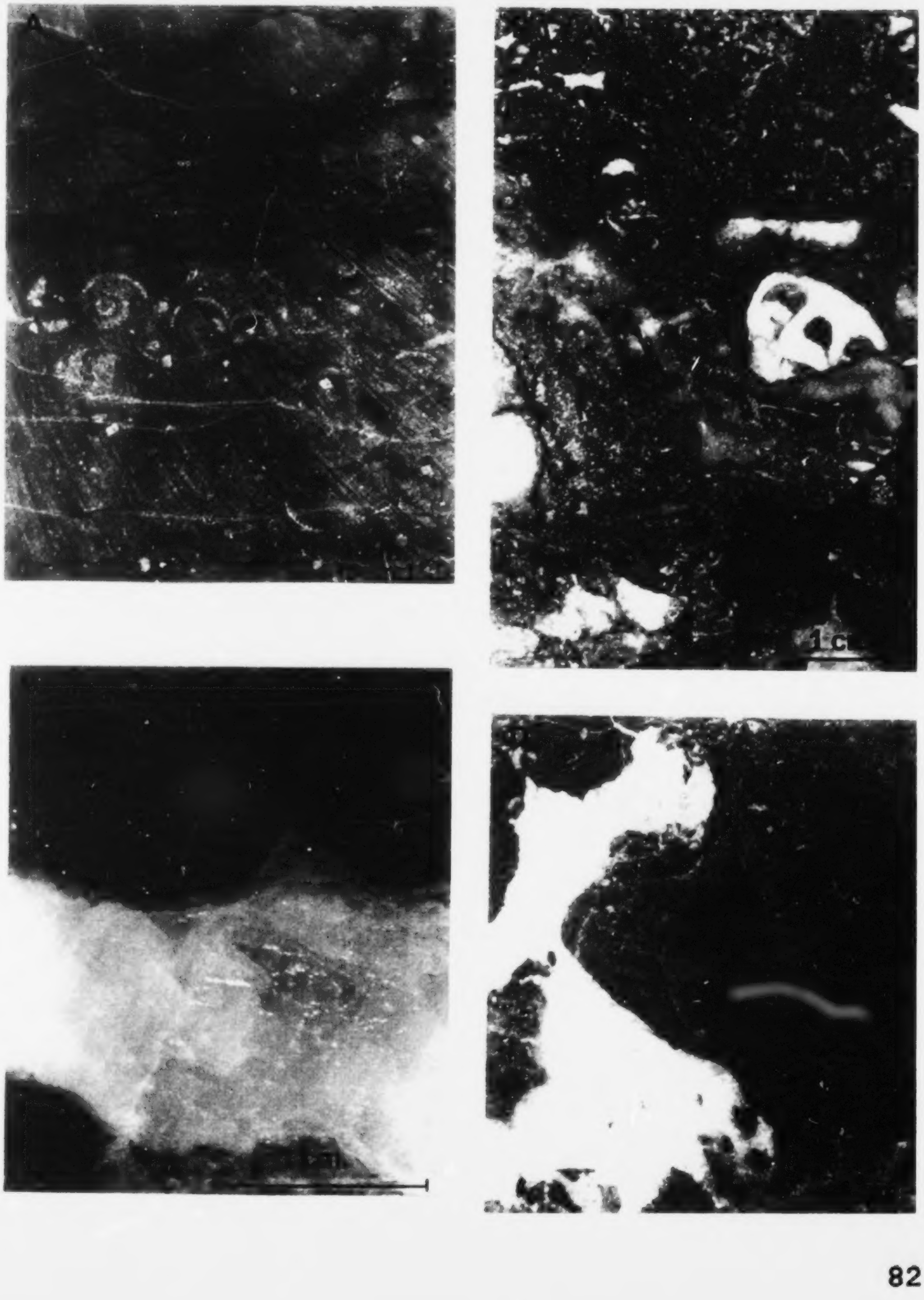
A
1 c

partially or completely filling porosity.

Both primary and secondary anhydrite are represented in the study area. Primary anhydrite (Event 2, Figure 3-6), which occurs only in the Upper Blueridge, formed in intertidal to supratidal depositional environments. It is commonly milky white to light grey, interbedded with dolomite (A and B, Figure 3-10). This anhydrite probably provided the source of the sulfate which migrated downward into the underlying Winterburn and Woodbend Groups, resulting in the formation, during burial, of the secondary anhydrite. Secondary anhydrite (Event 8, Figure 3-6) occurs in all depositional facies, either replacive and/or as a cement. Subsequent dissolution of replacive anhydrite has been identified as one of the mechanisms responsible for the generation of vuggy porosity (Murray, 1960). Locally, anhydrite tends to replace the replacement dolomite matrix and/or the dolomite cement, producing large vugs in which the anhydrite abuts directly against the host dolomite. This replacive anhydrite can mimic the dolomite crystal shape. As shown by Machel and Burton (1991), replacive secondary anhydrite nodules are commonly associated with bitumen and bituminous argillaceous seams and contain inclusions of the matrix dolomite. Where anhydrite forms a cement, partially filling moldic and fracture porosity, the crystals postdate the dolomite cement phase and occur as idiotopic fibrous to bladed laths, with dimensions ranging from millimeter to centimeter size (C, Figure 3-10). When filling larger vugs, or replacing the matrix, anhydrite generally is felted, being more massive and fine grained (D, Figure 3-10). Anhydrite is commonly replaced pseudomorphically by calcite. Where present, anhydrite replacement and cement together comprise, on average, up to 5% of the rock.

Pyrite (Events 2 and 13, Figure 3-6) occurs as disseminated crystals and as clusters in intercrystalline porosity, associated with moldic, vuggy, and fracture porosity. It is also common along stylolites (A, Figure 3-11). Pyrite can range in size from commonly <1mm (B, C, and D, Figure 3-11) to >0.5cm large clusters (B and D, Figure 3-11). Locally, pyrite replaces fossils, as well as dolomite and calcite, and occurs along bedding planes. Pyrite occurs as early-diagenetic biogenic pyrite (Event 2, Figure 3-6) and as late-diagenetic pyrite (Event 13, Figure 3-6). Where authigenic pyrite is seen to overgrow the late dolomite and calcite cement, secondary anhydrite, and other late diagenetic phases,

Figure 3-10 A. and B. White to light grey primary anhydrite interbedded with medium grey dolomite; Upper Blueridge Member (hand samples 02/15-26-54-23W5; 4007m and 02/15-26-54-23W5; 4019.75m, respectively).

C. Anhydrite crystal laths partially infilling moldic porosity of medium grey replacive dolomite (hand sample 10-13-52-22W5; 4386.8m).

D. Felted anhydrite filling vuggy porosity and replacing the dolomite host rock (hand sample 10-13-52-22W5; 4381.2m).

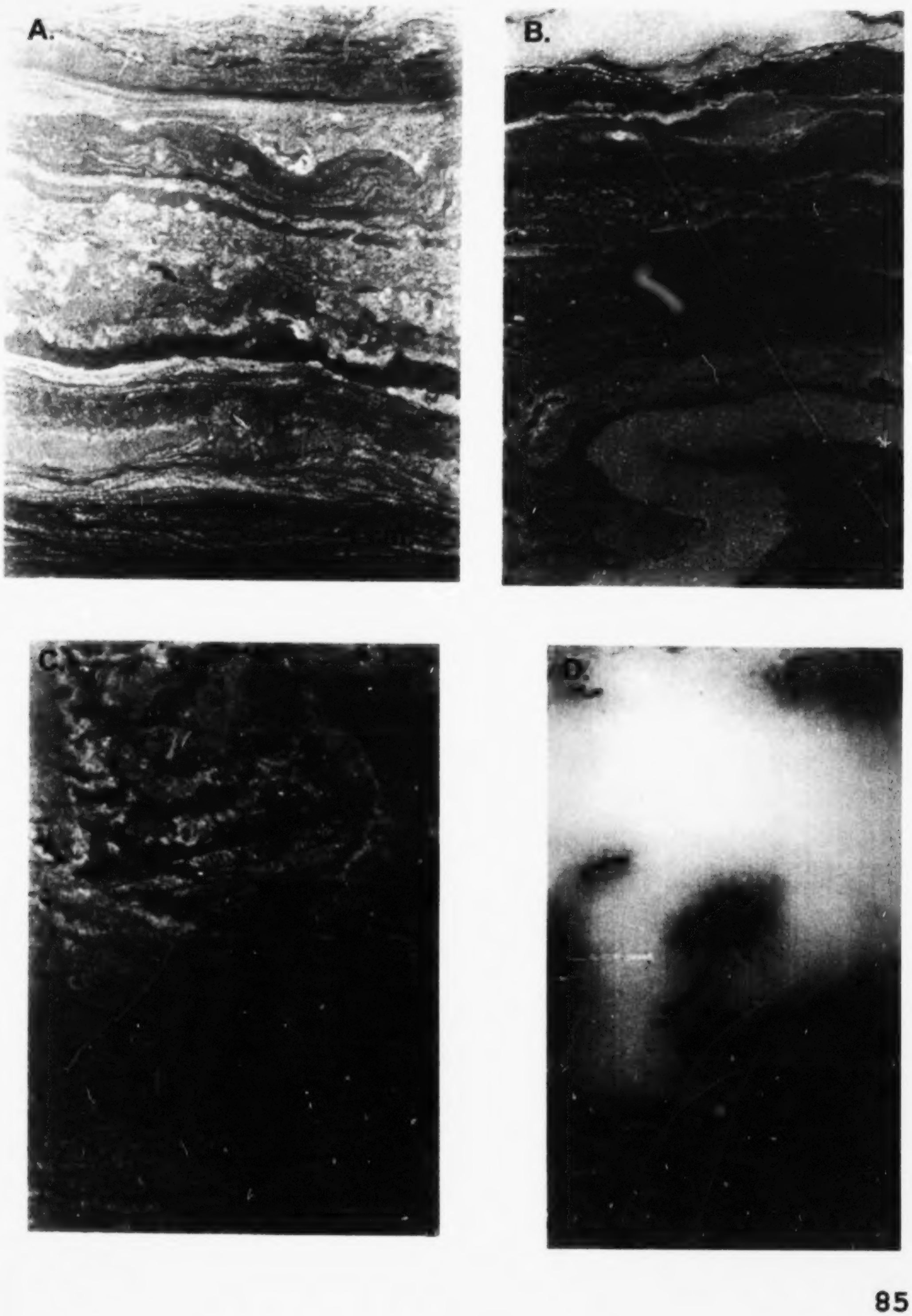
A.
B.
C.
D.

Figure 3-11 A. Pyrite ($\delta^{34}S$ = -7.18‰) along stylolite (hand sample 02/15-26-54-23W5; 4108.7m).

B. Photomicrograph (30X magnification; plane polarization) of pyrite along stylolites, disseminated in replacive dolomite matrix, and as clusters (thin section, sample 11-35-54-23W5; 13661.5′).

C. Disseminated pyrite ($\delta^{34}S$ = 13.23‰) in medium brown replacive dolomite matrix (hand sample 5-23-55-22W5; 12785.6′).

D. Photomicrographs (30X magnification; plane polarization) of intercrystalline pyrite and pyrite clusters (thin section, sample 2-36-54-23W5; 13350′).

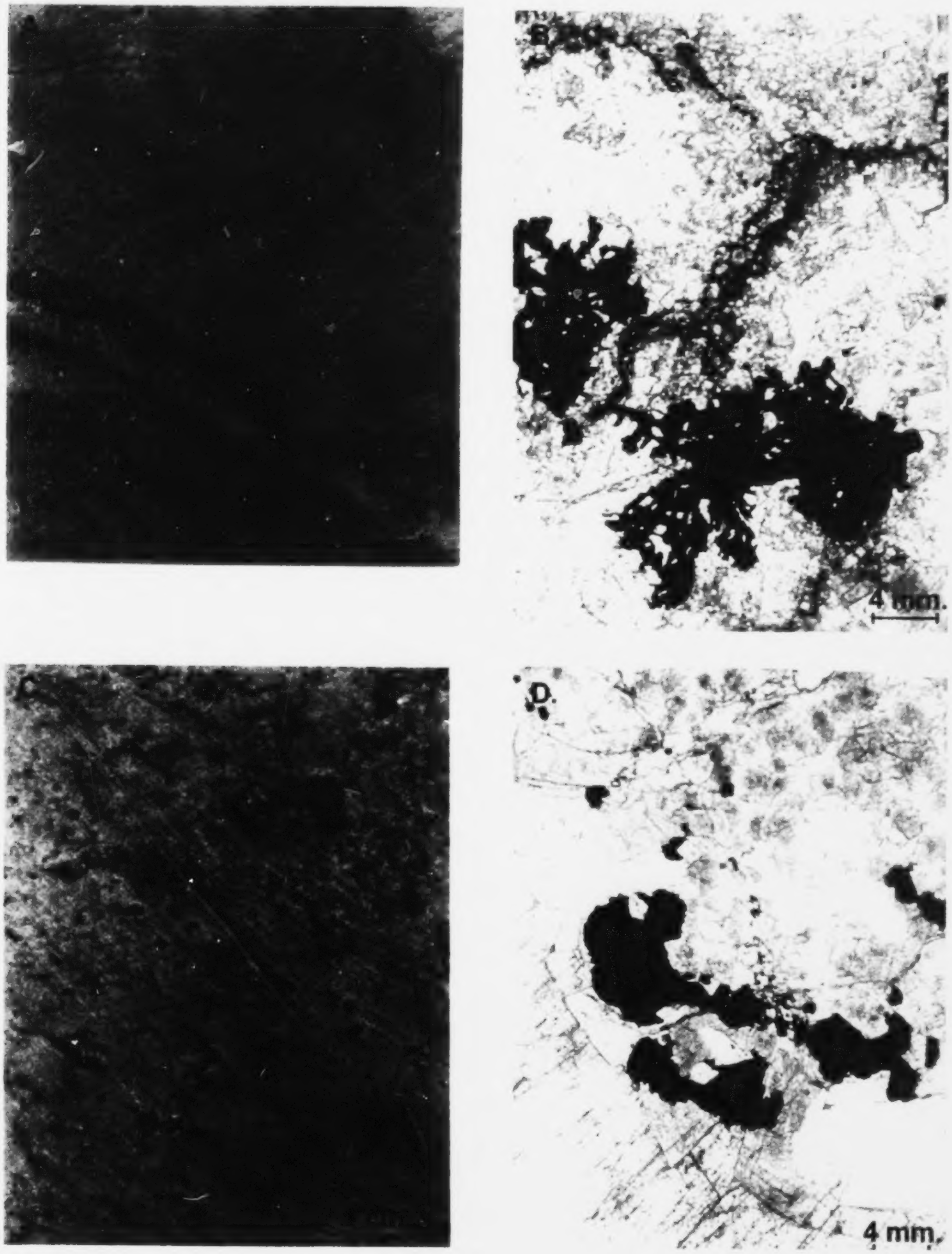
B
4 mm.
D.
4 mm.

it is interpreted to be late-diagenetic. Locally, pyrite can also appear as inclusions in these late-diagenetic phases, and is thus inferred to have been formed earlier. The sparse amounts of pyrite and paucity of textural relationships make it difficult to constrain the relative timing of pyrite-forming diagenetic events, which seem to have occurred over a long interval of time. There are no morphological characteristics of the samples collected for this study which allow for an unambiguous distinction between early and late pyrite. Pyrite occurrences are volumetrically small, less than 1%.

Elemental sulfur (Event 14, Figure 3-6) occurs throughout the Woodbend and Winterburn Groups of the study area in intercrystalline voids and is commonly associated with replacement dolomite and calcite cement, especially where the calcite replaces anhydrite and appears sucrosic. Sulfur also occurs in moldic and vuggy porosity where it is associated with late dolomite and calcite cements, as well as pyrite. It can also be found in fractures and along skeletal boundaries of fossils. Large euhedral to subhedral (A, Figure 3-12), anhedral (B, Figure 3-12), and fine grained disseminated (C and D, Figure 3-12) crystals of sulfur are seen in thin section and hand specimen. Elemental sulfur constitutes less than 1% of the rock.

3.3.4 Other Diagenetic Phases

There are several other diagenetic features in the paragenetic sequence which will be briefly addressed. Horizontal, inclined, and vertical fractures vary in abundance from nil to greater than 5%, and the fractures range in width from about 200-500 micrometers to several millimeters, and in length to several centimeters. Late-diagenetic fractures are most commonly filled with fine to coarse crystalline calcite cement, but other fracture-fills include dolomite, anhydrite, bitumen, and pyrite.

High amplitude stylolites may be associated with restricted deposition or short hiatuses, whereas low-amplitude stylolites and microstylolites are common features in low-energy lagoonal and basinal carbonates, and are commonly found along bedding planes and at the edges of skeletal fossils. Pyrite and clay minerals are often found along stylolites. Stylolites of varying thicknesses and amplitudes cross-cut the matrix dolomite; the average stylolite dimension is 1mm thick and greater than 7cm long.

Figure 3-12 A. Euhedral to subhedral elemental sulfur ($\delta^{34}S$ = 20.25‰), associated with white saddle dolomite cement and bitumen, partially infills the secondary moldic porosity of the medium grey to medium brown dolomite matrix (hand sample 7-1-53-24W5; 4532.25m).

B. Anhedral ("globular") native sulfur infills the moldic secondary porosity of medium grey replacive dolomite (hand sample 4-26-52-23W5; 4468.9m).

C. Native sulfur ($\delta^{34}S$ = 23.03‰) disseminated throughout felted calcite, which replaces anhydrite, and is associated with pyrite ($\delta^{34}S$ = 21.63‰; hand sample 7-15-52-22W5; 13738').

D. Photomicrograph (120X magnification; plane polarization and reflected light) of native sulfur disseminations in replacive dolomite matrix (thin section, sample 10-13-52-22W5; 4383.7m).

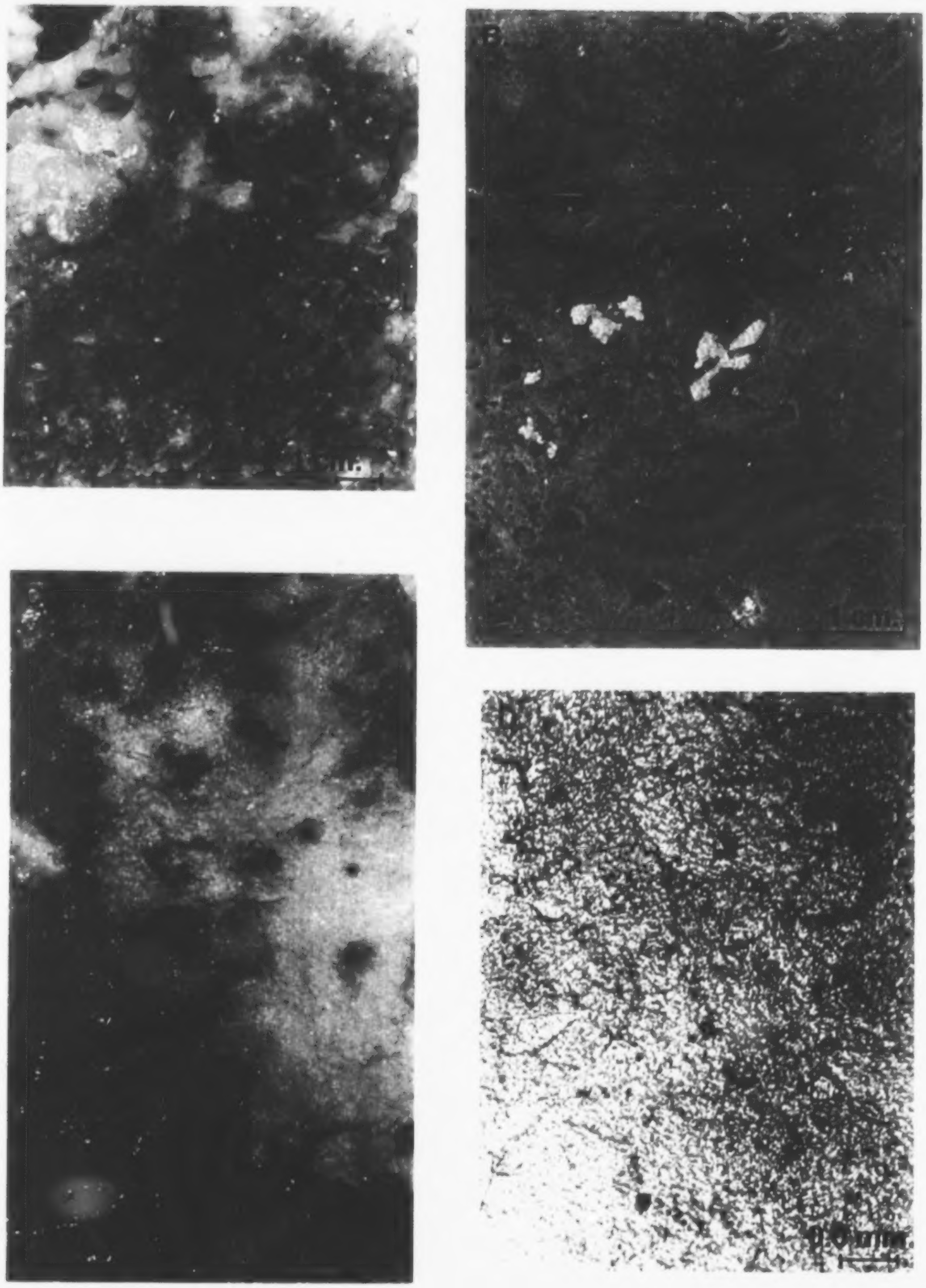
B
D
1.0 µm

Late-diagenetic bitumen is common, filling intercrystalline porosity, and is associated with late cements in moldic and vuggy porosity. Bitumen is also present in fractures and along faces of void-filling crystals. Bitumen commonly occurs disseminated through the matrix but may be present as clusters up to 0.5cm in diameter. The amount of solid bitumen varies considerably and is unpredictable. The average amount of bitumen ranges from nil to 5%. Quartz occurs rarely, as a very late porosity fill.

3.3.5 Porosity Generation and Destruction

In the Obed area, the highest porosities and permeabilities are encountered in the back-reef, reef crest, and reef slope environments. Porosity and permeability are controlled by a complex sequence of diagenetic events (Figure 3-6), with secondary porosity generated by dolomitization and modified by later dissolution. Secondary porosity types include intercrystalline, moldic, and vuggy porosities, and their occurrence depends on the types and abundances of leached fossils comprising the facies and/or the nature (fabric and texture) of the matrix. Fracturing of any facies assemblage can contribute to or account for the porosity present, if these fractures are not cemented.

Cementation of void spaces is common, voids being partially or completely infilled with secondary anhydrite, pyrite, native sulfur, as well as late planar and saddle dolomite cement and calcite cement. Facies and depositional environments of the Blueridge Member and Leduc Formation intervals were characterized by detailed core study and mapping (Figure 3-5). Porosity types are related to the types and sizes of skeletal debris, which in turn are related to depositional facies. Moldic (up to 2cm diameter) and vuggy (greater than 5cm diameter) porosity of various shapes, sizes, and percentages occur in places where fossils were present. Intercrystalline (less than 1mm diameter) porosity, with an absence of mud, is common in high energy environments, such as reefal environments where the fine grained material is washed away leaving interstitial voids. When not filled with late cements, these voids remain open and also add to the porosity. Hence, the reefal facies of the Blueridge Member, Nisku Formation, and Leduc Formation make good reservoir rocks where moldic, vuggy, or intercrystalline porosity (Choquette and Pray, 1970), or any combination of these porosity types with good permeability, exists.

3.4. INORGANIC GEOCHEMISTRY - EFFECTS OF BSR AND TSR

The formation of hydrogen sulfide and related mineralic sulfur phases involves the reduction of sulfate and the oxidation of organic compounds either by bacterial sulfate reduction (BSR) or thermochemical sulfate reduction (TSR). BSR is usually facilitated by disseminated organic matter (kerogen). In this area of the Western Canada Sedimentary Basin, oil migration and maturation took place in the Late Cretaceous to Early Tertiary (Kaufman *et al.*, 1990), and provided the organic materials necessary for TSR. BSR and TSR processes occur in mutally exclusive thermal regimes (Orr, 1977; Machel, 1987a; Wade *et al.*, 1989). Thermochemical sulfate reduction is an exothermic process producing H_2S and other diagenetic products in high-temperature environments with 80 to 100 < T < 150 to 200°C, corresponding to depths of about 2000 to 6000m at normal geothermal gradients (Machel *et al.*, 1995). Bacterial sulfate reduction occurs in low-temperature diagenetic environments, 0 < T < 60 to 80°C at depths less than 2000 to 2500m (Machel *et al.*, 1995), to produce biodegraded hydrocarbons, and H_2S. The uppermost temperature limit for BSR is based on the temperature below which the bacteria will metabolize and be active; the lower limit for TSR is the temperature below which the reaction rates are too slow to be significant over tens of millions of years (Kiyosu and Krouse, 1990). The end products of BSR and TSR depend on initial reactants. The common redox reactions operating in both of these diagenetic regimes generate hydrogen sulfide and inorganic phases such as calcite, dolomite, pyrite, and elemetal sulfur. These inorganic products are the focus of this study. Also important is primary anhydrite, considered to be representative of the reactant, or initial, sulfate necessary to produce these diagenetic phases by BSR or TSR.

Figure 3-13 illustrates the net mass and charge balanced reactions representative of the geochemical processes responsible for the dissolution of sulfates and generation of H_2S, and the products and byproducts of TSR and BSR. Reactions 1 and 2 are specific to BSR and thermal cracking, respectively, whereas most redox reactions involving hydrocarbons and inorganic sulfur compounds are valid for both BSR and TSR (Machel *et al.*, 1995). A comprehensive overview of the redox reactions responsible for BSR and TSR is found in Machel *et al.* (1995) and is the basis for the following summary of these

Figure 3-13 Reaction scheme for bacterial and thermochemical sulfate reduction.

BSR and TSR REACTIONS

REACTION 1

paraffinic hydrocarbons → biodegraded hydrocarbons

REACTION 2

crude oil → light crude oil + H_2S (+ PS) + CH_4

REACTION SET 3

$4R - CH_3 + 3SO_4^{2-} + 6H^+ \rightarrow 4R - COOH + 4H_2O + 3H_2S$

$R - CH_3 + 2R = CH_2 + CH_4 + 3SO_4^{2-} + 5H^+ \rightarrow 3R - COOH + HCO_3^- + 3H_2O + 3H_2S$

$2CH_2O + SO_4^{2-} \rightarrow 2HCO_3^- + H_2S$

REACTION SET 4

$2H_2S + O_2 \rightarrow 2S^0 + 2H_2O$

$3H_2S + SO_4^{2-} + 2H^+ \rightarrow 4S^0 + 4H_2O$

$H_2S + SO_4^{2-} + 2H^+ \rightarrow S^0 + 2H_2O + SO_2$

H_2S + hydrocarbons → S^0 + altered hydrocarbons

$S^{2-} \rightarrow S^0$

REACTION 5

$4S^0 + 1.33\ (-CH_2-) + 2.66\ H_2O + 1.33\ OH^- \rightarrow 4H_2S + 1.33\ HCO_3$

REACTION 6

hydrocarbons + SO_4^{2-} → altered hydrocarbons

+ solid bitumen + HCO_3^- (CO_2) + H_2S (HS^-) + heat reactions necessary to generate the diagenetic phases of geochemical interest for the Obed study area. These reactions have been developed on the basis of reactants and their products found in nature or experimentally, as outlined in Machel (1987a, and 1995), and references therein.

Dissolved primary anhydrite, with an isotopic composition representative of Devonian seawater, is considered to be the sulfate source for the generation of hydrogen sulfide during both bacterial sulfate reduction (BSR) and thermochemical sulfate reduction (TSR). Aerobic biodegradation of hydrocarbons is necessary at low temperature regimes for BSR to occur at significant rates (Reaction 1; Figure 3-13). Very small percentages of H_2S can be generated during BSR as long as conditions and nutrients are sufficient to sustain the bacteria. Microbial sulfate production in petroleum reservoirs is very limited in terms of hydrogen sulfide (produces 1-3% H_2S; Orr, 1977) but its products may act as a catalyst for TSR. At moderate burial or temperature regimes, maturation, or thermal cracking, responsible for oil generation, migration, and accumulation in reservoirs, occurs. This process is responsible for the formation of minor amounts of H_2S, methane, and polysulfides through the decomposition of organic sulfur compounds (Reaction 2; Figure 3-13). The high concentration of H_2S present at Obed (up to 30%) was generated at deep burial where maturation was accompanied and followed by TSR reactions (Machel *et al.*, 1995, Reactions 3 and 5 via 4; Figure 3-13). The third reaction set (Figure 3-13), with differences in reactions dependent on the reactants, deals with the initial S-O bond breakage and reduction of sulfur species (S^{6+} reduced to S^{2-}). The important reaction products are organic acids, bicarbonate ions and hydrogen sulfide, with bitumen being a possible by-product. The partial reoxidation of the hydrogen sulfide produced by these reactions yields elemental sulfur and various other products and by-products (Reaction set 4, Figure 3-13). This reaction set represents the abiological oxidation of H_2S by molecular oxygen, excess dissolved sulfate, or saturated hydrocarbons under varying conditions. Oxidation of sulfide ions may also be mediated by anaerobic or aerobic bacteria, as illustrated by the valence change of sulfur shown in the last equation of reaction set 4 (Figure 3-13). Elemental sulfur formed in this reaction does not generally survive as a separate phase but is reduced to S^{2-} as in reaction 5 (Figure 3-13). Main reaction products of reduction of elemental sulfur are bicarbonate ions, hydrogen sulfide, and possibly bitumen. Hydrogen sulfide, elemental sulfur, and polysulfides are partially recycled in reactions 3, 4, and 5. Therefore, these reactions are summarized in the net mass balance reaction, reaction 6 (Figure 3-13), which assumes all the elemental sulfur produced in reaction 4 was used up in reaction 5. This reaction summarizes the TSR process: hydrocarbons react with sulfate to produce altered hydrocarbons, solid bitumen, bicarbonate ions and/or carbon dioxide, hydrogen sulfide and/or HS^-, and heat. The initial order of these reactions and their degree of completion may vary depending on ambient conditions and reactants present. If reaction 5 does not proceed to completion, native sulfur will be present. If Fe^{2+} is present in the system, pyrite will form. Precipitation of carbonates (calcite and saddle dolomite) result from the presence of alkaline earth metals. Once reactions 3, 4, and 5 are started, they will proceed simultaneously at or near the aerobic (reaction 4 bacteria)/anaerobic (reaction 3 and 5 bacteria) interface, which could be the hydrocarbon/water contact (Machel *et al.*, 1995). Hydrogen sulfide, dissolved in formation water, evolves as a gas once its concentation exceeds its aqueous solubility. Thermochemical sulfate reduction accounts for high H_2S concentrations present in sour gas fields such as Obed.

The solid phases investigated in this study are the source sulfate (primary anhydrite), redistributed sulfate (secondary anhydrite), pyrite, elemental sulfur, and carbonates (calcite and dolomite). Porosity, accompanying the generation of the late sulfur phases, is generated during BSR and TSR by partial dissolution of the carbonate host rock during the acid-generating precipitation of sulfides, acidity due to the release of carbon dioxide, dissolution of anhydrite, and by various other factors (Machel *et al.*, 1995). The sulfur phases have been affected by the redox reactions either syndepositionally, during early burial, or during deep burial conditions. The phases studied generally occur in the porous, permeable reefal facies, with very few late carbonate and sulfur phases being present in the basinal facies.

3.4.1. Carbonates

The presence of alkali earth metals (Ca and Mg derived from seawater or dissolution of sedimentary and early-diagenetic carbonate minerals, Sr) at the reaction sites of bacterial sulfate reduction (BSR) and thermochemical sulfate reduction (TSR), where carbonate ions are produced, can result in the precipitation of calcite and/or dolomite. Late calcite and dolomite may form as a cement and/or as a replacement. Carbon and oxygen isotope ratios of authigenic calcite and dolomite can be used to identify reaction products of recrystallization and late precipitation. Strontium isotope data can provide additional information on the possible sources of the fluids and the pathways used for migration. As discussed in the paragenetic sequence (Figure 3-6), dolomitization of platform carbonates probably occurred relatively early by pervasive replacement of the original limestones. Later cementation of porosity involved precipitation of planar and saddle dolomite, as well as calcite, which formed under deeper burial conditions. Early marine calcites are difficult to sample for geochemical analysis because of their small volume as replacements of organisms, such as brachiopods, in the basinal limestone units. Neomorphism (recrystallization) of some limestone fossils is visible in thin section.

Calcites from the Obed area form two groups of calcites, herein called "early" and "late", which are distinguishable mainly on the basis of thin section petrography and hand sample observations, and confirmed by geochemical analyses. Early calcite samples are much less common than the late calcites and consist of limestone matrix and fossil replacement. The late calcites include the fine to very coarse crystalline diagenetic cement, and the fine grained calcite that replaces anhydrite. These calcites have $\delta^{18}O$ values ranging from -4.7 to -11.9‰ PDB (Peedee Belemnite) and $\delta^{13}C$ values ranging from 2.8 to -27.1‰ PDB. The $^{87}Sr/^{86}Sr$ ratios range from 0.7081 to 0.7255 (Table B-1; Appendix B).

A distinction can also be made between early and late dolomite, and these differences are reflected in geochemical signatures. Early pervasive replacement dolomites comprise the carbonate matrix, while later saddle dolomites are volumetrically less common. Dolomites have $\delta^{18}O$ values that range from -2.4 to -6.7‰ PDB and $\delta^{13}C$ values that range from 5.0 to -1.1‰ PDB. The $^{87}Sr/^{86}Sr$ ratios range from 0.7089 to 0.7153 (Table B-2; Appendix B).

The data sets are illustrated in Figures 3-14 and 3-15, and for each plot, samples were assigned an "early" or "late" symbol on the basis of observations made prior to plotting and interpretation. In the plot of $\delta^{13}C$ versus $\delta^{18}O$ (Figure 3-14) for calcites and dolomites, there are two distinct populations in the data, based primarily on their $\delta^{13}C$ values. One group comprises the early calcites, early dolomites, and late dolomites. This group shows a wide range in $\delta^{18}O$ over a relatively small range in $\delta^{13}C$. Similar ranges elsewhere in the Western Canada Sedimentary Basin (eg. Mountjoy *et al.*, 1990) have been attributed to formation or recrystallization at increasingly higher temperatures, trending away from values for Devonian seawater calcite at 25°C (MC, Figure 3-14). The other group, late calcites, displays almost a 30‰ $\delta^{13}C$ variation over a 6‰ change in $\delta^{18}O$. Both early and late dolomites have significantly lower $\delta^{18}O$ values than early calcites.

In the plot of $^{87}Sr/^{86}Sr$ ratios versus $\delta^{18}O$ (Figure 3-15), four populations, representative of the four groups of carbonates (early and late calcites and dolomites) are illustrated. The four early calcites analysed in this study have values ranging from 0.7082 to 0.7088. Late calcites have a much larger range of values from 0.7086 to 0.7252. A slight negative correlation of $\delta^{18}O$ is observed for these late calcites. Early replacement dolomites range in $^{87}Sr/^{86}Sr$ ratios from 0.7094 to 0.7113. Late saddle dolomites vary from 0.7118 to 0.7152, containing more radiogenic strontium than that of replacement dolomite but with similar $\delta^{18}O$. Late calcites show the most significant variations in strontium isotope ratios.

Also illustrated on these diagrams (Figures 3-14 and 3-15), are fields for calcite (MC) and dolomite (MD) which would have formed in equilibrium with Late Devonian seawater. The $\delta^{18}O$ and $\delta^{13}C$ values of relatively unaltered marine calcites are taken from Carpenter *et al.* (1991) and references therein. Calculated values of marine dolomites are from Amthor *et al.* (1993) and references therein. The Late Devonian seawater $^{87}Sr/^{86}Sr$ ratio is taken from Burke *et al.* (1982) as 0.7080 to 0.7083.

3.4.2. Anhydrite

Syndepositional, or primary, anhydrite of the Upper Blueridge Member, described

Figure 3-14 Plot of $\delta^{13}C$ versus $\delta^{18}O$ for early calcites, late calcites, early dolomites, and late dolomites (see legend). The fields of Late Devonian marine calcite and dolomite are labelled as MC and MD, respectively.

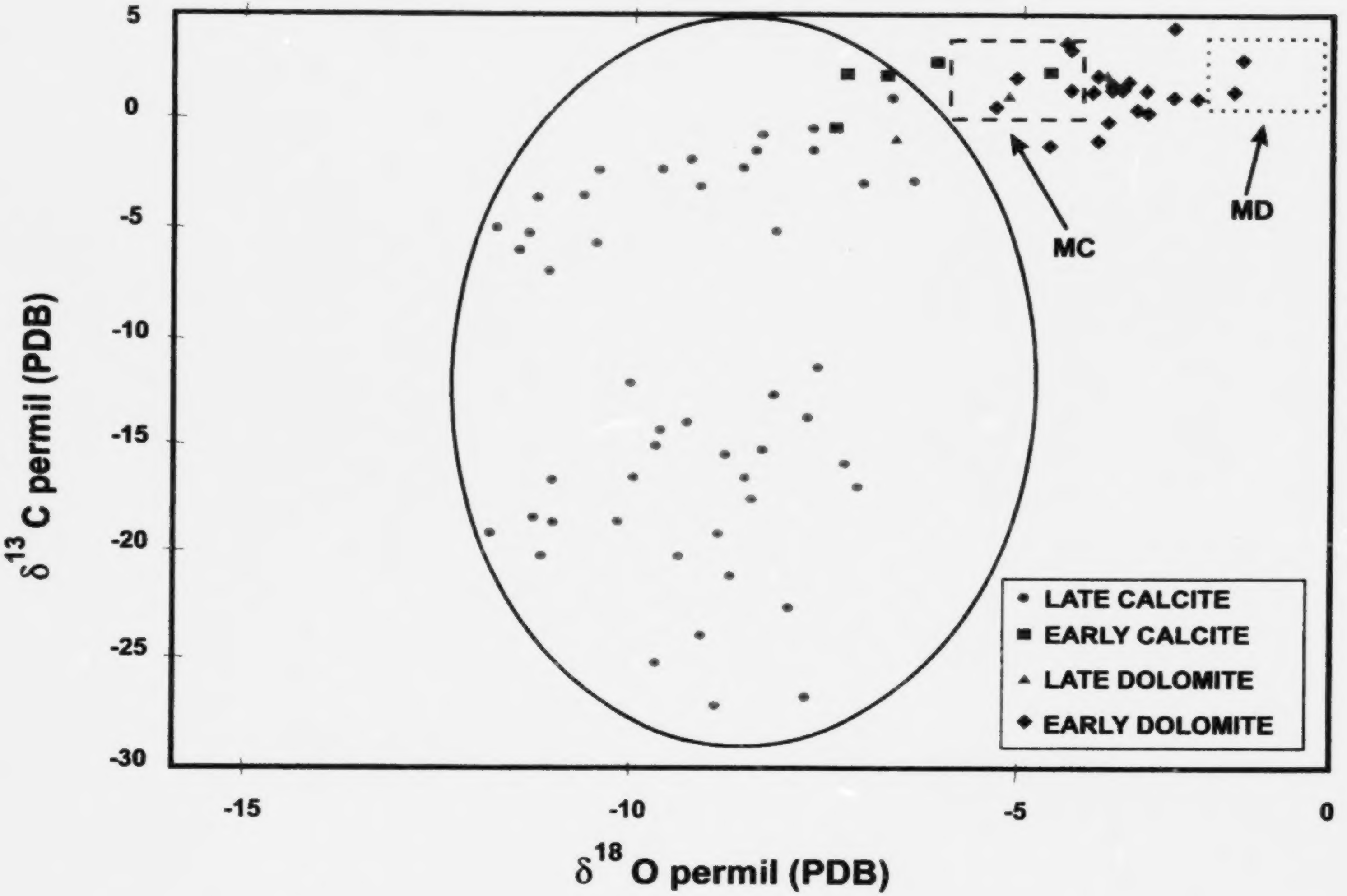
5
0
-5
-10
-15
-20
-25
-30
-15
-10
-5
0
δ13 C permil (PDB)
δ18 O permil (PDB)
MC
MD
● LATE CALCITE
■ EARLY CALCITE
▲ LATE DOLOMITE
◆ EARLY DOLOMITE

Figure 3-15 Plot of $^{87}Sr/^{86}Sr$ versus $\delta^{18}O$ of early and late calcites and dolomites (see legend). The fields of Late Devonian marine calcite and dolomite are labelled as MC and MD, respectively.

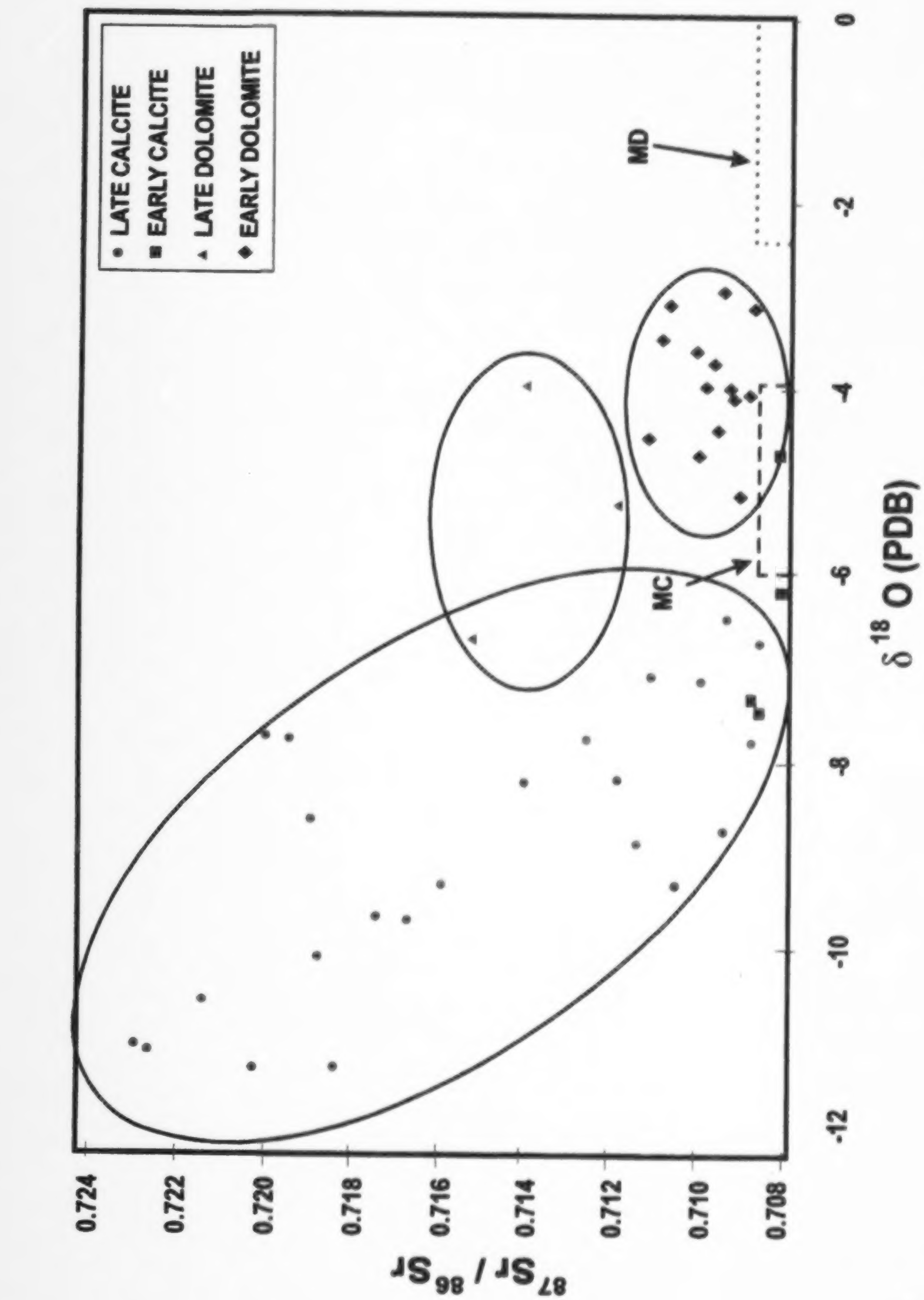
LATE CALCITE
EARLY CALCITE
LATE DOLOMITE
EARLY DOLOMITE
MD
MC
$^{87}Sr / ^{86}Sr$
0.724
0.722
0.720
0.718
0.716
0.714
0.712
0.710
0.708
-12
-10
-8
-6
-4
-2
0
$\delta^{18}O$ (PDB)

in section 3.3.3., is considered to be the sulfate source for the Obed complex. It regionally overlies the area and has an isotopic composition ($\delta^{18}O$ and $\delta^{34}S$) indicative of formation from Devonian seawater. An integration of Nisku data from Machel (1985) and Claypool *et al.* (1980) estimates the isotopic ratios of $\delta^{18}O$ at 14.7‰ SMOW (Standard Mean Ocean Water) and $\delta^{34}S$ at 25‰ CDT (Canyon Diablo Triolite) for primary anhydrite of the Late Devonian (Figure 3-16). This helps to define an isotopic realm for anhydrites which could have formed, during the Late Devonian, in the supratidal to intertidal facies of the Upper Blueridge Formation in the Obed area. $\delta^{34}S$ (CDT) versus $\delta^{18}O$ (SMOW) data for analysed anhydrites are plotted in Figure 3-17. Five anhydrite samples of Blueridge evaporitic, syn-depositional (primary), anhydrite were analysed and found to have an isotopic range in values of 13.8 to 15.4‰ SMOW for $\delta^{18}O$ and 25.6 to 26.4‰ for $\delta^{34}S$. A few other samples of syn-depositional, primary anhydrite are enriched in $\delta^{18}O$ (up to 21.3‰) and $\delta^{34}S$ (up to 35‰).

Machel and Burton (1991) discussed the processes affecting sulfur and oxygen isotopic changes of Late Devonian sulfate using vectors and areal distributions on a $\delta^{34}S$ versus $\delta^{18}O$ plot. Sulfur and oxygen isotope ratios of Nisku primary and secondary anhydrites for their plot (Figure 3-16) were compiled from data provided by Nakai and Jensen (1964), Hitchon and Friedman, 1969, Rees (1973), Krouse (1977), Holser *et al.* (1979), Claypool *et al.* (1980), Chiba *et al.* (1981), Jeffries *et al.* (1984), Pierre (1988), and references therein. The essential features of the Machel and Burton (1991) plot (Figure 3-16) are shown with the Obed data in Figure 3-17. Since the syndepositional (primary) bedded anhydrite of the Obed area is considered representative of Late Devonian seawater sulfate, the aforementioned (Machel and Burton, 1991) interpretations can be applied to the Late Devonian Blueridge primary and secondary anhydrite samples as well. The evolution of the anhydrites in the Obed area can be interpreted by application of the aforementioned vector plot to the available data in the Winterburn (Blueridge Member) and Woodbend (Leduc Formation) Groups of the Obed area (Figure 3-17).

Data for Lower and Upper Blueridge anhydrites show ranges from 13.2 to 21.3 ‰ SMOW for $\delta^{18}O$ values and 20.5 to 35.3 ‰ CDT for $\delta^{34}S$ signatures. These values

Figure 3-16 Plot of $\delta^{34}S$ versus $\delta^{18}O$ of Nisku primary and secondary anhydrites and processes affecting isotopic changes of Late Devonian sulfate, represented as vectors and areal distributions. Late Devonian marine gypsum/anhydrite plots as the origin of the vector family. **a**: isothermal, closed system removal of sulfate minerals, depleting the remaining dissolved sulfate for both oxygen and sulfur isotope ratios in direction a; **b** and **b'**:bacterial sulfate reduction, enriching the remaining dissolved sulfate isotopically in the direction of the area between these two vectors; **c**: mixing with sulfate from the underlying Middle Devonian evaporites; **d/d'**: oxygen isotope equilibriation with carbonate-equilibrated waters of variable oxygen isotope composition; **e**: sulfur enrichment of sulfate remaining during thermochemical sulfate reduction; **F** (coarse stipple pattern): reoxidation of reduced sulfur species that were formed during bacterial sulfate reduction; **G** (fine stipple pattern): reoxidation of the reduced sulfur species formed during thermochemical sulfate reduction (Machel and Burton, 1991)

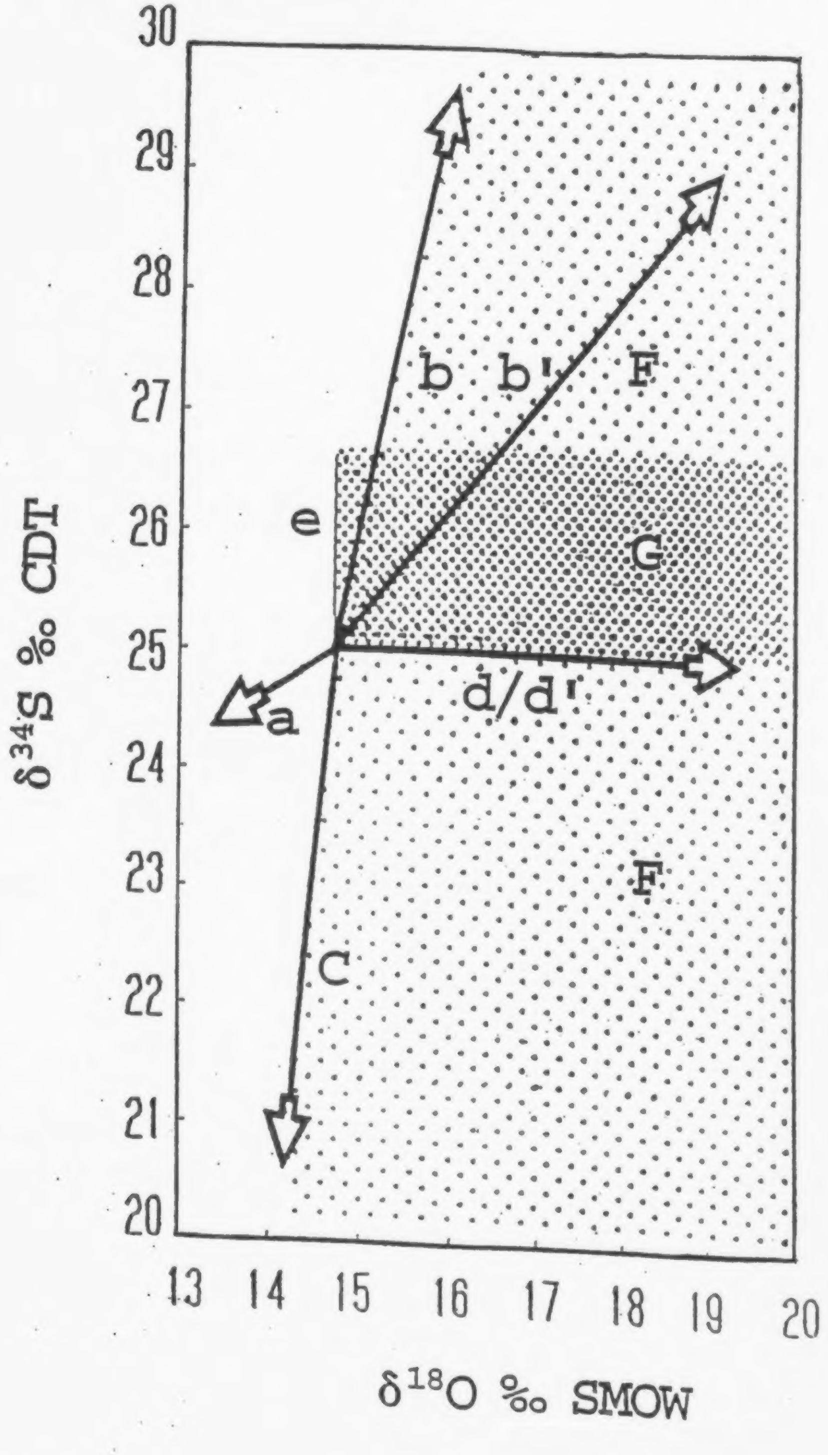
30
29
28
27
26
25
24
23
22
21
20
δ34S ‰ CDT
13
14
15
16
17
18
19
20
δ18O ‰ SMOW
a
b
b'
C
d/d'
e
F
G
F

Figure 3-17 Plot of $\delta^{34}S$ versus $\delta^{18}O$ of Woodbend (Leduc) and Winterburn (Blueridge) primary and secondary anhydrite samples (see legend). Primary anhydrites are only present in the Upper Blueridge; the rest are secondary. A field of primary anhydrite representative of Devonian seawater sulfate is outlined as the origin of the vector diagram. This vector plot is explained in Machel and Burton (1990; see also Figure 3-16) and its application to the data from the Obed area is explained in the text. A vector labelled BSR shows the direction of enhancement of $\delta^{34}S$ and $\delta^{18}O$ during bacterial sulfate reduction (BSR). The data above this vector are also affected by BSR. The data below this vector are representative of sulfate formed by reoxidation of isotopically depleted, reduced sulfur species that were initially formed during bacterial sulfate reduction (probably iron sulfides). A vector in the direction of isotopic signatures representative of mixing with Middle Devonian sulfate is also shown. Vertical bars in the left portion of the figure illustrate the ranges of $\delta^{34}S$ values for the anhydrite samples of the Winterburn and Woodbend Groups.

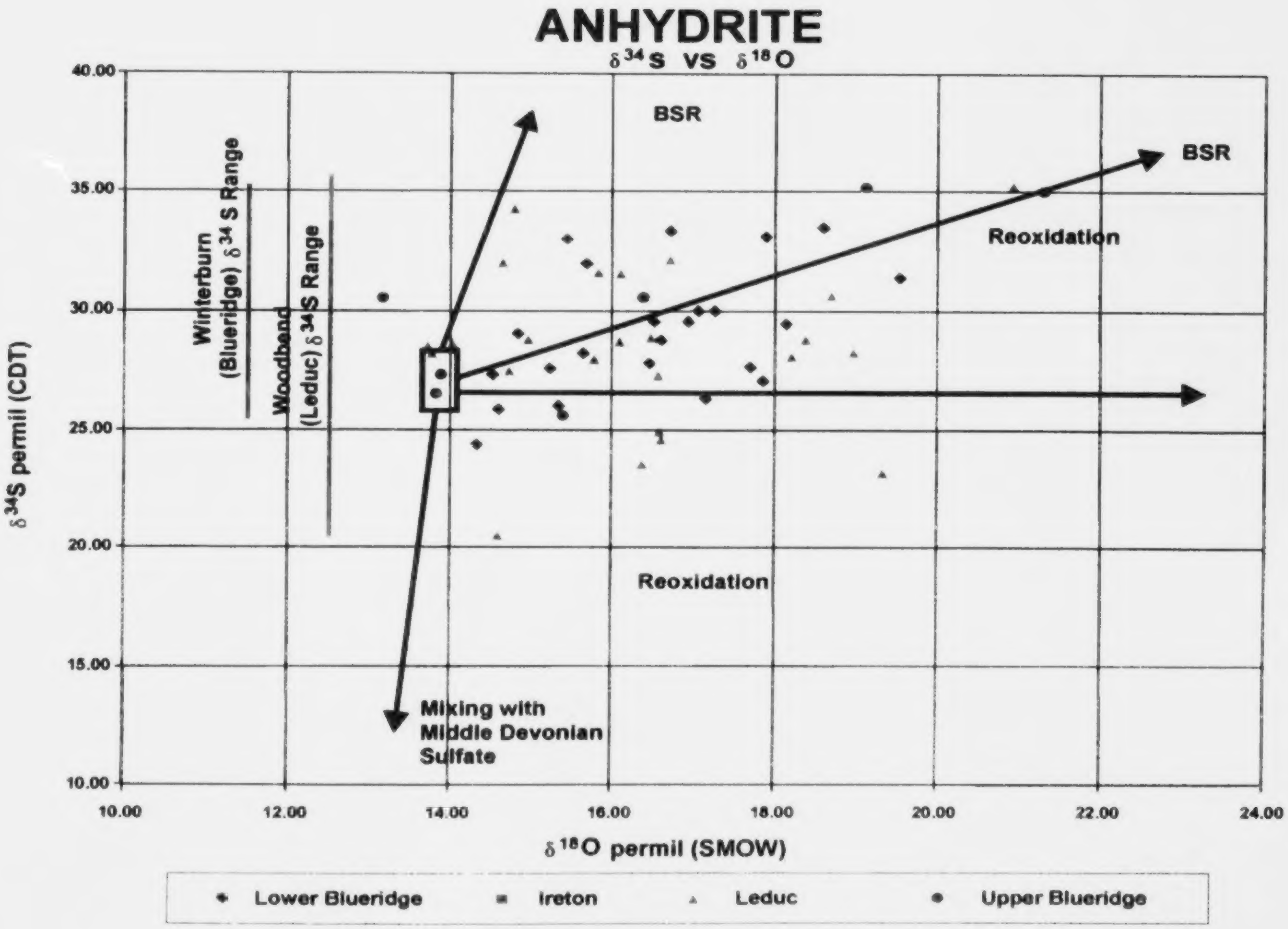
ANHYDRITE
δ34S VS δ18O
BSR
BSR
Reoxidation
Reoxidation
Mixing with Middle Devonian Sulfate
Winterburn (Blueridge) δ34 S Range
Woodbend (Leduc) δ34S Range
δ34S permil (CDT)
40.00
35.00
30.00
25.00
20.00
15.00
10.00
δ18O permil (SMOW)
10.00
12.00
14.00
16.00
18.00
20.00
22.00
24.00
Lower Blueridge
Ireton
Leduc
Upper Blueridge

overlap the primary, Devonian seawater signature and include compositions for primary anhydrites, as well as depositionally primary anhydrites which display subsequent alteration. A regression line drawn through these anhydrite data points (Figure 3-17) corresponds to an isotopic change consistent with bacterial sulfate reduction, along a vector with a slope of about 1.2 (Figure 3-16). The data below the aforementioned vector are representative of sulfate formed by reoxidation of isotopically depleted, reduced sulfur species that were initially formed during bacterial sulfate reduction and probably precipitated in the form of iron sulfides. There is no evidence for mixing with sulfate which might have migrated by fluid flow from the underlying Middle Devonian (Figure 3-17) along faults. There may be a relationship of the sulfur isotopic compositions with depth and formation. There is a 4 ‰ difference in the lowermost sulfur isotope value between the samples from the Winterburn Group and those of the Woodbend Group. The ranges of $\delta\ ^{34}S$ values are from 20.5 to 35.3 ‰ in the Leduc Formation and 24.5 to 35.18 ‰ in the Blueridge Member (Figure 3-17; vertical bars in the left portion of the figure).

3.4.3. Pyrite

When iron cations are present at the reaction site of BSR and/or TSR, they react with sulfide produced by the redox reactions to form iron sulfides, including pyrite. Clay minerals of the shales of the Ireton Formation are the most likely source to provide iron to the Obed reefal complex.

The sulfur isotope values for the pyrite samples analysed in the Obed area (Figure 3-18) have a spread of approximately 50‰ CDT. $\delta^{34}S$ values range from -23 to +30 ‰ CDT. Riciputi *et al.* (1994) determined a negative fractionation of up to 50‰ of sulfur isotopes between pyrite and the source sulfate during early BSR. Kiyosu and Krouse (1990) determined a negative fractionation of about 10-20‰, at temperatures of 200 to 100°C, respectively, during TSR. For this study, 10‰ is considered the maximum possible sulfur isotope fractionation during TSR.

Although the habit of biogenic pyrite is generally framboidal and that of

Figure 3-18 Plot of depth below the Graminia Silt marker versus $\delta^{34}S$ of Woodbend (Leduc) and Winterburn (Blueridge) pyrite (see legend). The bars at the base of the figure represent the range of $\delta^{34}S$ values of the primary (Upper Blueridge) anhydrite,and the ranges of values due to TSR and BSR relative to a $\delta^{34}S$ value of 25‰ CDT, taken as representative of Late Devonian seawater sulfate. A dashed vertical line at 15. A dashed vertical line at 15‰ CDT represents the lower limit of values possible due to TSR.

PYRITE

Depth Below Graminia vs $\delta^{34}S$

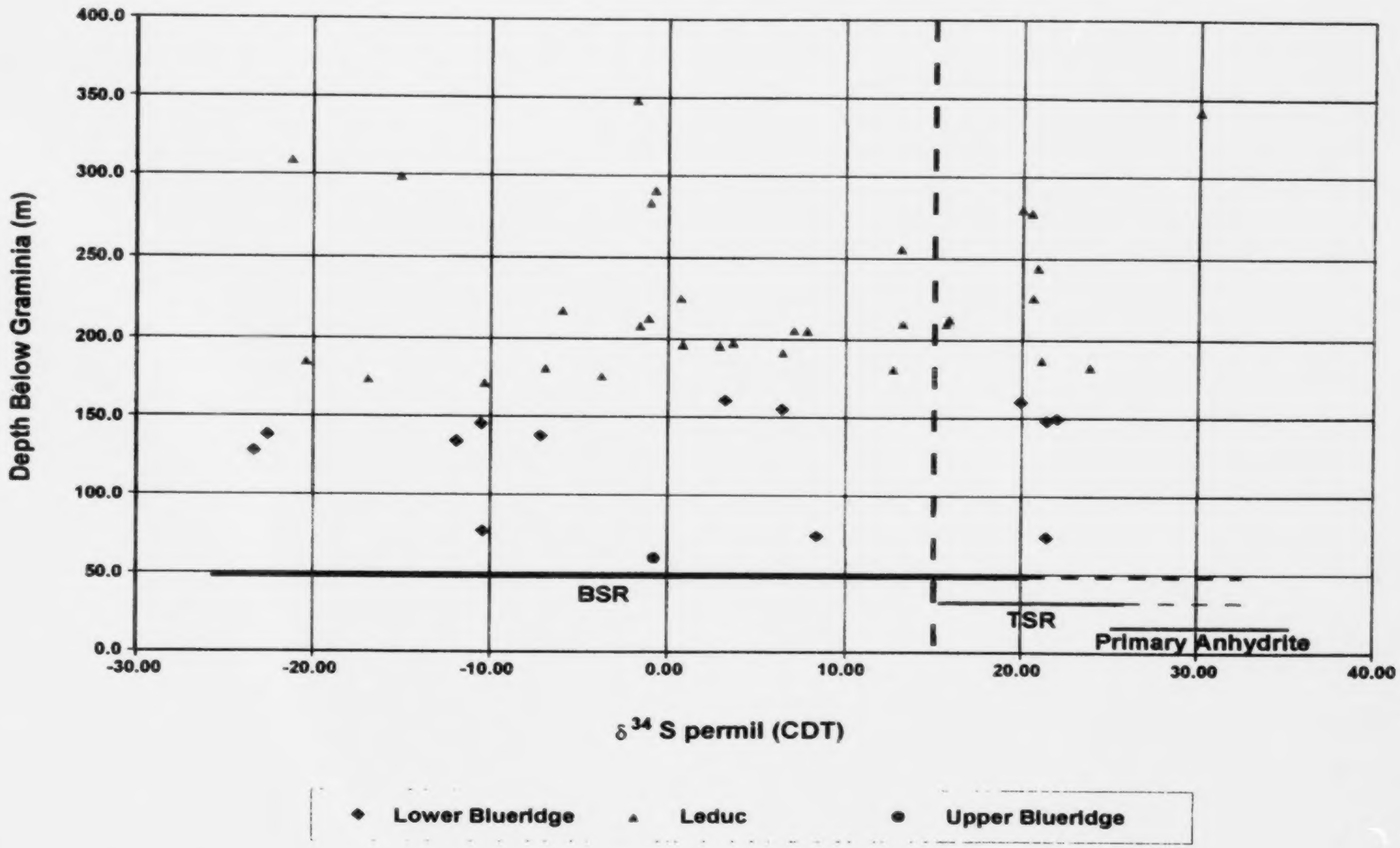

thermogenic pyrite is commonly cubic (Machel, 1989; Riciputi *et al.*, 1994), there are no morphological characteristics in this study which allow for the unambiguous distinction between early and late pyrite. The pyrite which contains reduced sulfur of a definite biogenic origin has $\delta^{34}S$ values of <15‰ (Figure 3-18). The pyrite which contains sulfur with $\delta^{34}S$>15‰ is either from BSR or from TSR (Figure 3-18). There seems to be no correlation of enrichment or reduction of ^{34}S with texture, depth, or depositional facies. The highest $\delta^{34}S$ value is also the deepest Leduc sample, but there is insufficient data to support a statement that there is enrichment with depth.

The $\delta^{34}S$ values reported here for pyrite samples were determined on bulk sample powders which combined many pyrite grains in an individual sample. In contrast, Riciputi *et al.* (1994) used an ion microprobe to analyse individual crystals *in situ* from the Obed area. This method allows for the recognition that $\delta^{34}S$ values of individual pyrite grains within thin section-sized samples that vary as much as 50‰. A trend of increasing sulfur isotope ratio with increasing grain size has been observed in pyrite from the Obed field by Riciputi *et al.* (1994). They also observed that the isotopically heavy pyrites tend to be replacive and corroded, thereby considered to be late and formed during TSR.

3.4.4. Elemental Sulfur

Native sulfur occurs as a reaction product of the previously discussed redox reactions (BSR and TSR) when reaction 5 (Figure 3-13) does not go to completion. For example, elemental sulfur may form when the concentration of reactive hydrocarbons is low or they are not supplied fast enough to the reaction site (Machel *et al.*, 1995). As in the case of pyrite, the sulfur isotope signatures reflect the sulfide produced by BSR and TSR. Sulfide for the sulfur is provided by reduction of sulfate from the primary anhyrites of the Upper Blueridge.

The sulfur isotope values for the native sulfur samples analysed in the Obed area (Figure 3-19) range from 15 to 28‰ CDT. Since the fractionation during the reaction of sulfide to elemental sulfur (Reaction Set 4, Figure 3-13) is negligible, the same sulfur isotope fractionations discussed with respect to pyrite are applicable to the interpretation

Figure 3-19 Plot of depth below the Graminia Silt marker versus $\delta^{34}S$ of Woodbend (Leduc) and Winterburn (Blueridge) native sulfur (see legend). Bars at the base of the figure represent the range of $\delta^{34}S$ values of the primary (Upper Blueridge) anhydrite,and the ranges of values due to TSR. Red vectors to the right of the figure illustrate the ranges of $\delta^{34}S$ values of primary and secondary anhydrite for the Winterburn and Woodbend Groups. Three populations of sample values are circled: values from the Windfall area, Leduc Formation in the Obed area, and Blueridge Member in the Obed area.

NATIVE SULFUR

Depth Below Graminia vs δ34S

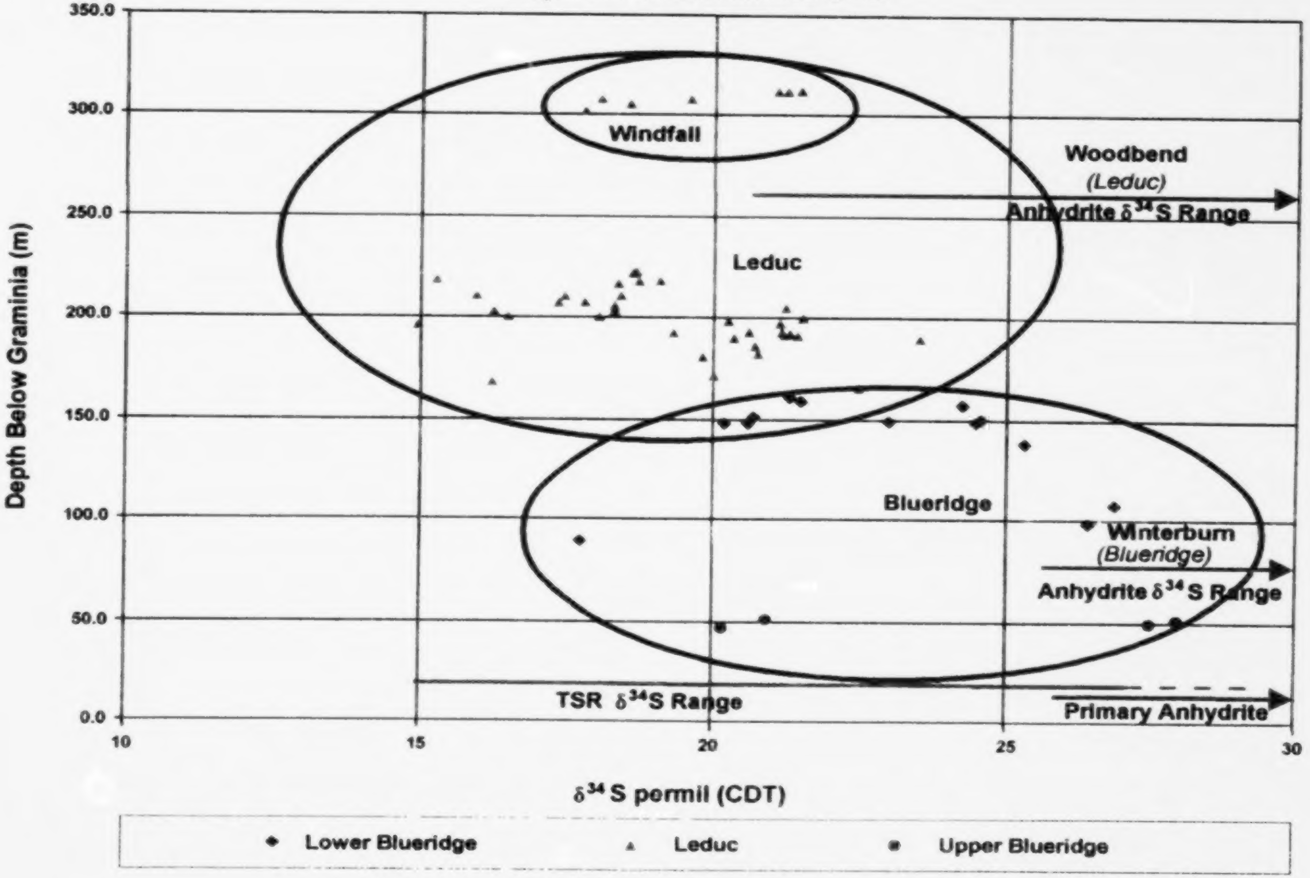

of elemental sulfur compositions. Considering that the range of values for the primary source anhydrite is from 26 to 35‰, all of the observed values are consistent with TSR.

There appear to be three populations of $\delta^{34}S$ values based on stratigraphy and geographic location (Figure 3-19). The shallowest population is not discussed here because these samples are from a well which is probably part of the Windfall complex, rather than part of the Obed area. The Leduc Formation is the lowermost unit stratigraphically in Obed, and elemental sulfur samples from this unit show a range of $\delta^{34}S$ values from 15.0-23.5‰, while the sulfur samples from depositional cycles within the Lower Blueridge Member exhibit values of 17.8-27.0‰. The highest values, 27.5-28.3‰ CDT, are from sulfur which is associated with anhydrite, and these samples are from basinal facies of the Upper Blueridge, directly underlying the supratidal/intertidal facies.

There is no correlation of morphology of the native sulfur mineralization with the $\delta^{34}S$ signatures. Ambient conditions such as temperature, pH, and concentration of sulfur control the presence of euhedral to subhedral crystalline sulfur versus anhedral sulfur with a "globular" appearance, which must have been liquid at depth.

3.5. DISCUSSION AND CONCLUSIONS

The carbonate buildups of the Blueridge Member, Nisku Formation, and Leduc Formation have undergone a complex diagenetic history (Figure 3-6). Dolomitization of the Obed platform carbonates occurred relatively early by pervasive replacement of the original limestones, and later by coarser cement. The amount of porosity and permeability of the reef complex was a key factor affecting the flow of fluids that were responsible for the early dolomitization and late precipitation of carbonates (calcite and dolomite) and sulfur phases (anhydrite, pyrite, and native sulfur). The fluids and their reactions with the components of the carbonate reef rocks, for example, the reaction of hydrocarbons with dissolved sulfate, are responsible for the geochemical signatures found in the Devonian subsurface rocks.

Bacterial sulfate reduction (BSR) and thermochemical sulfate reduction (TSR) occur in a wide range of sedimentary and diagenetic environments unless kinetically inhibited. They occur in different thermal regimes but their reaction products and by-products are identical and include altered hydrocarbons, hydrogen sulfide, pyrite, native sulfur, and carbonates. Primary depositional anhydrite plays a very important role in these chemical reactions as a reactant, with a sulfate signature representative of Devonian seawater. Secondary anhydrite is derived through dissolution and reprecipitation of the aforementioned primary anhydrite. Petrography has helped to determine the paragenetic sequence of the diagenetic events and occurrences of the diagenetic phases in the Obed study area. Identification of the origins (BSR or TSR) for each of the inorganic phases can be addressed through petrography and isotope geochemistry. The carbon isotope ratios of the carbonates and sulfur isotope ratios of the sulfates, sulfides, and native sulfur, as well as oxygen isotope ratios, where applicable, have provided evidence for the thermal regimes and processes during their formation. Strontium isotope ratios provide additional information on fluid history.

Carbon, oxygen, and strontium isotope compositions determined for the carbonates of the Obed area show indications of recrystallization. Early fossil replacement calcites have $\delta^{13}C$ values similar to those of Late Devonian seawater (MC), but lower $\delta^{18}O$ (Figure 3-14). They have $^{87}Sr/^{86}Sr$ ratios similar to Late Devonian seawater in two samples, but have higher values in two samples (Figure 3-15). These calcites are interpreted to have recrystallized from fluids evolved from Devonian seawater. The late calcites from the Obed area have lower $\delta^{18}O$ and much lower $\delta^{13}C$ values than those of the early calcites and Late Devonian marine calcites (MC). This suggests that the late calcites formed at deeper burial depths, and at higher temperatures than the early, slightly recrystallized, calcites. Carbon in the late calcites is isotopically highly depleted ($\delta^{13}C$ with a minimum of -27.1‰ PDB), and this is indicative of incorporation of oxidized organic carbon from thermochemical sulfate reduction. The late calcite cements have $^{87}Sr/^{86}Sr$ ratios up to 0.7255, the highest ratios found to date for carbonates in the Western Canada Sedimentary Basin. Carbonate veins cutting Proterozoic Miette Group clastics and carbonates in outcrop in the Rocky Mountains (Jasper Basin) have $^{87}Sr/^{86}Sr$ ratios of 0.7387 to 0.7741 (Koffyberg, 1994). This suggests that a very radiogenic soluble strontium fluid component was present just west of Obed to deposit these veins. Given these values, the close stratigraphic correlation of the Obed area with the Jasper Basin, and the fact that the Southesk-Cairn complex extends into the Jasper Basin and underlies the Obed platform, thus creating a migration pathway, it is possible that ^{87}Sr-enriched fluids were derived from the Rocky Mountain fold and thrust belt, driven by the Laramide orogeny into the Obed area.

The early replacive dolomites have significantly depleted $\delta^{18}O$ values (up to 5‰) and slightly depleted $\delta^{13}C$ values compared to those of Late Devonian marine dolomites (MD) in the Obed area (Figure 3-14). The $\delta^{18}O$ composition of the early replacive dolomites is likely a reflection of the fluids responsible for pervasive dolomitization during shallow to intermediate burial, having been modified or evolved from Devonian seawater. Several early replacive and late saddle dolomites are slightly depleted in $\delta^{13}C$. Incorporation of isotopically light carbon is evidence of recrystallization of replacive dolomite and precipitation of saddle dolomite during or after the production of oxidized organic carbon by TSR (eg. Machel, 1987b). The similar isotopic signatures of these dolomite samples suggests a correlation of timing of events. The ^{87}Sr/^{86}Sr ratios for the Obed dolomites are significantly higher than marine dolomite isotopic signatures, with the late dolomite being more radiogenic than the early dolomites (Figure 3-15). These ratios are best explained by the presence of ^{87}Sr-enriched fluids for recrystallization and cementation during deep burial (Figure 3-4) in the Late Cretaceous to Early Tertiary. A lesser degree of depletion of $\delta^{18}O$ and $\delta^{13}C$ occurred in late dolomites, as opposed to late calcites. This may be due to the ^{87}Sr-enriched fluids entering the Obed area at a later stage than hydrocarbon migration (and TSR). The ^{87}Sr-enriched fluids responsible for the precipitation of the late calcites post-date the formation of the saddle dolomite cements. These late dolomite cements were likely formed from earlier fluids than those responsible for the aforementioned late calcites, and are associated with hydrocarbon migration.

The most likely sulfate source in the Obed area is the bedded anhydrites of the Upper Blueridge Member. Dissolved sulfate, carried to lower stratigraphic levels, is involved in BSR and TSR reactions, as well as being responsible for the precipitation of secondary anhydrite. BSR was the main process affecting the sulfur and oxygen isotopic ratios in the early diagenetic regimes, syn- and post-depostional. Subsequent isotopic modifications due to thermochemical sulfate reduction of sulfur phases at deep burial depths are rare and relatively minor in extent. Some petrographically primary anhydrite is enriched in $\delta^{18}O$ (up to 21.3‰) and $\delta^{34}S$ (up to 35‰), and is interpreted as being altered by bacterial sulfate reduction, either during or shortly after deposition (Figure 3-17). Secondary anhydrite, filling void spaces and/or replacing host rock, occurs in any depositional facies assemblage and fits the main criteria outlined by Machel and Burton (1991), and references therein, for a burial origin. Samples of secondary anhydrite from the Lower Blueridge Member and Leduc Formation, show $\delta^{34}S$ values very close to those of the primary anhydrites, as well as higher values indicating alteration by bacterial sulfate reduction (Figure 3-17). At shallow depths, bacteria preferentially reduce the light sulfur isotopes from the sulfate, leaving behind anhydrite carrying heavier sulfur isotopic signatures. Also contributing to the wide spread in geochemical signatures of the secondary anhydrite is the partial reoxidation of isotopically lighter, reduced sulfur species (mainly pyrite) that were formed during bacterial sulfate reduction. Most sulfates resulting from the reoxidation of sulfides, with or without intermediate formation of elemental sulfur, would have about the same sulfur isotope compositions as the isotopically light parent sulfides, with only slight fractionations (Machel *et al.*, 1995). Primary evaporitic sulfate from the Upper Blueridge, which is extensive over the Obed area and precipitated from Devonian seawater, could provide a sufficient volume of sulfate to account for all secondary anhydrite in the underlying Winterburn and Woodbend Groups. The main process responsible for the geochemical signatures of the primary and secondary anhydrites is bacterial sulfate reduction. There is no correlation of sulfur isotopic data with facies, except for the fact that primary anhydrites are found only in the Upper Blueridge. Hydrologic flow carrying dissolved sulfate must have proceeded downwards through the Upper Blueridge during syndepositional and shallow to intermediate burial diagenesis. There appears to have been no mixing with soluble sulfate from the underlying Middle Devonian. There is no obvious explanation for the 4 ‰ difference in the lowermost sulfur isotope value of the samples from the Winterburn and Woodbend

Groups.

Secondary anhydrite, filling void spaces, is less common in the Leduc Formation of the updip portion of the Obed platform in wells near gas production. This can be accounted for by TSR which removed much of the secondary anhydrite to produce H_2S. The hydrocarbons that facilitated TSR probably migrated from the Woodbend platform into the Leduc reefs, then up into the Winterburn carbonates. Thus, the hydrocarbons had more time to react with and diminish the amount of sulfates in the Leduc Formation compared to the overlying reefal carbonates. Secondary anhydrite is present in the Winterburn Group throughout the platform.

The broad range of sulfur isotope ratios for pyrite observed in the Obed data (Figure 3-18) is indicative primarily of Rayleigh fractionation common to early diagenetic BSR, with the possibility of additional fractionation during TSR. Because of the large spread in $\delta^{34}S$ values, it can be assumed that the system was partially closed.

In carbonates, the concentration of reactive iron and metabolizable organic matter is much lower than in shales, and in this environment sulfate reduction to produce pyrite may be due to TSR as well as BSR (Riciputi *et al.*, 1994 and references therein). Since the range of $\delta^{34}S$ values for the primary source anhydrite is from 26 to 35 ‰, the range of values possible as a result of TSR and that as a result of BSR overlap for values greater than 15‰ (Figure 3-17). This overlap in the spread of $\delta^{34}S$ values of fractionation for TSR and BSR is supported by anhydrite samples derived from basinal limestones, whose values should clearly be indicative of BSR but also lie in the range indicative of TSR. Samples from basinal limestones are only affected by very early, shallow burial bacterial sulfate reduction, considering that there is a permeability barrier due to the tight nature of basinal shales and limestones.

Native sulfur formed in the late, deep burial diagenetic environment, after saddle dolomite (Figure 3-6), through TSR, and only where metal ions were not present for the formation of metal sulfides. Although native sulfur is commonly located in the water-wet portion of the reservoir, the amount in any given core interval can be unpredictable and variable. Considering the geochemical constraints (Figure 3-13), elemental sulfur most likely formed in the gas-water transition/contact zone. However, elemental sulfur may also form in the hydrocarbon-bearing zone if significant water is present to allow for its precipitation. In the Obed area, all native sulfur must have formed from TSR, which is consistent with their range of $\delta^{34}S$ values.

The two distinct native sulfur $\delta^{34}S$ populations of the Woodbend Group (Leduc Formation) and Winterburn Group (Blueridge Member) can possibly be explained by the range in $\delta^{34}S$ values of the source anhydrites in these two intervals (Figure 3-19). Elemental sulfur from the Leduc Formation shows a mean $\delta^{34}S$ value of 19‰, while the samples from the Blueridge Member have a mean value of 23‰, a difference of 4‰. This corresponds to the 4‰ difference, as discussed previously, in isotopic ranges of the $\delta^{34}S$ values for anhydrite in the Leduc Formation and the Blueridge Member, with the Leduc having a lower $\delta^{34}S$ range. The sulfur isotopic compositions of the native sulfur apparently reflects the compositions of the anhydrite from which the sulfur was derived. Depositional facies are similar, as well as sulfur morphology, in both the Leduc Formation and Blueridge Member. Therefore, there is no correlation of sulfur isotope ratios with these factors.

Concentrations of hydrogen sulfide in gas produced by thermochemical sulfate reduction-related reactions are not limited except by the availability of sulfate and organic matter (Orr, 1977). TSR (and BSR) not only accounts for accumulations of sour gas (H_2S) such as those of the Winterburn and Woodbend Groups of the Obed field, but it resulted in the formation of diagenetic calcite, dolomite, pyrite and native sulfur. An understanding of the timing and geochemical nature of the diagenetic phases, and thus the fluids and reactions responsible for their deposition, can assist in the exploration of hydrocarbons in the Alberta deep basin.

3.6. REFERENCES

Amthor, J.E., Mountjoy, E.W., and Machel, H.G., 1993, Subsurface dolomites in Upper Devonian Leduc formation buildups, central part of Rimbey-Meadowbrook reef trend, Alberta, Canada, Bulletin of Canadian Petroleum Geology, v. 41, p. 69-185.

Anderson, N.L., Hills, L.V., Cederwall, D.A. (editors), 1989, Geophysical Atlas of Western Canadian Hydrocarbon Pools, Alberta Research Council, 344p.

Andrews, G.D., 1987, Devonian Leduc outcrop reef-edge models and their potential seismic expression, *In* Devonian of the World, Proceedings of the Second International Symposium on the Devonian System, N.M., McMillan, A.F. Embry, and D.J. Glass (*eds.*), Can. Soc. Petrol. Geol., Memoir 14, v. II, p. 427-450.

Baadsgaard, H., Chaplin, C., and Griffin, W.L., 1986, Geochronology of the Gloserneia pegmatite, Froland, Southern Norway: Norsk Geologisk Tidsskift, v. 64, p. 111-119.

Burke, W.H., Denison, R.E., Hetherington, E.A., Koepnick, R.B., Nelson, H.F., and Otto, J.B., 1982, Variations in seawater $^{87}Sr/^{86}Sr$ throughout Phanerozoic time, Geology, v. 10, p. 516-519.

Carpenter, S.J., Lohmann, K.C., Holden, P., and Walter, L.M., 1991, $\delta^{18}O$ values, $^{87}Sr/^{86}Sr$ and Sr/Mg ratios of Late Devonian abiotic marine calcite: implications for the composition of ancient seawater, Geochemica Cosmochimica Acta, v. 55, p. 1991-2010.

Chiba, H., Kusakabe, M., Hirano, S.I., Matsudo, S., and Somiya, S., 1981, Oxygen isotope fractionation factors between anhydrite and water from 100-550°C: Earth and Planetary Science Letters, v. 53, p. 55-62.

Claypool, G.E., Holser, W.T., Kaplan, I.R., Sakai, H., and Zak, I., 1980, The age curves of sulfur and oxygen isotopes in marine sulfate and their mutual interpretation: Chemical Geology, v. 28, p. 199-260.

Choquette, P.W. and Pray, L.C., 1970, Geologic nomenclature and classification of porosity in sedimentary carbonates, American Association of Petroleum Geologists Bulletin, v. 54, p. 207-250.

Dickson, J.A.D., 1965, A modified staining technique for carbonates in thin sections, Nature, v. 205, p. 587.

Drivet, E., 1993, Diagenesis and reservoir characteristics of Upper Devonian Leduc dolostones, southern Rimbey-Meadowbrook reef trend, central Alberta, M.Sc. thesis, Department of Earth and Planetary Sciences, McGill University.

Energy Resources Conservation Board, 1993, Alberta's reserves of crude oil, oil sands, gas, natural gas liquids and sulphur (December 31, 1992), Report Series ERCB93-18, 32nd Edition, Alberta Energy Conservation Board, Calgary, Alberta.

Epstein, S., Graf, D.L., and Degens, E.T., 1964, Oxygen isotope studies on the origin of dolomites. In Craigh, H., Miller, S.L., and Wasserburg, G.J. (eds.), Isotopic and cosmic chemistry. North-Holland Publishing Co., Amsterdam, p. 169-180.

Folk, R.L., 1962, Spectral subdivision of limestone types, In Classification of Carbonate Rocks, AAPG Memoir 1, p. 62-84.

Hitchon, B. and Friedman, I., 1969, Geochemistry and origin of formation waters in the Western Canada Sedimentary Basin - I: stable isotopes of hydrogen and oxygen: Geochimica et Cosmochimica Acta, v. 33, p. 1321-1349.

Holser, W.T., Kaplan, I.R., Sakai, H., and Zak, I, 1979, Isotope geochemistry of oxygen in the sedimentary sufate cycle: Chemical Geology, v. 25, p. 1-17.

Hudson, J.D. and Anderson, T.F., 1989, Ocean temperatures and isotopic compositions through time, Transactions of the Royal Society of Edinburgh: Earth Sciences, v. 80, no. 3-4, p. 183-192.

Jeffries, M.O., Krouse, H.R., Shakur, M.A., and Harris, S.A., 1984, Isotope geochemistry of stratified Lake "A", Ellesmere Island, N.W.T., Canada: Canadian Journal of Earth Sciences, v. 21, p. 1008-1017.

Kaufman, J., Meyers, W.J., and Hanson, G.N., 1990, Burial cementation in the Swan Hills Formation (Devonian), Rosevear Field, Alberta, Canada, Journal of Sedimentary Petrology, v. 60, p. 918-939.

Kiyosu, Y. and Krouse, H.R., 1990, The role of organic acid in the abiogenic reduction of sulfate and the sulfur isotope effect, Geochemical Journal, v. 24, p. 21-27.

Koffyberg, A.M., 1993, Strontium isotopic constraints on the geochemistry and origins of regional vein-forming fluids in the southern Canadian Cordillera, M.Sc. thesis, Edmonton, Alberta, University of Alberta, 102p.

Krouse, H.R., 1977, Sulfur isotope studies and their role in petroleum explorartion: Journal of Geochemical Exploration, v. 7, p. 189-211.

Krouse, H.R., 1983, Stable isotope research of more effective utilization of gas fields in Alberta, Canada Energy Resource Research Fund Agreement U-30, p. 1-100.

Machel, H.G., 1985, Facies and diagenesis of the Upper Devonian Nisku Formation in the subsurface of Alberta, Ph.D. dissertation, McGill University.

Machel, H.G., 1987a, Some aspects of diagenetic sulfate-hydrocarbon redox-reactions, In Diagenesis of sedimentary sequences (ed. J.D. Marshall), Geological Society Special Publication, No. 36, p. 15-28.

Machel, H.G., 1987b, Saddle dolomite as a by-product of chemical compaction and thermochemical sulfate reduction, Geology, v. 15, p. 936-940.

Machel, H.G., 1989, Relationships between sulfate reduction and oxidation of organic compounds to carbonate diagenesis, hydrocarbon accumulations, salt domes, and metal sulfide deposits, Carbonates and Evaporites, v. 4, p. 137-151.

Machel, H.G. and Burton, E.A., 1991, Burial-diagenetic sabkha-like gypsum and anhydrite nodules. Journal of Sedimentary Petrology, Vol. 61, No. 3, p. 394-405.

Machel, H.G., Krouse, H.R., and Sassen, R., 1995, Products and distinguishing criteria of bacterial and thermochemical sulfate reduction, accepted by Applied Geochemistry.

McCrea, J.M., 1950, On the isotopic chemistry of carbonates and a paleothermometer scale, Journal of Chemical Physics, v. 18, p. 849-857.

Mountjoy, E.W., Qing, H., and McNutt, 1992, Strontium isotopic composition of Devonian dolomites, Western Canada Sedimentary Basin: significance of sources of dolomitizing fluids, Applied Geochemistry, v. 7, p. 59-75.

Murray, R.C., 1960, Origin of porosity in carbonate rocks, Journal Sedimentary Petrology, V. 30, No. 1, p. 59-84.

Nakai, N.J. and Jensen, M.L., 1964, Kinetic isotope effect in bacterial reduction and oxidation of sulfur: Geochimica et Cosmochimica Acta, v. 28, p. 1893-1912.

Orr, W.L., 1977, Geologic and geochemical controls on the distribution of hydrogen sulfide in natural gas. In Advances in Organic Geochemistry (ed. R. Campos and J. Goni), p. 571-597. Enadisma.

Pierre, C., 1988, Applications of stable isotope geochemistry to the study of evaporites, *in* Schreiber, B.C., ed., Evaporites and Hydrocarbons: New York, Columbia University Press, p. 300-344.

Rees, C.E., 1973, A steady-state model for sulfur isotope fractionation in bacterial reduction systems: Geochimica Cosmochimica Acta, v. 37, p. 1141-1162.

Riciputi, L.R., Cole, D.R., and Machel, H.G., 1994, Sulfide formation in reservoir carbonates of the Devonian Nisku Formation, Alberta, Canada: an ion microprobe study, Submitted to Geochemica et Cosmochimica Acta.

Shakur, M.A., 1982, δ^{34}S and δ^{18}O variations in terrestrial sulfates [unpubl. Ph.D. diss.]: University of Calgary, 300p.

Switzer, S.B., Holland, W.G., Christie, D.S., Graf, G.C., Hedinger, A.S., McAuley, R.J., Wierzbicki, R.A., Packard, J.J., 1994, Devonian Woodbend-Winterburn strata of the Western Canada Sedimentary Basin. In Geologic Atlas of the Western Canada Sedimentary Basin. G.D. Mossop and I. Shetsen (compilers). Calgary, Canadian Society of Petroleum Geologists and Alberta Research Council, p. 165-195.

Ueda, A. and Krouse, H.R., 1986, Direct conversion of sulphide and sulphate minerals to SO_2 for isotope analyses, Geochemical Journal, v. 20, p. 209-212.

Wade, W.J., Hanor, J.S., and Sassen, R., 1989, Controls on H_2S concentration and hydrocarbon destruction in the eastern Smackover Trend, Transactions Gulf Coast Association of Geological Societies, v. 39, p. 309-320.

Walls, R.A., Mountjoy, E.W., and Fritz, P., 1979, Isotopic composition and diagenetic history of carbonate cements in Devonian Golden Spike Reef, Alberta, Canada, Geol. Soc. Am. Bull., v. 10, p. 1963-1982.

CHAPTER 4:
CONCLUSIONS AND RECOMMENDATIONS

The Upper Devonian carbonates in the Whitecourt area of west-central Alberta continue to be a primary target in the deep basin gas plays. The Obed area is one of the many Devonian reefal complexes that rim the Wild River sub-basin (Switzer *et al.*, 1994). The stratigraphy is complex and the constituent carbonates have been extensively dolomitized and record a complex diagenetic history. Relatively early diagenetic events, such as pervasive dolomitization and replacive anhydrite emplacement, occurred during the Late Devonian to Mississippian, whereas hydrocarbon migration and late diagenetic alteration and cementation occurred in the Late Cretaceous to Early Tertiary (Kaufman et al., 1990).

The Geological Atlas of the Western Canada Sedimentary Basin (Mossop and Shetsen, 1994) states that no significant hydrocarbon reserves have been assigned to the Blueridge Formation (Switzer et al., 1994). However, as is the case in the Obed area, the stratigraphy is not well understood and, therefore, designations of producing fields are not accurate. In Obed, one of the hydrogen sulfide pools is considered to be of Nisku age but with the incorporation of detailed mapping and correlations, I have interpreted it to be part of the cycles of the Lower Blueridge Formation. The overall pattern exhibited within the Simla of the southern Jasper Basin can be applied as a model for bank to basin geometries of the Lower Blueridge Formation in the Obed area, and thus may be readily applied to the subsurface of Alberta (Hedinger and Workum, 1989). The same physical relationships can be seen in the older Nisku stratigraphic interval of the West Pembina area (Exploration Staff, Chevron Standard Limited, 1979).

Geochemistry (carbon, oxygen, strontium, and sulfur isotope data) of the inorganic phases (calcite, dolomite, anhydrite, pyrite, and sulfur) in the Devonian carbonates of the Obed area provides information regarding fluid flow history and timing in relation to burial and hydrocarbon migration. Also, it can help to recognize recrystallization and discriminate phases generated by thermochemical sulfate reduction (TSR) from other processes, such as bacterial sulfate reduction (BSR). According to the ERCB publication on Alberta's reserves of gas and sulfur (1993), the Obed field has an H_2S gas content of 24-29%. This amount of gas may be attributed to the process of TSR. The processes of TSR and BSR are important because they occur in a wide range of sedimentary and diagenetic environments and several of their reaction products and byproducts are of economic significance.

In the Obed area, the understanding of Frasnian carbonate sedimentology, stratigraphy, and diagenesis, is valuable to the exploration of hydrocarbons in the Devonian sediments. Recommendations for further research in this area of the Western Canada Sedimentary Basin are as follows:

- More than one structural block may be present in the Obed platform area. This may lead to exploration potential in the updip portion of another structural block, if present, south of the Obed field. Seismic data should be studied and a structural assessment done.
- Mapping and correlations should be traced regionally, coupled with biostratigraphy, or other dating data, to attain greater cofidence in the correlations made in this study. With a more detailed data set and focussed sampling, geochemical distributions and correlations of late diagenetic phases, such as native sulfur, may be traced with respect to the gas/water contact.
- $^{87}Sr/^{86}Sr$ ratios for anhydrites should be analysed and applied to the data set presented in this study.
- Geochemical data should be obtained from the Devonian outcrops of the Jasper Basin and applied to that presented for the Devonian of the subsurface. The Obed complex is a promontory of the Southesk-Cairn complex (Jasper Basin) and geochemical correlations may be made, as has been made with the stratigaphy.
- Organic geochemistry of gas and gas condensates of the Obed area should be analysed and examined in terms of thermochemical sulfate reduction.
- Fluid flow modeling, as well as elemental and isotopic compositions of formation water, may help in the understanding of the fluid evolution.
- Fluid inclusion studies would provide information on paleotemperatures.
- Chromatographic, elemental and isotopic compositions of inorganic phases would be useful.

- Cathodluminesence should be utilized to study dolomitization.

REFERENCES

Energy Resources Conservation Board, 1993, Alberta's reserves of crude oil, oil sands, gas, natural gas liquids and sulphur (December 31, 1992), Report Series ERCB93-18, 32nd Edition, Alberta Energy Conservation Board, Calgary, Alberta.

Exploration Staff, Chevron Standard Limited, 1979, Geology, geophysics and significance of the Nisku reef discoveries, West Pembina area, Alberta, Canada, Bull. Can. Petrol. Geol., v. 27, p. 326-359.

Hedinger, A.S. and Workum, R.H., 1989, Uppermost Frasnian reefs, Jasper Basin, Alberta, *In* Reefs, Canada and Adjacent Areas, H.H.J. Geldsetzer, N.P. James, and G.E. Tebbutt (eds.), Can. Soc. Petrol. Geol., Memoir 13, p. 466-470.

Kaufman, J., Meyers, W.J., and Hanson, G.N., 1990, Burial cementation in the Swan Hills Formation (Devonian), Rosevear Field, Alberta, Canada, Journal of Sedimentary Petrology, v. 60, p. 918-939.

Mossop, G.D, and Shetsen, I. (compilers), 1994, Geologic Atlas of the Western Canada Sedimentary Basin. Calgary, Canadian Society of Petroleum Geologists and Alberta Research Council, 510p.

Switzer, S.B., Holland, W.G., Christie, D.S., Graf, G.C., Hedinger, A.S., McAuley, R.J., Wierzbicki, R.A., Packard, J.J., 1994, Devonian Woodbend-Winterburn strata of the Western Canada Sedimentary Basin. In Geologic Atlas of the Western Canada Sedimentary Basin. G.D. Mossop and I. Shetsen (compilers). Calgary, Canadian Society of Petroleum Geologists and Alberta Research Council, p. 165-195.

APPENDIX A:
CORE INFORMATION

There are over 52 wells in the Obed area that penetrate the Wabamun Group and 32 of these wells have core (Table A-1). These cores were logged at the Energy Resource Conservation Board (ERCB) and over 300 samples were obtained, 200 thin sections were prepared at the University of Alberta and through Core Laboratories, and 700 core photos were taken. These core logging descriptions, samples, thin sections,and photographs are available through contacting the author and/or Dr. Hans G. Machel at the University of Alberta.

TABLE A-1

WELL NUMBER WITH CORE
16-16-52-21W5
10-13-52-22W5
07-15-52-22W5
02-22-52-22W5
09-30-52-22W5
04-26-52-23W5
07-18-52-24W5
10-27-52-24W5
15-23-53-21W5
12-15-53-22W5
06-12-53-23W5
14-23-53-23W5
07-01-53-24W5
06-28-54-21W5
07-06-54-22W5
08-05-54-23W5
16-05-54-23W5
05-07-54-23W5
05-13-54-23W5
11-13-54-23W5
09-23-54-23W5
06-24-54-23W5
15-26-54-23W5
02/15-26-54-23W5
11-35-54-23W5
02-36-54-23W5
11-30-55-20W5
09-31-55-20W5
07-25-55-21W5
08-06-55-22W5
10-09-55-22W5
05-23-55-22W5
08-01-55-23W5

APPENDIX B:
GEOCHEMISTRY ANALYSES

B.1. Carbon and Oxygen Isotope Analysis

Calcite and dolomite samples were prepared by the author for carbon and oxygen isotope analyses under supervision at U of A (University of Alberta) and U of C (University of Calgary). Calcite analyses were performed at both the University of Calgary (UC) and the University of Alberta (UA). Table B-1 provides the calcite data obtained from these labs labelled as follows: UA = samples prepared by Karlis Muehlenbachs in his lab at U of A; UA1 = samples prepared by Kim Manzano in Karlis Muehlenbachs' lab at U of A and run in 1993 on an old mass spectrometer (MS); UA2 = same as UA1 except samples were run in 1995 on the new MS; UC = samples prepared and run in Roy Krouse's lab at the U of C. All carbon and oxygen isotope analyses of dolomite (Table B-2) were provided by Roy Krouse's lab at the University of Calgary. Data were collected from samples which include replacive dolomite (ED), dolomite cement (LD), fossil replacement calcite (EC), and calcite cement (LC).

Moore (1994, and references therein) and Koffyberg (1994) provide a detailed description of the theory and preparation involved in the analysis of carbon and oxygen isotope ratios. The analytical procedures are outlined in McCrea (1950) and Epstein *et al.* (1964).

B.2. Strontium Isotope Analysis

Samples for strontium isotope analyses were prepared by the author at the University of Alberta under the supervision of Pat Cavell, who also carried out the mass spectrometry. Data were collected from the same sample set as the carbon and oxygen isotope analyses (EC and LC, Table B-1; ED and LD, Table B-2). Moore (1994) and Koffyberg (1994) provide descriptions and theory of sample preparation and analytical procedures, also originally outlined in Baadsgaard *et al.* (1986).

Also analysed and included in the table are lead isotope ratios for calcites and dolomites (Table B-1 and B-2). Samples for $^{206}Pb/^{204}Pb$ analyses were collected during the procedure discussed above for strontium isotope analyses. These data were not discussed in this study since they contributed very little to the interpretation of the diagenesis of the Obed area.

B.3. Sulfur and Oxygen Isotope Analysis

Samples for the analysis of sulfur and oxygen isotope ratios were collected and prepared by the author. Sulfur isotope ratios of anhydrite, pyrite, and elemental sulfur (Table B-3, Table B-4, and Table B-5, respectively) were prepared and measured using the procedures outlined by Ueda and Krouse (1986) and Krouse (1983).

TABLE B-1: CALCITE GEOCHEMISTRY

WELL ID	DESCRIPTION	DEPTH (ft, m)	DEPTH (m)	87/86Sr	206/204Pb	del13C permil (PDB)	del18O permil (PDB)	CALCITE TYPE	LAB LOCATION
16-16-52-21W5	BASINAL WELL	13509.5	4117.7	0.71591	18.465	-1.80	-9.35	LC	UC
		13509.5	4117.7			-2.21	-10.54	LC	UA1
07-15-52-22W5	PLATFORM WELL	13737.5	4187.2	0.71119	18.438	-2.88	-7.10	LC	UC
		13745.5	4189.7	0.71141	18.258	-15.33	-8.86	LC	UA1
		13745.5	4189.7	0.71156				LC	
		13747.3	4190.2	0.71057	18.464	-13.88	-9.34	LC	UA1
		13774.5	4198.5			-16.36	-10.02	LC	UA2
02-22-52-22W5	PLATFORM WELL	4224.6	4224.6	0.71190	18.392	-12.66	-8.21	LC	UC
		4257.6	4257.6	0.71881	18.234	-12.04	-10.10	LC	UA1
		4257.8	4257.8			-4.94	-11.46	LC	UA2
09-30-52-22W5	PLATFORM WELL	4533.5	4533.5			-4.87	-11.87	LC	UA2
07-18-52-24W5	PINNACLE WELL	4823.3	4823.3	0.72266	18.858	-6.84	-11.13	LC	UC
		4823.3	4823.3			-2.97	-9.19	LC	UC
		4823.3	4823.3			-3.31	-10.72	LC	UA1
		4835.4	4835.4			-15.33	-8.35	LC	UA1
		4854.6	4854.6			-1.19	-8.52	LC	UA1
10-27-52-24W5	PLATFORM WELL	4686.5	4686.5	0.71957	18.905	-0.32	-7.79	LC	UC
		4686.5	4686.5			-0.51	-8.46	LC	UA1
14-23-53-23W5	CROSS-SECTION B	4126.1	4126.1	0.72148	18.284	-5.49	-10.58	LC	UC
		4126.1	4126.1			-5.87	-11.58	LC	UA1
07-01-53-24W5	PLATFORM WELL	4524.4	4524.4	0.71842	18.467	-3.39	-11.32	LC	UA2
		4529.3	4529.3	0.72550	18.475	-2.08	-9.73	LC	UA
		4529.3	4529.3	0.72493				LC	

TABLE B-1: CALCITE GEOCHEMISTRY

WELL ID	DESCRIPTION	DEPTH (ft, m)	DEPTH (m)	87/86Sr	206/204Pb	del13C permil (PDB)	del18O permil (PDB)	CALCITE TYPE	LAB LOCATION
06-28-54-21W5	BASINAL WELL	12376.7	3772.5	0.70865		1.12	-6.73	LC	UC
		12878.0	3925.3	0.71139	18.448			LC	
		13076.0	3985.6	0.70884	18.643			LC	
		13076.0	3985.6	0.70815				LC	
07-06-54-22W5	BASINAL WELL	12878.0	3935.2			-7.14		LC	UA2
		12910.5	3985.6	0.70884		2.33	-7.34	EC	UA1
		13076.0	3985.6			2.28	-6.83	EC	UA1
		13076.0	3985.6	0.70815		2.76	-6.21	EC	UC
05-07-54-23W5	CROSS-SECTION B	4381.3	4381.3	0.72010		-1.37	-7.77	LC	UC
11-13-54-23W5	CROSS-SECTION A	4012.2	4012.2	0.71668		-25.11	-9.72	LC	UA
		4012.2	4012.2			-20.25	-9.42	LC	UA
09-23-54-23W5	CROSS-SECTION A	3971.1	3971.1			-15.16		LC	UA2
		3977.4	3977.4	0.72301	18.151	-18.68	-11.08	LC	UA1
		3991.0	3991.0	0.71263	18.683	-26.72	-7.77	LC	UC
		3991.0	3991.0			-27.10	-8.95	LC	UA1
06-24-54-23W5	CROSS-SECTION A	4091.0	4091.0			-4.91		LC	UA2
		4103.0	4103.0			-19.21	-8.95	LC	UA2
15-26-54-23W5	PLATFORM WELL	13361.0	4072.4			-23.76	-9.14	LC	UC

TABLE B-1: CALCITE GEOCHEMISTRY

WELL ID	DESCRIPTION	DEPTH (ft, m)	DEPTH (m)	87/86Sr	206/204Pb	del13C permil (PDB)	del18O permil (PDB)	CALCITE TYPE	LAB LOCATION
02/15-26-54-23W	CROSS-SECTION A	4031.0	4031.0	0.71404		-4.95	-8.23	LC	UA1
		4068.6	4068.6	0.72027		-18.42	-11.32	LC	UA1
		4089.7	4089.7			-15.01	-9.74	LC	UA1
		4108.5	4108.5			-25.80		LC	UA2
11-35-54-23W5	CROSS-SECTION A	13833.4	4216.4	0.71744		-14.35	-9.68	LC	UA
02-36-54-23W5	CROSS-SECTION A	12926.0	3939.9			-20.28	-11.22	LC	UA1
		13040.0	3974.6	0.71012	18.502			EC	
		13435.0	4095.0			-19.20	-11.86	LC	UA1
		13637.0	4156.6			-11.40	-7.70	LC	UA1
07-25-55-21W5	BASINAL WELL	13570.0	4136.2	0.70820	18.450			EC	
		13657.0	4162.7	0.70812	18.216			EC	
		13657.0	4162.7	0.70824	18.886	2.30	-4.73	EC	UC
08-06-55-22W5	CROSS-SECTION A	4015.8	4015.8			-18.63	-10.19	LC	UA1
		4029.9	4029.9			-16.69	-11.09	LC	UA1
		4050.8	4050.8			-15.86	-7.31	LC	UC
		4050.8	4050.8			-22.64	-8.02	LC	UC
		4051.3	4051.3	0.70922		-21.08	-8.79	LC	UA1
		4067.9	4067.9			-16.54	-8.59	LC	UA1
		4089.3	4089.3	0.70994	18.277	-16.97	-7.14	LC	UC
		4089.3	4089.3			-17.55	-8.58	LC	UA1
		4089.3	4089.3			-16.96	-7.16	LC	UC
10-09-55-22W5	CROSS-SECTION A	3824.5	3824.5	0.70865		-0.21	-7.48	EC	UC
		3824.5	3824.5	0.70942		-2.65	-6.50	LC	UC

TABLE B-1: CALCITE GEOCHEMISTRY

WELL ID	DESCRIPTION	DEPTH (ft, m)	DEPTH (m)	87/86Sr	206/204Pb	del13C permil (PDB)	del18O permil (PDB)	CALCITE TYPE	LAB LOCATION
05-23-55-22W5	BASINAL WELL	12789.0	3898.1	0.71901		-2.02	-8.65	LC	UC
08-01-55-23W5	CROSS-SECTION A	4028.8	4028.8	0.70881		-13.65	-7.79	LC	UC

TABLE B-2: DOLOMITE GEOCHEMISTRY

WELL ID	DESCRIPTION	DEPTH (ft, m)	DEPTH (m)	87/86Sr	206/204Pb	del18O (PDB)	del13C (PDB)	DOLOMITE TYPE
16-16-52-21W5	BASINAL WELL	13466.5	4104.6	0.71179		-5.26	1.27	LD
10-13-52-22W5	BASINAL WELL	4383.7	4383.7	0.70961	18.781	-4.49	3.45	ED
07-15-52-22W5	PLATFORM WELL	13737.5	4187.2	0.70970		-3.74	2.02	ED
02-22-52-22W5	PLATFORM WELL	4224.6	4224.6	0.71097		-3.51	0.55	ED
09-30-52-22W5	PLATFORM WELL	4538.9	4538.9	0.70994	18.721	-3.98	2.14	ED
		4556.1	4556.1	0.70930		-4.12	2.30	ED
15-23-53-21W5	PINNACLE WELL	4046.5	4046.5	0.71525		-6.71	-0.75	LD
12-15-53-22W5	BASINAL WELL	13133.4	4003.1	0.71075		-3.15	1.28	ED
		13133.4	4003.1	0.71012				ED
06-12-53-23W5	PLATFORM WELL	4092.6	4092.6	0.70914				ED
		4103.2	4103.2			-4.19	1.45	ED
07-01-53-24W5	PLATFORM WELL	4529.3	4529.3			-2.38	1.73	ED
		4532.25	4532.25			-2.84	1.23	ED
		4532.25	4532.25			-5.41	0.72	ED
07-06-54-22W5	BASINAL WELL	12880.0	3925.8	0.71015		-3.62	0.71	ED
09-23-54-23W5	CROSS-SECTION	3937.5	3937.5	0.70939		-4.02	0.27	ED
		3971.1	3971.1	0.71093	19.718	-3.50	1.69	ED
		4002.0	4002.0	0.71010	18.698			LD
		4002.0	4002.0	0.71182	18.611			ED
		4102.0	4102.0			-3.82	1.69	ED
		4102.0	4102.0			-3.94	1.69	ED

TABLE B-2: DOLOMITE GEOCHEMISTRY

WELL ID	DESCRIPTION	DEPTH (ft, m)	DEPTH (m)	87/86Sr	206/204Pb	del18O (PDB)	del13C (PDB)	DOLOMITE TYPE
06-24-54-23W5	CROSS-SECTION	4092.6	4092.6			-2.69	5.00	ED
		4103.2	4103.2	0.71112	19.281			ED
02/15-26-54-23W5	CROSS-SECTION	4067.0	4067.0	0.70887		-3.16	4.40	ED
		4118.4	4118.4	0.71129		-4.55	3.62	ED
11-35-54-23W5	CROSS-SECTION	13854.5	4222.9	0.70898		-4.10	1.53	ED
02-36-54-23W5	CROSS-SECTION	13411.0	4087.7	0.71397		-3.98	2.25	LD
		13411.0	4087.7	0.71001		-4.76	-1.05	ED
08-06-55-22W5	CROSS-SECTION	4022.7	4022.7			-3.94	1.87	ED
		4050.8	4050.8	0.70446				ED
		4051.3	4051.3			-4.14	-0.62	ED
		4067.9	4067.9			-4.46	1.59	ED
05-23-55-22W5	BASINAL WELL	12834.0	3911.8	0.70910		-5.19	2.03	ED

TABLE B-3: ANHYDRITE GEOCHEMISTRY

WELL ID	DESCRIPTION	DEPTH (ft,m)	DEPTH (m)	del34S permil	del18O permil
10-13-52-22W5	BASINAL WELL	4369.2	4369.2	28.33	13.75
		4372.6	4372.6	28.49	13.72
		4378.8	4378.8	28.12	18.20
		4382.5	4382.5	28.16	
		4383.0	4383.0	27.48	
		4383.7	4383.7	28.68	16.09
		4385.9	4385.9	25.24	
		4388.7	4388.7	31.50	
		4391.1	4391.1	32.14	
07-15-52-22W5	PLATFORM WELL	13720.5	4183.1	32.05	15.71
		13730.5	4186.1	28.09	15.65
		13738.0	4188.4	33.10	18.60
		13764.0	4196.3	30.08	16.96
		13773.8	4199.3	26.08	15.37
		13774.0	4199.4	26.06	14.68
		13774.5	4199.5	32.90	17.89
		13775.0	4199.7	24.52	14.26
02-22-52-22W5	PLATFORM WELL	4225.5	4225.5	29.62	16.08
		4241.0	4241.0	28.72	14.95
		4254.0	4254.0	28.84	16.46
09-30-52-22W5	PLATFORM WELL	4521.5	4521.5	30.05	
		4533.5	4533.5		11.59
		4534.7	4534.7	27.92	15.76
		4537.7	4537.7	31.99	14.65
		4544.5	4544.5	24.53	16.59
		4554.7	4554.8	24.99	16.58

TABLE B-3: ANHYDRITE GEOCHEMISTRY

WELL ID	DESCRIPTION	DEPTH (ft,m)	DEPTH (m)	del34S permil	del18O permil
04-26-52-23W5	PLATFORM WELL	4461.4	4461.4	34.29	14.76
		4464.5	4464.5	20.51	14.60
		4468.9	4468.9	27.23	16.54
		4472.8	4472.8	28.72	16.07
07-18-52-24W5	PLATFORM WELL	4825.7	4825.7	21.65	
	BR PINNACLE	4834.6	4834.6		14.12
		4836.5	4836.5	28.64	14.05
		4852.3	4852.3	27.44	14.71
		4852.4	4852.4	26.10	
		4859.7	4859.7	31.58	15.80
		4859.8	4859.8	32.13	16.70
15-23-53-21W5	BASINAL WELL	4038.9	4038.9	23.12	19.31
	BR PINNACLE	4041.6	4041.6		18.70
		4044.8	4044.8	25.69	14.35
		4049.3	4049.3	30.63	18.69
		4049.7	4049.7	23.57	16.36
		4050.9	4050.9	31.54	16.11
		4051.1	4051.1	35.33	20.93
		4052.1	4052.1	28.70	18.37
12-15-53-22W5	BASINAL WELL	13133.4	4004.1	29.84	17.08
		13185.7	4020.0	31.25	19.54

TABLE B-3: ANHYDRITE GEOCHEMISTRY

WELL ID	DESCRIPTION	DEPTH (ft,m)	DEPTH (m)	del34S permil	del18O permil
06-12-53-23W5	PLATFORM WELL	4091.4	4091.4	27.64	17.80
		4092.6	4092.6	26.99	17.93
		4100.4	4100.4	29.52	18.15
		4101.6	4101.6	25.79	11.91
		4105.6	4105.6	28.92	14.81
06-28-54-21W5	BASINAL WELL	12336.0	3761.0	30.45	13.17
		12376.7	3773.4	35.18	19.12
05-13-54-23W5	CROSS-SECTION A	13375.0	4077.7	28.28	18.98
11-13-54-23W5	CROSS-SECTION A	3932.1	3932.1	25.60	15.41
		3946.7	3946.7	30.49	16.37
		3969.6	3969.6	27.34	14.47
		3972.7	3972.7	27.53	15.18
09-23-54-23W5	CROSS-SECTION A	3950.9	3950.9		14.69
02/15-26-54-23W5	CROSS-SECTION A	4007.0	4007.0	26.54	
		4016.1	4016.1	26.91	
		4017.0	4017.0	26.99	
		4019.7	4019.7	25.69	
		4099.9	4099.9	25.44	
		4100.0	4100.0	26.90	
		4106.2	4106.2	22.83	
		4108.2	4108.2	19.69	
		4109.6	4109.6	17.27	
		4133.4	4133.4	29.93	
		4150.8	4150.8	29.04	

TABLE B-3: ANHYDRITE GEOCHEMISTRY

WELL ID	DESCRIPTION	DEPTH (ft,m)	DEPTH (m)	del34S permil	del18O permil
11-35-54-23W5	CROSS-SECTION A	13323.5	4062.0	26.43	13.80
		13377.0	4078.4	27.29	13.87
		13389.0	4081.0	30.23	
		13394.5	4083.7	34.10	
		13838.3	4219.0	28.59	
02-36-54-23W5	CROSS-SECTION A	13005.0	3964.9	33.00	15.39
		13115.0	3998.5	33.70	16.67
10-09-55-22W5	BASINAL WELL	3832.5	3832.5	26.50	17.21
11-30-55-20W5	BASINAL WELL	3889.9	3889.9	34.97	21.28
08-01-55-23W5	CROSS-SECTION A	4017.4	4017.4	27.88	16.42
		4017.6	4017.6	27.78	16.47
		4037.0	4037.0	28.70	16.52
		4047.0	4047.0	29.50	16.41

TABLE B-4: PYRITE GEOCHEMISTRY

WELL ID	DESCRIPTION	DEPTH (ft,m)	DEPTH (m)	DEPTH BELOW GRAMINIA (m)	del 34S per mil
10-13-52-22W5	BASINAL WELL	4378.8	4378.8	341.8	30.11
		4386.4	4386.4	349.4	-1.87
07-15-52-22W5	PLATFORM WELL	13737.5	4188.3	148.3	21.69
		13738.0	4188.4	148.4	21.63
		13742.0	4189.6	149.6	22.09
		13761.0	4195.4	155.4	6.54
		13774.5	4199.5	159.5	3.15
		13775.0	4199.7	159.7	19.90
02-22-52-22W5	PLATFORM WELL	4257.7	4257.7	183.7	-20.52
07-18-52-24W5	BASINAL WELL	4833.5	4833.5	191.5	6.57
	BR PINNACLE				
10-27-52-24W5	PLATFORM WELL	4685.0	4685.0	187.0	21.21
15-23-53-21W5	BASINAL WELL	4038.0	4038.0	299.0	-15.13
	BR PINNACLE	4049.9	4049.9	310.9	-21.36
14-23-53-23W5	CROSS-SECTION B	4122.9	4122.9	176.0	-3.79
		4126.9	4126.9	179.9	12.69
		4128.5	4128.5	181.5	23.91
07-06-54-22W5	BASINAL WELL	12934.0	3943.3	63.3	-0.54
		13076.0	3986.6	106.6	-7.91
11-13-54-23W5	CROSS-SECTION A	3972.7	3972.7	77.7	-10.47
09-23-54-23W5	CROSS-SECTION A	3950.9	3950.9	73.9	21.49

TABLE B-4: PYRITE GEOCHEMISTRY

WELL ID	DESCRIPTION	DEPTH (ft,m)	DEPTH (m)	DEPTH BELOW GRAMINIA (m)	del 34S per mil
02/15-26-54-23W5	CROSS-SECTION A	4099.9	4099.9	127.9	-23.37
		4106.1	4106.1	134.1	-11.96
		4108.5	4108.5	136.5	-22.68
		4108.7	4108.7	136.7	-7.18
		4116.9	4116.9	144.9	-10.60
		4121.6	4121.6	149.6	-13.98
		4150.8	4150.8	178.8	16.08
		4151.0	4151.0	179.0	17.95
11-35-54-23W5	CROSS-SECTION A	13838.3	4219.0	204.0	7.82
		13849.0	4222.3	207.3	-1.57
		13857.8	4224.9	209.9	15.78
		13863.5	4226.7	211.7	15.94
02-36-54-23W5	CROSS-SECTION A	13346.0	4068.9	194.9	2.83
		13348.0	4069.5	195.5	0.76
		13350.0	4070.1	196.1	3.69
		13403.0	4086.3	212.3	-1.18
		13420.6	4091.6	217.6	-5.99
		13619.0	4152.1	278.1	20.57
		13627.3	4154.7	280.7	20.11
09-31-55-20W5	BASINAL WELL	3983.8	3983.8	225.8	20.72

TABLE B-4: PYRITE GEOCHEMISTRY

WELL ID	DESCRIPTION	DEPTH (ft,m)	DEPTH (m)	DEPTH BELOW GRAMINIA (m)	del 34S per mil
08-06-55-22W5	CROSS-SECTION A	4014.8	4014.8	171.8	-10.40
		4016.3	4016.3	173.3	-16.89
		4022.7	4022.7	179.7	-6.95
		4048.0	4048.0	205.0	7.22
		4050.8	4050.8	207.8	13.36
		4067.9	4067.9	224.9	0.66
		4088.0	4088.0	245.0	21.01
05-23-55-22W5	BASINAL WELL	12785.6	3898.0	256.0	13.23
		12876.0	3925.6	283.6	-1.03
		12899.8	3932.9	290.9	-0.70
08-01-55-23W5	CROSS-SECTION A	4013.2	4013.2	74.2	8.50

TABLE B-5: NATIVE SULFUR GEOCHEMISTRY

WELL ID	DESCRIPTION	DEPTH (ft,m)	DEPTH (m)	DEPTH BELOW GRAMINIA (m)	del 34S per mil
07-15-52-22W5	PLATFORM WELL	13734.5	4187.3	147.3	20.60
		13736.5	4188.0	148.0	20.20
		13738.0	4188.4	148.4	23.03
		13747.3	4191.3	151.3	20.70
		13764.0	4196.3	156.3	24.26
		13769.0	4197.9	157.9	21.50
		13773.8	4199.3	159.3	21.31
02-22-52-22W5	PLATFORM WELL	4223.0	4223.0	149.0	24.53
		4224.3	4224.3	150.3	24.62
		4240.4	4240.4	166.4	22.48
09-30-52-22W5	PLATFORM WELL	4533.5	4533.5	200.5	18.04
		4537.3	4537.3	204.3	18.29
		4538.9	4538.9	205.9	18.26
		4540.8	4540.8	207.8	17.83
		4544.9	4544.9	211.9	18.42
		4547.5	4547.5	214.5	18.37
		4548.8	4548.8	215.8	18.38
		4550.6	4550.6	217.6	19.06
		4551.1	4551.1	218.1	18.72
		4554.7	4554.7	221.7	18.61
		4555.2	4555.2	222.2	18.68
		4556.3	4556.3	223.3	18.68

TABLE B-5: NATIVE SULFUR GEOCHEMISTRY

WELL ID	DESCRIPTION	DEPTH (ft,m)	DEPTH (m)	DEPTH BELOW GRAMINIA (m)	del 34S per mil
04-26-52-23W5	PLATFORM WELL	4456.6	4456.6	195.6	14.95
		4461.1	4461.1	200.1	16.48
		4464.5	4464.5	203.5	16.24
		4468.9	4468.9	207.9	17.34
		4472.0	4472.0	211.0	15.95
07-18-52-24W5	PLATFORM WELL	4820.5	4820.5	168.5	16.24
	BR PINNACLE	4834.6	4834.6	192.6	19.30
		4848.1	4848.1	206.1	18.31
		4852.3	4852.3	210.3	17.40
		4859.7	4859.7	217.7	15.25
10-27-52-24W5	PLATFORM WELL	4677.7	4677.7	179.7	19.78
		4681.1	4681.1	183.1	20.75
		4685.0	4685.0	187.0	20.71
		4689.3	4689.3	191.3	21.15
		4689.6	4689.6	191.6	21.43
		4689.9	4689.9	191.9	21.26
		4691.0	4691.0	193.0	21.13
15-23-53-21W5	BASINAL WELL	4041.6	4041.6	302.6	17.78
	BR PINNACLE	4044.8	4044.8	305.8	18.56
		4046.5	4046.5	307.5	18.04
		4047.2	4047.2	308.2	19.58
		4050.8	4050.8	311.8	21.11
		4050.9	4050.9	311.9	21.18

TABLE B-5: NATIVE SULFUR GEOCHEMISTRY

WELL ID	DESCRIPTION	DEPTH (ft,m)	DEPTH (m)	DEPTH BELOW GRAMINIA (m)	del 34S per mil
		4051.1	4051.1	312.1	21.46
12-15-53-22W5	BASINAL WELL	13133.4	4004.1	49.1	27.79
06-12-53-23W5	PLATFORM WELL	4102.5	4102.5	89.5	17.77
07-01-53-24W5	PLATFORM WELL	4523.7	4523.7	189.7	23.52
		4524.4	4524.4	190.4	20.35
		4526.6	4526.6	192.6	20.58
		4532.3	4532.3	198.3	20.25
06-28-54-21W5	BASINAL WELL	12336.0	3761.0	51.0	28.25
07-06-54-22W5	BASINAL WELL	12879.0	3926.5	46.5	20.18
		12894.0	3931.1	51.1	20.95
05-13-54-23W5	CROSS-SECTION A	13351.0	4070.4	196.4	21.12
		13362.0	4073.8	199.8	21.55
		13378.5	4078.8	204.8	21.21
02/15-26-54-23W5	CROSS-SECTION A	4109.9	4109.9	137.9	25.35
11-35-54-23W5	CROSS-SECTION A	13389.0	4081.0		26.95
		13389.8	4081.2		26.40
08-06-55-22W5	CROSS-SECTION A	4014.8	4014.8	171.8	20.00
08-01-55-23W5	CROSS-SECTIO	4037.0	4037.0	98.0	26.44
		4047.0	4047.0	108.0	26.88

REFERENCES CITED IN APPENDICES

Baadsgaard, H., Chaplin, C., and Griffin, W.L., 1986, Geochronology of the Gloserneia pegmatite, Froland, Southern Norway: Norsk Geologisk Tidsskift, v. 64, p. 111-119.

Epstein, S., Graf, D.L., and Degens, E.T., 1964, Oxygen isotope studies on the origin of dolomites. In Craigh, H., Miller, S.L., and Wasserburg, G.J. (eds.), Isotopic and cosmic chemistry. North-Holland Publishing Co., Amsterdam, p. 169-180.

Koffyberg, A.M., 1993, Strontium isotopic constraints on the geochemistry and origins of regional vein-forming fluids in the southern Canadian Cordillera, M.Sc. thesis, Edmonton, Alberta, University of Alberta, 102p.

Krouse, H.R., 1983, Stable isotope research of more effective utilization of gas fields in Alberta, Canada Energy Resource Research Fund Agreement U-30, p. 1-100.McCrea, J.M., 1950, On the isotopic chemistry of carbonates and a paleothermometer scale, Journal of Chemical Physics, v. 18, p. 849-857.

McCrea, J.M., 1950, On the isotopic chemistry of carbonates and a paleothermometer scale, Journal of Chemical Physics, v. 18, p. 849-857.

Moore, S.L.O., 1994, Dolomitization styles, Yoho National Park, unpublished M.Sc. thesis, University of Calgary.

Shakur, M.A., 1982, $\delta^{34}S$ and $\delta^{18}O$ variations in terrestrial sulfates [unpubl. Ph.D. diss.]: University of Calgary, 300p.

Ueda, A. and Krouse, H.R., 1986, Direct conversion of sulphide and sulphate minerals to SO_2 for isotope analyses, Geochemical Journal, v. 20, p. 209-212.